

**DEGRADATION STUDIES OF MULTILAYER COATINGS EXHIBITING  
ANGULAR DEPENDENT TRANSMITTANCE**

By

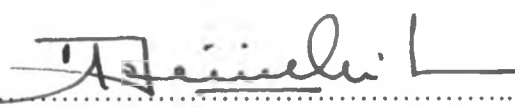
Musembi    Robinson    Juma

**A THESIS SUBMITTED IN PARTIAL FULFILMENT OF THE  
REQUIREMENT FOR THE MASTER OF SCIENCE DEGREE OF THE  
UNIVERSITY OF NAIROBI**


**UNIVERSITY OF NAIROBI  
2002**

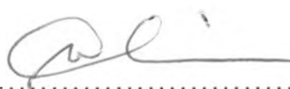
## DECLARATION

This Thesis is my own work and has not been examined or submitted for examination in any other University

Signed.....  
Musembi, Robinson Juma Reg.No. I/56/7066/98  
Date..... 19th/8/2002

This thesis has been submitted for examination with our approval as supervisors

1 Supervisor.....  
Dr. Julius M. Mwabora  
Department of Physics  
University of Nairobi  
P.O. Box 30197  
Nairobi  
Kenya  
Date..... 10/8/2002

2 Supervisor.....  
Dr. Godfrey W. Mbise  
Department of Physics  
University of Dar es Salaam  
P.O. Box 35063  
Dar es Salaam  
Tanzania  
Date..... 20/8/2002

# DEDICATION

To my Parents

## ACKNOWLEDGMENT

My special thanks go to Dr. Julius M. Mwabora and Dr. Godfrey W. Mbise whom I owe a lot for introducing me into thin film optics and vacuum technology. Many thanks go to them jointly for encouraging me to take this project. I have benefited a lot from the numerous discussions I have held with them, from time to time, and for instilling in me a firm inspiration in applied optics, a subject I have come to love and enjoy.

I also wish to thank jointly again Dr. Mwabora and Dr. Mbise, who were my supervisors for their excellent guidance, unrivalled kindness and their broad knowledge and experience especially in thin films. Their cooperation during the entire period of this work made everything run smoothly.

I highly appreciate the coordination and swift action of Prof. Lennart Hasselgren, Prof. Rogath T. Kivaisi and Dr. Godfrey Mbise who went into great length to make sure the optical spectrophotometer that could have stalled this work was back into its proper working condition just in time.

The six month period of research fellowship at Solar Energy Lab., Physics Department, University of Dar es Salaam, was sponsored by International Programs in Physical Sciences (IPPS), through the Condensed Matter Research Group, University of Nairobi and the Solar Energy Research Group, University of Dar es Salaam.

Special thanks to our Condensed Matter Research Group leader Prof. B.O. Aduda, whom I have benefited from his knowledge and experience in materials science, which came into handy in the course of doing this work. His kindness and readiness to help, plus his skilful leadership are highly acknowledged.

The skilful technical assistance of Boniface Muthoka and Josephine Ochola of the Condensed Matter Research Group, University of Nairobi; Khalfani Mtelela of Solar

Energy Group, D. Lameck of central science workshop, and M. Suya of Zoology Department, at the University of Dar es Salaam. Their efforts in technical assistance are acknowledged.

I would also wish to express my deep gratitude to all other people who helped me in one way or another during the course of this work

I also wish to express my gratitude to Mr. Mghendi Mwamburi, Physics Department, Moi University, Kenya, for helping and discussing MathCAD programming. The programme was very useful in the final analysis of this work. Many thanks again to Mr. Mghendi Mwamburi for providing me with ISO 9845 AM 1.5 and ISO 10526 illuminant (Eye) data files.

## ABSTRACT

Multilayer coatings exhibiting angular dependent transmittance were prepared by evaporation method. Different multilayer combinations have been studied, which included  $\text{MgF}_2/\text{Ag}/\text{MgF}_2$ ,  $\text{MgF}_2/\text{Al}/\text{MgF}_2$ ,  $\text{TiO}_2/\text{Ag}/\text{TiO}_2$  and  $\text{TiO}_2/\text{Al}/\text{TiO}_2$ . Among these combinations,  $\text{MgF}_2/\text{Ag}/\text{MgF}_2$  multilayer has been found to display the best optical properties, that is, high transmittance in the visible region and low transmittance in the near infrared region and substantial angular dependency (i.e. tendency of optical transmittance and reflectance to depend on variation of angle of incidence beam).

$\text{MgF}_2/\text{Ag}$  based multilayer coating was adopted for degradation study due to their superior optical properties. Transmittance and reflectance were measured before and after the samples were exposed to degradation environment. The environment could be extreme temperature, inflated humidity, saline solution, organic solvents or aquatic condition for the case of accelerated degradation study. For non-accelerated degradation studies, the samples were left to age naturally in the normal atmosphere for predetermined duration.

The samples' spectral properties were found to insignificantly degrade after they were subjected to various degradation environments. The highest change in transmittance and reflectance was registered for samples soaked in saline solution while no change was noted for samples kept in room environment (i.e. normal atmosphere). The changes observed can be attributed to changes in crystallographic structure (amount of defects and dislocations), packing density and surface roughness of the multilayer films. It is concluded that the optical properties of  $\text{MgF}_2/\text{Ag}/\text{MgF}_2$  multilayer coatings are virtually unaffected by most of the adverse weather conditions considered in this study.

## TABLE OF CONTENTS

DECLARATION.....	ii
DEDICATION.....	iii
ACKNOWLEDGEMENT.....	iv
ABSTRACT.....	vi
TABLE OF CONTENTS.....	vii
LIST OF SYMBOLS.....	x
LIST OF FIGURES.....	xiii
LIST OF TABLES.....	xix

### CHAPTER ONE: INTRODUCTION

1.1. Introduction.....	1
1.2. Statement of the Problem.....	2
1.3. Significance of the Study.....	3
1.4. Main Objectives of This Work.....	4

### CHAPTER TWO: LITERATURE REVIEW

2.1. Ambient Radiation.....	6
2.2. Coatings with Angularly Dependent Transmittance.....	9
2.3. Degradation Studies.....	11
2.4. Survey of Window Coatings for Different Climatic Regions..	12
2.5. Protection for Film.....	14

**CHAPTER THREE: THEORY FOR MULTILAYER COATINGS  
EXHIBITING ANGULAR DEPENDENT  
TRANSMITTANCE**

3.1.	Introduction.....	19
3.2.	Maxwell's Equations.....	19
3.3.	Boundary Conditions.....	21
3.4.	Fresnel's Equations for Angle Dependent Coatings.....	22
3.5.	The Characteristic Matrix of a Homogeneous Media.....	26
3.6.	Quantitative Performance Parameters.....	27

**CHAPTER FOUR: EXPERIMENTAL TECHNIQUES**

4.1.	Introduction.....	29
4.2.	Cleaning the Substrate.....	29
4.3.	Deposition of the Films.....	30
4.4.	Optical Characterization.....	32
4.5.	Ageing Treatment.....	33
4.5.1.	<i>Elevated Temperatures</i> .....	34
4.5.2.	<i>Low Temperatures</i> .....	34
4.5.3.	<i>Humid Environment</i> .....	34
4.5.4.	<i>Saline Solution</i> .....	35
4.5.5.	<i>Organic Solvents</i> .....	36
4.5.6.	<i>Outdoor Environment</i> .....	36
4.5.7.	<i>Aquatic Condition</i> .....	36



## CHAPTER FIVE: RESULTS AND DISCUSSION

5.1.	Introduction.....	37
5.2.	Degradation Studies.....	38
5.2.1.	<i>Elevated Temperatures</i> .....	38
5.2.2.	<i>Low Temperatures</i> .....	45
5.2.3.	<i>Humid Environment</i> .....	52
5.2.4.	<i>Saline Solution</i> .....	55
5.2.5.	<i>Organic Solvents</i> .....	60
5.2.6.	<i>Outdoor Environment</i> .....	65
5.2.7.	<i>Aquatic Condition</i> .....	68
5.3.	MgF <sub>2</sub> /Ag/MgF <sub>2</sub> Coatings.....	70
5.4.	TiO <sub>2</sub> Based Coatings.....	72

## CHAPTER SIX: CONCLUSION AND SUGGESTIONS FOR FURTHER STUDIES

6.1.	Conclusion.....	77
6.2.	Suggestions for Further Studies.....	78

REFERENCES.....	80
-----------------	----

<b>APPENDIX:</b>		
	<b>A: TABULATED OPTICAL PROPERTIES OF</b>	
	<b>MgF<sub>2</sub>/ Ag/ MgF<sub>2</sub> MULTILAYER COATINGS</b>	86
	<b>B: PROGRAM MOONRAKER 7</b>	90

## LIST OF SYMBOLS

<b>A</b>	Aged sample
<b>AM 1.5</b>	Air Mass at azimuthal angle
<b>B</b>	Magnetic Induction vector
<b>B<sub>j</sub></b>	Magnetic induction vector for medium $j$ , $j = 1, 2, \dots$
<b><i>b</i></b>	Back side of sample
<b><i>c</i></b>	Speed of light
<b><i>d</i></b>	Thickness of the film
<b>D</b>	Electric displacement vector
<b>D<sub>j</sub></b>	Electric displacement vector for medium $j$ , $j = 1, 2, \dots$
<b>E</b>	Electric energy vector
<b>E<sub>j</sub></b>	Electric energy vector for medium $j$ , $j = 1, 2, \dots$
<b>E<sub>i</sub></b>	Incident electric energy vector
<b>E<sub>r</sub></b>	Reflected electric energy vector
<b>E<sub>t</sub></b>	Transmitted electric energy vector
<b>E<sub>rp</sub></b>	Reflected p polarized energy vector
<b>E<sub>ip</sub></b>	Incident p polarized energy vector
<b>E<sub>rs</sub></b>	Incident s polarized energy vector
<b>E<sub>is</sub></b>	Incident s polarized energy vector
<b>E<sub>tp</sub></b>	Transmitted p polarized energy vector
<b>E<sub>ts</sub></b>	Transmitted s polarized energy vector
<b>EM</b>	Electromagnetic
<b><i>f</i></b>	Front side of sample
<b>H</b>	Magnetic intensity vector
<b>H<sub>j</sub></b>	Magnetic intensity vector for medium $j$ , $j = 1, 2, \dots$
<b>ISO</b>	International Standard Organization
<b><i>i</i></b>	Complex quantity ( $i^2 = -1$ )
<b>J</b>	Electric current density vector
<b><i>k</i></b>	Wave vector
<b>La<sub>3</sub>O<sub>3</sub></b>	Lanthanum Oxide

$m_{ij}$	Elements of a characteristic matrix
<b>M</b>	Characteristic matrix
<b>N</b>	New (fresh) sample
$n$	Refractive index
$n_j$	Refractive index of medium $j$ , $j = 0, 1, 2, 3, \dots$
<b>nm</b>	Nanometers = $10^{-9}$ m
<b>NIR</b>	Near Infrared
<b>P</b>	Measured spectral radiometric property (reflectance or transmittance)
$r$	Rate of deposition
<b>R</b>	Reflectivity
$R_j$	Reflectivity of medium $j$ , $j = 1, 2, 3, \dots$
<b>RE</b>	Reflectance
$R_{lum}$	Luminous reflectance
$R_{sol}$	Solar reflectance
<b>RH</b>	Relative humidity
$r_{2s}, r_{2p}$	Fresnel reflection coefficient for s and p field respectively
$r_{ij}, t_{ij}$	Reflectance and transmittance from medium $i$ to medium $j$ respectively. $i \neq j$ , $i = 1, 2, 3, \dots, j = 1, 2, 3, \dots$
<b>T</b>	Transmissivity
$T_j$	Transmissivity of medium $j$ , $j = 1, 2, 3, \dots$
<b>TR</b>	Transmittance
$T_{lum}$	Luminous transmittance
$T_{sol}$	Solar transmittance
$t_{2s}, t_{2p}$	Fresnel transmission coefficient for s and p field respectively
<b>TE</b>	Transmitted energy
<b>TIR</b>	Total Internal Reflection
<b>UV</b>	Ultra Violet *
$\delta$	Phase difference
$\epsilon$	Dielectric constant
$\epsilon_j$	Dielectric constant of medium $j$ , $j = 1, 2, 3, \dots$

$\epsilon$	Emmittance
$\lambda$	Wavelength
$\mu$	Magnetic permeability
$\pi$	Angle in radians
$\theta_1$	Oblique incidence angle
$\theta_2$	Normal incidence angle
$\theta_i$	Angle of incidence
$\theta_r$	Angle of reflection
$\theta_t$	Angle of transmission
$\rho$	Charge density
$\sigma$	Electrical conductivity
$\hat{n}$	Normal unit vector
$\omega$	Angular frequency
$\nabla$	$\nabla = \mathbf{i} \frac{\partial}{\partial x} + \mathbf{j} \frac{\partial}{\partial y} + \mathbf{k} \frac{\partial}{\partial z}$
$\Phi$	Weighting function for the strength of source (sunlight or thermal)
$\text{\AA}$	Ångström = $10^{-10}$ m
$\mu\text{m}$	Micrometer = $10^{-6}$ m

## LIST OF FIGURES

	Page
Figure 2.1. Spectra for (a) blackbody radiation (b) solar radiation outside the earth atmosphere (c) typical absorption across atmosphere envelope (d) relative sensitivity of human eye (Granqvist, 1991)	7
Figure 2.2. Effects of the rate of deposition on the reflectance of SiO coated aluminium (Heavens, 1965)	15
Figure 2.3a. Spectral transmittance of Ag and ZnS/Ag/ZnS coatings, deposited on cleaned glass substrate. Fresh sample a and c, aged sample b and d. The insert curves are expanded to show the visible region (Mbise, <i>et. al.</i> , 1990)	17
Figure 2.3b. Spectral transmittance of Ag and ZnS/Ag/ZnS coatings, deposited on uncleaned glass substrates. Fresh sample a and c, aged sample b and d. The insert curves are expanded to show the visible region (Mbise, <i>et. al.</i> , 1990)	17
Figure 3.1. Light path passing from a less dense medium into a denser medium; the incident, reflected and transmitted rays and angles are indicated	21
Figure 3.2. The path of light ray passing from air across the film into the air or another medium of refractive index less than that of the film	24

- Figure 5.2.1a. Spectral transmittance and reflectance of  $\text{MgF}_2/\text{Ag}/\text{MgF}_2$  multilayer for fresh sample and a sample laid in an oven maintained at  $50 \pm 1^\circ\text{C}$  for indicated duration 39
- Figure 5.2.1aa. The variation with time of wavelength integrated luminous transmittance for sample annealed at  $50^\circ\text{C}$ . Fresh sample A and C, aged sample B and D. (NB. A and B denotes oblique incidence; C and D denotes normal incidence) 40
- Figure 5.2.1b. Spectral transmittance and reflectance of  $\text{MgF}_2/\text{Ag}/\text{MgF}_2$  for fresh sample and a sample laid in an oven maintained at  $100 \pm 1^\circ\text{C}$  for indicated duration. 41
- Figure 5.2.1bb. The variation with time of wavelength integrated luminous transmittance for sample annealed at  $100^\circ\text{C}$ . Fresh sample A and C, aged sample B and D. (NB. A and B denotes oblique incidence; C and D denotes normal incidence) 42
- Figure 5.2.1c. Spectral transmittance and reflectance of  $\text{MgF}_2/\text{Ag}/\text{MgF}_2$  multilayer for fresh sample and a sample laid in an oven maintained at  $200 \pm 1^\circ\text{C}$  for indicated duration 43
- Figure 5.2.1cc. The variation with time of wavelength integrated luminous transmittance for sample annealed at  $200^\circ\text{C}$ . Fresh sample A and C, aged sample B and D. (NB. A and B denotes oblique incidence; C and D denotes normal incidence) 44
- Figure 5.2.2a. Spectral transmittance and reflectance of  $\text{MgF}_2/\text{Ag}/\text{MgF}_2$  multilayer for fresh sample and a sample laid in freezer maintained at  $-10 \pm 1^\circ\text{C}$  for indicated duration 46

- Figure 5.2.2aa. The variation with time of wavelength integrated luminous transmittance for sample laid in freezer maintained at 10 °C. Fresh sample A and C, aged sample B and D. (NB. A and B denotes oblique incidence; C and D denotes normal incidence) 47
- Figure 5.2.2b. Spectral transmittance and reflectance of MgF<sub>2</sub>/Ag/MgF<sub>2</sub> multilayer for fresh sample and a sample laid in freezer maintained at -18 ±1°C for indicated duration 48
- Figure 5.2.2bb. The variation with time of wavelength integrated luminous transmittance for sample laid in freezer maintained at -18 °C. Fresh sample A and C, aged sample B and D. (NB. A and B denotes oblique incidence; C and D denotes normal incidence) 49
- Figure 5.2.2c. Spectral transmittance and reflectance of MgF<sub>2</sub>/Ag/MgF<sub>2</sub> multilayer for fresh sample and a sample covered in ice (frost) at -20 ±1°C for indicated duration 50
- Figure 5.2.3a. Spectral transmittance and reflectance of MgF<sub>2</sub>/Ag/MgF<sub>2</sub> multilayer for fresh sample and a sample laid in humidity chamber maintained at 86 ±1% relative humidity for indicated duration 53
- Figure 5.2.3b. The variation with time of wavelength integrated luminous transmittance for sample laid in chamber maintained at 86% relative humidity. Fresh sample A and C, aged sample B and D. (NB. A and B denotes oblique incidence; C and D denotes normal incidence) 54

- Figure 5.2.4a. Spectral transmittance and reflectance of  $\text{MgF}_2/\text{Ag}/\text{MgF}_2$  multilayer for fresh sample and a sample soaked in salt (NaCl) solution of concentration 20 gm/100ml water for indicated duration 56
- Figure 5.2.4b. Spectral transmittance and reflectance of  $\text{MgF}_2/\text{Ag}/\text{MgF}_2$  multilayer for fresh sample and a sample soaked in salt (NaCl) solution of concentration 20 gm/100ml water for indicated duration 57
- Figure 5.2.4c. Spectral transmittance and reflectance of  $\text{MgF}_2/\text{Ag}/\text{MgF}_2$  multilayer for fresh sample and a sample soaked in salt (NaCl) solution of concentration 20 gm/100ml water for indicated duration 58
- Figure 5.2.4d. The variation with time of wavelength integrated luminous transmittance for sample soaked in saline solution. Fresh sample A and C, aged sample B and D. (NB. A and B denotes oblique incidence; C and D denotes normal incidence) 59
- Figure 5.2.5a. Spectral transmittance and reflectance of  $\text{MgF}_2/\text{Ag}/\text{MgF}_2$  multilayer for a fresh sample and a sample soaked in acetone of purity 99.8% for indicated duration 61
- Figure 5.2.5aa. The variation with time of wavelength integrated luminous transmittance for sample soaked in acetone. Fresh sample A and C, aged sample B and D. (NB. A and B denotes oblique incidence; C and D denotes normal incidence) 62



Figure 5.2.5b. Spectral transmittance and reflectance of  $MgF_2/Ag/MgF_2$  multilayer for fresh sample and a sample soaked in ethanol of purity 99.8% for indicated duration 63

Figure 5.2.5bb. The variation with time of wavelength integrated luminous transmittance for sample soaked in ethanol. Fresh sample A and C, aged sample B and D. (NB. A and B denotes oblique incidence; C and D denotes normal incidence) 64

Figure 5.2.6a. Spectral transmittance and reflectance of  $MgF_2/Ag/MgF_2$  multilayer for a fresh sample and a sample exposed into normal outside atmosphere environment, temperature range  $20 - 34 \pm 1^\circ C$ ; humidity range  $60 - 70 \pm 1\% RH$  for duration indicated 66

Figure 5.2.6b. The variation with time of wavelength integrated luminous transmittance for sample exposed into outdoor environment. Fresh sample A and C, aged sample B and D. (NB. A and B denotes oblique incidence; C and D denotes normal incidence) 67

Figure 5.2.7a. Spectral transmittance and reflectance of  $MgF_2/Ag/MgF_2$  multilayer for a fresh sample and a sample soaked in water in room environment for indicated duration 69

Figure 5.2.7b. The variation with time of wavelength integrated luminous transmittance for sample soaked in distilled water. Fresh sample A and C, aged sample B and D. (NB. A and B denotes oblique incidence; C and D denotes normal incidence) 70

Figure 5.3.1. Spectral transmittance (TR) and reflectance (RE) for MgF <sub>2</sub> /Al/MgF <sub>2</sub> coating	71
Figure 5.4.1. Spectral transmittance (TR) and reflectance (RE) for TiO <sub>2</sub> /Ag/TiO <sub>2</sub> coating	73
Figure 5.4.2. Spectral transmittance (TR) and reflectance (RE) for TiO <sub>2</sub> /Al/TiO <sub>2</sub> coating	74
Figure 5.4.3 Spectral normal transmittance (TR) and near normal reflectance (RE) (Granqvist, 1991)	76
Figure 5.4.4 Measured optical transmittance (TR) and reflectance (RE) of a 180-Å TiO <sub>2</sub> / 180- Å Ag/ 180- Å TiO <sub>2</sub> film on Corning 7059 Glass (John and Bachner, 1976)	76

## LIST OF TABLES

Table 2.1.	Stability of selective coatings in air (Kivaisi, 1976)	18
Table 4.1.	Material used in this work, their purity and the type of hearth used	31
Table 4.2.	Concentration of graded solution used to maintain the atmosphere at constant humidity at $29 \pm 1$ °C	35
Table 5.3.1.	Material type used in this work with respective crystal structure and density (Besancon, 1986; Pulker, 1999)	72
Table 5.4.1.	Properties of TiO <sub>2</sub> at different substrate temperature (Pulker, 1999).	74
Table A1.	Changes in optical properties for samples heated at 50 °C for duration shown	86
Table A2.	Changes in optical properties for samples heated at 100 °C for duration shown	86
Table A3.	Changes in optical properties for samples heated at 200 °C for duration shown	86
Table A4.	Changes in optical properties for samples laid in freezer maintained at -10 °C for duration shown	87
Table A5.	Changes in optical properties for samples laid in freezer maintained at -18 °C for duration shown	87
Table A6.	Changes in optical properties for samples covered in ice (frost) at -20 °C for duration shown	87

Table A7. Changes in optical properties for samples laid in chamber maintained at 86% relative humidity for duration shown	88
Table A8. Changes in optical properties for samples soaked in saline solution of concentration 20gm/100ml, for duration shown	88
Table A9. Changes in optical properties for samples soaked in acetone of purity 99.8% for duration shown	88
Table A10. Changes in optical properties for samples soaked in ethanol of purity 99.8% for duration shown	89
Table A11. Changes in optical properties for samples exposed into outdoor environment for duration shown	89
Table A12. Changes in optical properties for samples soaked in distilled water for duration shown	89

## INTRODUCTION

### 1.1 Introduction

Multilayer coatings are obtained by deposition of multiple successions of thin plane parallel films on the same surface of the substrate. These coatings, which may be produced by evaporation and/or sputtering techniques, are widely used in mirrors, dichroic beam splitters, antireflection coatings, narrow and broadband interference filters, etc. Each of these applications often requires careful control of thickness and refractive indices for each layer in the stack (Coleman, 1978; Behrndt, 1964; Randlett *et. al.*, 1966; Mbise and Kivaisi, 1993).

Most of the applications of multilayer optical coatings have been confined to normal incidence, but there are few designs for oblique incidence (Mbise and Kivaisi, 1993; Mbise, 1998). Coatings whose transmittance of incidence radiation falling at off-normal angles is higher than transmittance of normally incidence radiation are said to exhibit angular dependent transmittance. Coatings with angular dependent transmittance find applications in energy efficient windows (an energy efficient window is a device capable of providing good lighting during the day and good thermal comfort both during the day and night at minimum demand of paid energy), particularly in automobile industry and architectural sectors. Each of these applications requires maximization of the angular performance. *Angular performance* is defined as the difference between the off-normal and normal incidence luminous transmittance, where it is expected that  $T_{\text{normal}} < T_{\text{off-normal}}$ .

The subject of dielectrics and metallic films has been extensively treated in the scientific literature. The materials that have been found suitable for combining high transmittance in the visible (VIS) range with low transmittance in the near infrared (NIR) range include; the noble metals i.e. Ag, Cu and Au (Johnson and Christy, 1972).

Kazem, *et. al.* 1988; Palik, 1985). Other materials are Al (Behrens and Ebel, 1981) or Cr (Johnson and Christy, 1974; Nestel and Christy, 1980). To enhance the luminous transmittance of these metallic materials, especially the noble metals, antireflection layer is usually applied either on top of the metal layer or the metal layer is embedded in between the dielectric material. Some of the materials suitable for the antireflection purpose include; ZnS (Palik, 1985), TiO<sub>2</sub> (Palik, 1985), CaF<sub>2</sub> (Driscoll and Vaughan, 1978), SiO<sub>2</sub> (Palik, 1985), MgF<sub>2</sub> (Driscoll and Vaughan, 1978) or WO<sub>3</sub> (Mbise and Kivaisi, 1993).

## 1.2 Statement of the Problem

Space conditioning of residential and commercial buildings accounts for substantial fraction of the annual energy consumption in many countries. In developing countries, roughly 3% of the annual energy consumption is tied to fenestration performance and it is believed that higher values are valid for industrialized countries (Granqvist, 1991). The 1970's energy crisis has made energy conservation one of the most important issues. Thus, for example, the insulation properties of buildings have been tremendously improved, particularly for walls and roofing materials which at the moment have a k-value (i.e. thermal conductance) of as low as  $1 \text{ Wm}^{-2}\text{K}^{-2}$ . However, the k-value for usual glass window is as bad as  $6 \text{ Wm}^{-2}\text{K}^{-2}$  or worse. Therefore, it is worth noting that, to date glass windows are still the main path for heat exchanges between building and surroundings. For a long time, efforts by scientist and industries were being geared towards developing windows with desired insulation. This has been achieved by reducing heat losses and condensation through windows by improving them in terms of their U-value (conductance of heat) or their R-value (resistance to heat flow) (Ling and Cheng, 1987).

A glass window with multilayer coatings exhibits angular dependent transmittance, which is desired in the tropical climate where the sun is high most of the day. These coatings have been shown to transmit (Mbise and Kivaisi, 1993) both solar and

luminous transmittance as high as 64% at oblique angle of incidence and as low as 48% at normal incidence.

Thus windows with angular dependent transmittance are suitable for louvers in the architecture and inclined windscreens in the motor vehicles. It should be noted that such fixtures are to be placed on the outside where they are exposed to different weather conditions varying from cold, rainy, humid, hot, permafrost, etc, whose intensity are sometimes drastic depending on time, location and season. These climatic changes are likely to degrade the radiative properties of multilayer coated glass windows. Needless to mention, the optical characteristics of these window coatings are expected to last for at least few decades, and are usually kept outdoors. It is for these reasons that there is need to perform degradation studies of these window coatings. To our knowledge, no degradation study of multilayer coatings exhibiting angular dependent transmittance has been reported, albeit its potentiality for application has been reported in literature (Mbise and Kivaisi, 1993; Granqvist, 1991; Rubin, *et. al.*, 1999).

### **1.3 Significance of the Study**

The properties of multilayer coatings exhibiting angular dependent transmittance are suitable for energy efficiency of windows. Durability of the material combination used in their fabrication is vital especially if they are to be kept outdoors, with possibility for harsh environments. The results of this work will provide at least preliminary information on the tolerance of these windows to various environmental conditions. The outcomes of the study will also act as an impetus and motivation to other workers already working in the field of window technology, and eventually bring this essential device into the market. This work consolidates various degradation test methods and may act as a good reference to future related studies.

## 1.4 Main Objectives of This Work

The major aim of the present work is to investigate the degradation of optical (transmittance and reflectance) properties of multilayer coatings exhibiting angular dependent transmittance. Particularly, the study aims at investigating the tolerance of such window coatings with respect to: extreme temperatures, humidity, organic solvents, saline solution, aquatic condition and normal atmospheric condition.

Specific objectives of this study are: -

1. To fabricate D/M/D multilayer coatings (D = dielectric; M = metal) on glass substrate. The fabricated coatings are hereinafter referred to as *samples*.
2. To perform accelerated degradation of the samples by subjecting them to different conditions as explained below:
  - (i) Anneal samples in air at temperatures between 50 and 200 °C for varying duration of time.
  - (ii) Keep the samples in freezing environment (temperatures lower than -10 °C) for varying duration of time.
  - (iii) Keep the samples exposed to high loads of relative humidity (> 80% RH) for varying duration of time.
  - (iv) Keep the samples soaked in organic solvent for varying duration of time.
  - (v) Keep the samples soaked in saline solution for varying duration of time.
  - (vi) Keep the samples soaked in aquatic condition for varying duration of time.
3. To employ spectrophotometry in obtaining the optical properties of freshly deposited samples and degraded samples for different angles of light incidence in the 300 – 2500 nm wavelength range.



4. To assess the energy efficiency inherent in the optical data and thereby evaluate the tolerance of samples to the conditions stated in objective 2

## LITERATURE REVIEW

### 2.1. Ambient Radiation

As defined earlier, an energy efficient window is a device capable of providing good lighting during the day and good thermal comfort both during the day and night at minimum demand of paid energy. Energy efficiency of a glass window can be achieved by applying thin surface coatings tailored so as to modify the radiative properties of the glass. The coating is supposed to control radiative inflows and heat losses due to radiation, conduction and convection (Granqvist, 1991; Mbise, 1995).

The key to energy efficient window lies in the clear understanding of the radiative properties of our natural surroundings. These properties are illustrated in Fig. 2.1.

As a preamble to the discussion, the properties of the radiation are conveniently expounded by starting with the ideal blackbody spectra, whose emitted spectrum is also known as the Planck's spectra, is uniquely defined if the absolute temperature is known. Figure 2.1(a) depicts the Planck's spectra for three temperatures and with a common logarithmic wavelength scale on the abscissa. The ordinate scale depicts power per unit area and per unit wavelength increment (hence the units  $\text{GWm}^{-3}$ ). The spectra are bell shaped and confined to the  $2.0 \times 10^3 < \lambda < 10^5$  nm range, where  $\lambda$  denotes the wavelength. The peaks in the spectra are characteristically displaced towards long wavelength as the temperature decreases, which is the manifestation of Wien's displacement law. At room environment, the peak lies at about  $10^5$  nm. The thermal radiation from a real body is obtained by multiplying the Planck's spectra by a numerical factor, the emittance,  $\epsilon$ , whose value lies in the range  $0 < \epsilon < 1$ . In general, the emittance is wavelength dependent (Granqvist, 1991; Mbise, 1995; Meinel and Meinel, 1979).

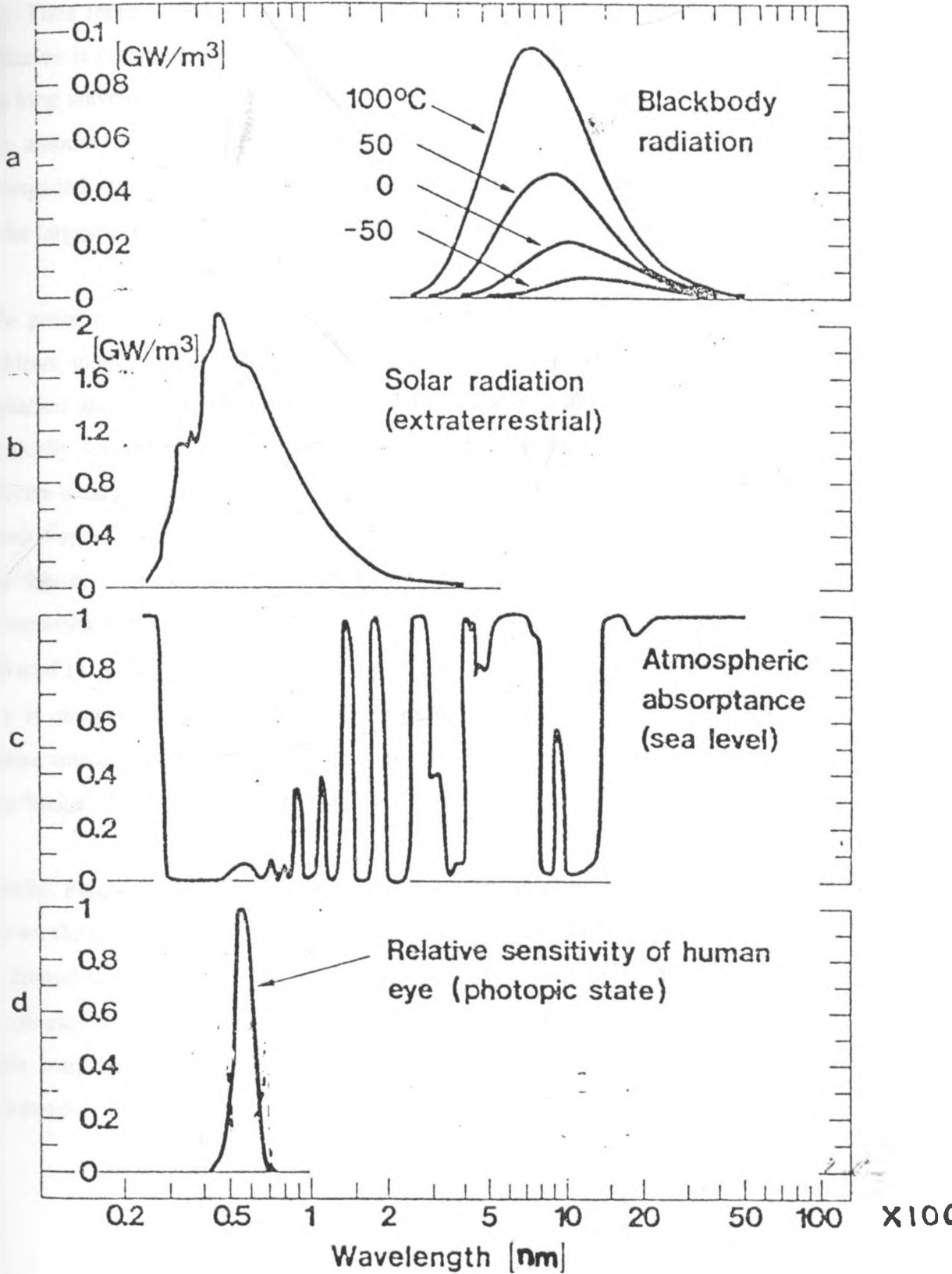


Figure 2.1 Spectra for (a) blackbody radiation (b) solar radiation outside the earth atmosphere (c) typical absorption across atmosphere envelope (d) relative sensitivity of human eye (Granqvist, 1991)

Figure 2.1(b) shows the spectrum of the extraterrestrial radiation. The curve has a bell shape defined by the sun's surface temperature ( $\sim 6000\text{ }^{\circ}\text{C}$ ). It can be observed that the solar spectrum is confined to the  $250 < \lambda < 3.0 \times 10^3\text{ nm}$  interval and it is peaked at around  $\lambda \approx 500\text{ nm}$ . Thus there is almost no overlap with the spectra for the thermal radiation. The solar radiation is comprised of a wide range of wavelength from the short wavelength ultraviolet to the long wavelength infrared. The integrated area under the curve gives the solar constant (i.e. the amount of energy incident in unit time on unit surface area exposed normally to unimpeded radiation from the sun, outside the atmosphere) of about  $1353 \pm 21\text{ Wm}^{-2}$ , which is the largest possible power density at the top of atmosphere (Mbise, 1989; Granqvist, 1991).

The present study is mainly concerned with radiation levels at the earth surface and it is of obvious interest to consider to what extent the atmospheric absorption influences solar radiation and thermal emission. Figure 2.1(c) illustrates absorption spectrum for irradiation vertically across the full atmospheric envelope at clear weather conditions, at sea level. The spectra is rather complicated, with bands of high absorption caused chiefly by carbon dioxide, water vapour and ozone, and intervening zones where atmosphere is very transparent. From the figure, it is clearly observed that the highest percentage of the solar radiation can be transmitted down to the ground level, and only fractions of the ultraviolet ( $\lambda < 400\text{ nm}$ ) and infrared ( $\lambda > 700\text{ nm}$ ) remains as damped. Thermal radiation from a surface exposed to clear sky is observed to be strongly absorbed except in the  $8.0 \times 10^3 < \lambda < 1.3 \times 10^4\text{ nm}$  range, where transmittance is large, but this only can happen at low humidity (Mbise, 1995; Meinel and Meinel, 1979; Granqvist, 1991).

Finally, Figure 2.1(d) illustrates a biophysical property of interest to application. The diagram shows the relative sensitivity of human eye in its light adapted (photopic) state. The bell shape is limited to  $400 < \lambda < 700\text{ nm}$  interval with its peak at  $555\text{ nm}$ . In its darkness adapted (scotopic) state, the eyes sensitivity is displaced about  $50\text{ nm}$  towards shorter wavelength. This small confinement tells us that most of the solar radiation comes as infrared radiation (Granqvist, 1991).

## 2.2 Coatings With Angularly Dependent Transmittance

Angular dependent window coatings can be designed from a variety of approaches, among which we mention polymer films, Total Internal Reflection (TIR) systems and multilayer films (Mbise, 1995). The work being reported in this thesis deals with the degradation studies of the latter films.

In the first example, the film, usually photopolymerized components having different refractive indices and reactivities, is coated on a flat substrate and then exposed to ultraviolet (UV) light to polymerize. The polymer film can be tailored to scatter incident light so that the overall throughput has an angular performance of ~70% by increasing the light incident angle from  $0^\circ$  to  $\sim 25^\circ$ . This kind of angular dependent window coating has been commercialized, under trademark <sup>®</sup> ANGLE 21, and is used for architecture in Japan (Mbise, 1995). On the other hand, TIR system has high transmittance for normal incidence light and dramatically blocks all obliquely incident light. From the earlier works, little research efforts have been devoted to this type of angular dependent window coating.

Multilayer coatings are obtained by deposition of multiple successions of thin plane parallel films on the same substrate. These coatings are widely used in mirrors, dichroic beam splitters, antireflection coatings, narrow and broadband interference filters, etc. Each of these applications requires careful control of thickness and refractive indices for each layer in the stack (Coleman, 1978; Behrnt, 1964; Randlett *et. al.*, 1966; Mbise and Kivaisi, 1993).

Although the history of multilayer films stretches far back to the work of Fraunhofer (Hilger, 1986), many topics have remained un-researched in this subject. To date, for example, most of the work in this field have been confined to normal incident. There are of-course a few designs for oblique incidence (Mbise *et. al.* 1989a-c; Kivaisi, 1982; Smith, 1989; Granqvist, 1989; Karlsson and Roos, 2000; Karlsson *et. al.* 2001). Few studies have been reported on experimental and theoretical work as well as for commercial devices. Turbadar (1964a,b) and Catalan (1961) have both reported theoretical models for angular dependent coatings. Turbadar reported a theoretical model for the all dielectric double layer (Turbadar, 1964a) and

triple layer (Turbadar, 1964b) coatings optimized for oblique incidence. Turbadar's model, however, were designed to work with either p or s polarized light and cannot be used with unpolarized light. These models were designed with thickness other than quarter wavelength to provide a broad region of low reflectance in the visible spectrum for either state of polarization. In order to achieve high transmittance for obliquely incidence light, Turbadar's model used completely different film thickness for different polarization. On the other hand Catalan (1961) reported a dielectric bilayer for p - polarized light only. Catalan's theoretical model included calculated curves giving the spectral reflectance for normal and oblique incidence and quantitative results showing the influence of the glass substrate and the effect of film thickness mismatching.

Few workers have reported theoretical models corroborated with experimental work. Cox *et. al.* (1954), Cox *et. al.* (1962), Mbise (1995) and Mbise and Kivaisi (1993) are some of the workers who have reported such studies. In reports by Cox *et. al.* (1954,1962), they reported an all dielectric double layer (Cox *et. al.*, 1954) and triple layer (Cox *et. al.*,1962) coatings optimized for un-polarized light. In both cases, the models were optimized for glass substrates of different refractive indices for various thickness combinations. The experimental work to test these models was done using a vacuum evaporation method whereby the substrate was heated to temperatures ranging between 150 - 300 °C in order to form scratch and abrasion resistance films. Mbise and Kivaisi (1993) in their work reported a dielectric/metal/dielectric and random dielectric/metal coatings design types. Mbise and Kivaisi's (1993) model was optimized to work for un-polarized light incident at oblique angle, in order to have high transmittance in the visible region with low near infrared transmittance. Thickness for different metals and dielectric combination were optimized by use of computer simulation program. The coatings were prepared in a conventional diffusion pumped coating system by evaporation method.

Currently a lot of interest and research efforts are in optical devices that have low transmittance at normal incidence than is in oblique incidence light. Mbise *et. al.* (1989a-c); Kivaisi (1982); Smith (1989); Granqvist (1989); Karlsson and Roos (2000) and Karlsson *et. al.* (2001) have done studies on angular dependent coatings, whereas, Tremblay *et. al.* (1987)

studied an angular reflector device. The angular dependent coatings (Mbise *et. al.* 1989a-c; Kivaisi, 1982; Smith, 1989; Granqvist, 1989; Karlsson and Roos, 2000; Karlsson *et. al.* 2001) have better indoor-outdoor contact and they open up new possibilities for energy efficient glazing and architectural design.

### 2.3 Degradation Studies

The term degradation can be defined as gradual loss of the original characteristics or ageing with time due to exposure of material to various conditions. Degradation study involves a careful study of possible factors that might cause ageing of the material in question.

Films are sometimes used at elevated temperatures or at very low temperatures, or they may be exposed to drastic changes in temperatures. These variations in temperature more often than not usually cause changes in the films structure, such as surface and volume imperfections, which include: surface roughness, rough internal boundaries or density fluctuations. Some of these changes are either reversible or irreversible. Good examples of reversible effect are the temperature dependency of the refractive index, and the electrical conductivity of the dielectric and metal films (Pulker, 1999; Heavens, 1965). On the other hand, irreversible effects include increase in void fraction, amount of defects and dislocations and electrical conductivity of the film after annealing (Pulker, 1999).

The use of thin film is not limited to the above stated environmental conditions, sometimes thin films have been exposed to chemically reactive environment and it is of great importance for films to be resistant to such environment. The atmospheric pollutants such as SO<sub>2</sub> and H<sub>2</sub>S usually do damage the optical properties of most coating materials by forming weak acids, which react with metallic, and non-metallic materials (Heavens, 1965; Pulker, 1999). The effect of humidity and saline water can be substantial in tropical climate or coastal regions. Humid environment usually damages hygroscopic film materials, while most materials normally react with saline solution, even when at very small concentration. Films should also be tolerant to liquid cleaning agents, to acids and also to fungus. The chemical compatibility

between the substrate and the film is also very important. The choice of substrate should be chemically compatible with the coating material, e.g. the glass constituent, PbO and the coating material such as  $\text{La}_2\text{O}_3$  may react and form optically absorbing metallic lead. A proper choice of substrate coating material should be put into consideration in order to avoid chemical degradation (Pulker, 1999; Heavens, 1965).

## 2.4 Survey of Window Coatings for Different Climatic Regions

Currently, there are several different types of energy efficient window coatings. These can be categorized broadly into two main classes, namely, STATIC window coatings and DYNAMIC window coatings. The former coatings have STATIC properties in the sense that their optical performance remains the same irrespective of external conditions while the latter changes with changes of the ambient.

The STATIC window coatings can conveniently be subdivided into coatings for *solar control* and coatings for providing low thermal emittance or *energy windows*.

In warm climate, it is frequently the case that solar energy that finds its way inside the building through the window is absorbed into the room and it eventually causes overheating. It is apparently energy effective to have *solar control* window that blocks the infrared part of the spectrum ( $700 < \lambda < 3000 \text{ nm}$ ) without excessive lowering of the luminous transmittance ( $400 < \lambda < 700 \text{ nm}$ ) (Mbise, 1989; Granqvist, 1991; Granqvist, 1984).

The *solar control* window utilizes coatings that function as heat diminishing devices and it is for this reason that these windows are also called transparent infrared reflector. Such window possesses a coating which transmits well in the luminous region of the solar radiation ( $400 < \lambda < 700 \text{ nm}$ ) and reflects the infrared radiation (Valkonen and Karlsson, 1985; John and Bachner, 1976), therefore the near infrared which carries large percentage of the total solar energy is restricted from passing through the window, while the visible radiation is transmitted. Whence, a good illumination combined with a low, comfortable, temperature



may be attained with decreased need for space conditioning which is costly in terms of paid energy. Materials reported to be suitable for fabricating these types of window as indicated by Granqvist (1984) are anti-reflected films of noble metals (Cu, Au and Ag). Dielectrics with high refractive indices (examples  $\text{In}_2\text{O}_3$ ,  $\text{Bi}_2\text{O}_3$ ,  $\text{TiO}_2$ ,  $\text{SnO}_2$ ,  $\text{ZnS}$  and  $\text{ZnO}$ ) are useful for creating the desired anti-reflection (Granqvist, 1991; Granqvist, 1984; Valkonen and Ribbing, 1984; Mbise, *et. al.* 1997).

In a cold climate, it is frequently the case that the window causes an undesired loss of energy, and hence space conditioning demands heating. It is thus energy effective to find ways and means of decreasing the heat losses. One of the ways of doing this is to diminish heat loss through convection. This can be done through use of multiple glazed windows incorporating one or more slabs essentially still gas. Diminishing the thermal radiation can further lower the heat transfer. Low thermal emittance can easily be achieved through suitable window coating (Granqvist, 1991; Granqvist, 1984; Mbise, 1989; Valkonen and Ribbing, 1984).

*Energy window* is the name given to those windows that display a low thermal emittance. These types of windows are preferably for cold climates since they reflect the thermal radiation  $3000 < \lambda < 10000\text{nm}$  and they usually have a high solar transmittance  $300 < \lambda < 3000 \text{ nm}$  (Granqvist, 1991). A good example of *energy window* is transparent infrared reflector. Two different types of coatings can be used to provide a low thermal emittance: an extremely thin metal film embedded between high refractive index dielectric layers with thickness chosen so as to maximize solar transmittance ( $T_{\text{sol}}$ ), and certain heavily doped oxide semiconductor layers. Examples include  $\text{SnO}_2$  doped by F or Sb,  $\text{In}_2\text{O}_3$  doped by Sn, and  $\text{ZnO}$  doped by Al (Granqvist, 1991; Granqvist, 1984; Mbise, 1989; Ling and Cheng, 1987; Valkonen and Ribbing, 1984; Mbise, *et. al.* 1997). The possible causes of degradation in these climates are: extreme cold weather, permafrost, rainy, etc.

The above two types of coatings are of great value for energy efficient windows. However, they suffer one major drawback in that their properties are static. In a temperate climate, these types of windows are not suitable. Such climate requires window coatings which can adjust according to variable demands on heating and lighting during the day or season.

A dynamic window coating popularly known as *smart window* is suitable for temperate climate. The "classes" of smart windows include: Photochromic (cf. those whose optical properties are dependent on irradiation); thermochromic (cf. those whose properties are dependent on temperature); and electrochromic (cf. those whose properties change in response to strength and direction of an applied electric field). (Granqvist, 1984; Granqvist, 1991; Granqvist, 1995; Mbise, 1989).

This work is devoted to particular design of static energy efficient window, that is multilayer coatings exhibiting angular dependent transmittance. Such coatings, which we discuss in the next section, fall under solar control window category and therefore are suitable for tropical climates.

## 2.5 Protection for Film

In many of the striking developments in multilayer technologies, little attention is often paid to film properties other than those needed to fulfill the optical requirements. A feature of considerable practical importance, if coatings were to be used outside the conducive environment of the laboratory, is the resistance of such coatings to degradation by the harsh elements of ordinary atmosphere.

The anti-reflectance coating, apart from their use to enhance transmittance in multilayer optical system, they are also used as protective overlayer (Ling and Cheng, 1987). Certain optical glasses have a poor resistance to atmospheric degradation. The aluminium films used in reflecting telescope are found to deteriorate with time unless some protection is applied (Heavens, 1965). The rate of deterioration is particularly high in coastal neighborhoods where salt-laden atmospheres are common.

In one of the stability studies reported (Heavens, 1965) for the protection of aluminium mirrors, the Al - SiO multilayer was subjected to (i) extended heating in air to 400 °C and (ii) boiling in 5% salt solution for one hour. It was found that, after subjecting the samples to

these severe conditions, the performance of the SiO coated surface improved considerably in terms of increasing the resistance to abrasion of the surfaces. The absorption of the monoxide in the ultraviolet resulted into poor reflectance for the wavelength below 350 nm. The effect was less severe for the films deposited at a lower rate than those deposited at a higher rate, and the absorption decreased on heating the film at 400 °C in air, owing to the conversion of the monoxide into SiO<sub>2</sub>. The prominent effect of the rate of deposition is illustrated in Fig. 2.2. Besides providing protection against atmospheric degradation, silicon monoxide films were found to give improved adhesion if deposited on the mirror blank prior to the deposition of the aluminium film. On the other hand, aluminium oxide overlayer was done by oxidizing the aluminium surface using an anodizing agent. The resulting surface had high resistance to abrasion and fair resistance to contaminating atmosphere. Protection using the latter oxide was found to be inferior to that provided by silicon oxide. Since the aluminium oxide film formed is highly transparent even at wavelength below 250 nm, the optical performance of the aluminium is slightly impaired.

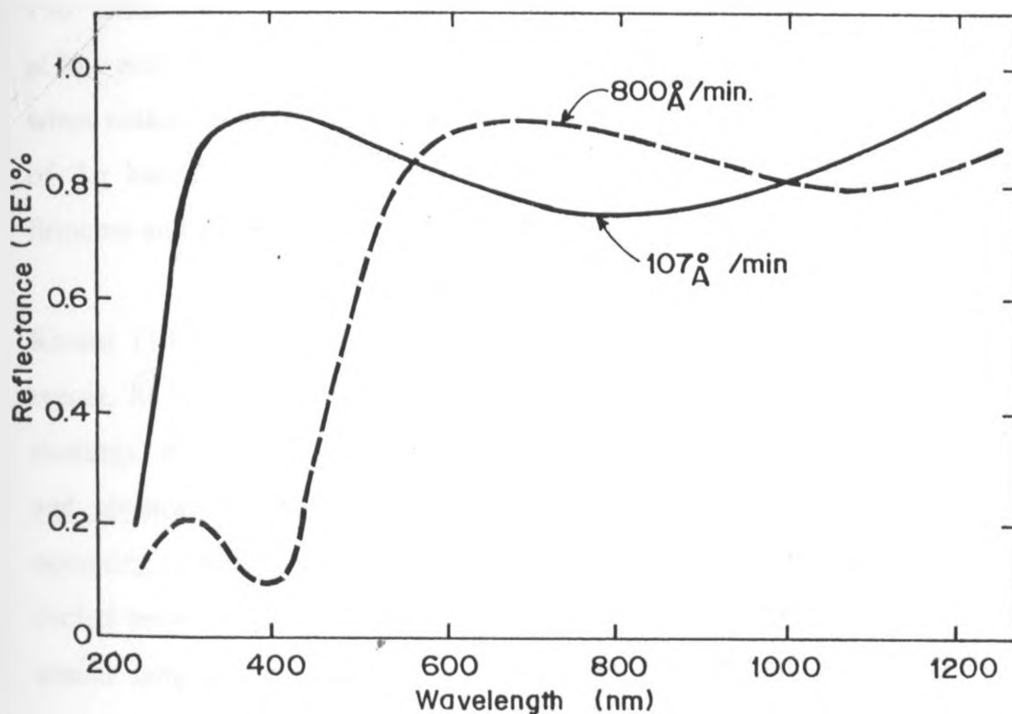


Figure 2.2 Effects of rate of deposition on the reflectance of SiO coated aluminium (Heavens, 1965)

Mbise *et. al.* (1990) have reported findings on environmental stability of optical properties of Ag film and ZnS/ Ag /ZnS multilayer. They found that the stability of the coating depended on several parameters, but more important were the surface cleanliness and vacuum condition during deposition. These results are depicted in figures 2.3 a and b, where it can be observed that, films coated on clean glass substrate were more stable than those coated on uncleaned glass substrate. Furthermore, it should be noted that stability was greatly enhanced for silver films embedded between an anti-reflection coatings which, beside enhancing transmittance, they acted as protection coating to the silver layer.

In a different study, Ling and Cheng (1987) reported studies on stability of two layer coatings, that is, a single metal layer coated with a single anti-reflection layer (c.f. SiO<sub>2</sub>/Cu, SiO<sub>2</sub>/Ag and TiO<sub>2</sub>/Cu). Their study focussed on (i) stability of coating as a function of applied temperature, that is, when coatings are laid up in high and / or low temperature environments, and (ii) when soaked in water. Their report showed that, the spectral properties change very little when coated substrates have been laid up at -40 °C for 24 hrs, at 100 °C for 10 hrs and at 150 °C for 4 hrs. The study showed that the coatings had good stability in transmittance both at low and elevated temperature. They also tested Cu and Ag based films on glass substrates, when soaked in water for 12 hrs, the Cu based coatings were still stable, but soaking stability of Ag based coatings were slightly poorer. Ling and Cheng (1987) suggested that, for firmness and stability, clean substrates and high deposition rate is recommended.

Kivaisi (1976) reported stability studies on selective absorbing thin film coatings. In his report, SiO was used as the anti-degradation material as well as the anti-reflectance for the coatings. A large number of coated samples were tested for possible deterioration of optical and physical properties that may result from medium temperature or humid environment operating conditions. The samples were placed in an oven at atmospheric pressure. They were cycled between room temperature and the desired operating temperature (~240 °C). Other similar samples were placed in a humid chamber. The relative humidity of the chamber varied from 90 to 96% at room temperature (25 °C). They were left in the chamber for period varying from 24 hrs to 168 hrs. After each test, the samples were removed and their reflectances were measured. Table 2.1 shows Kivaisi's results.

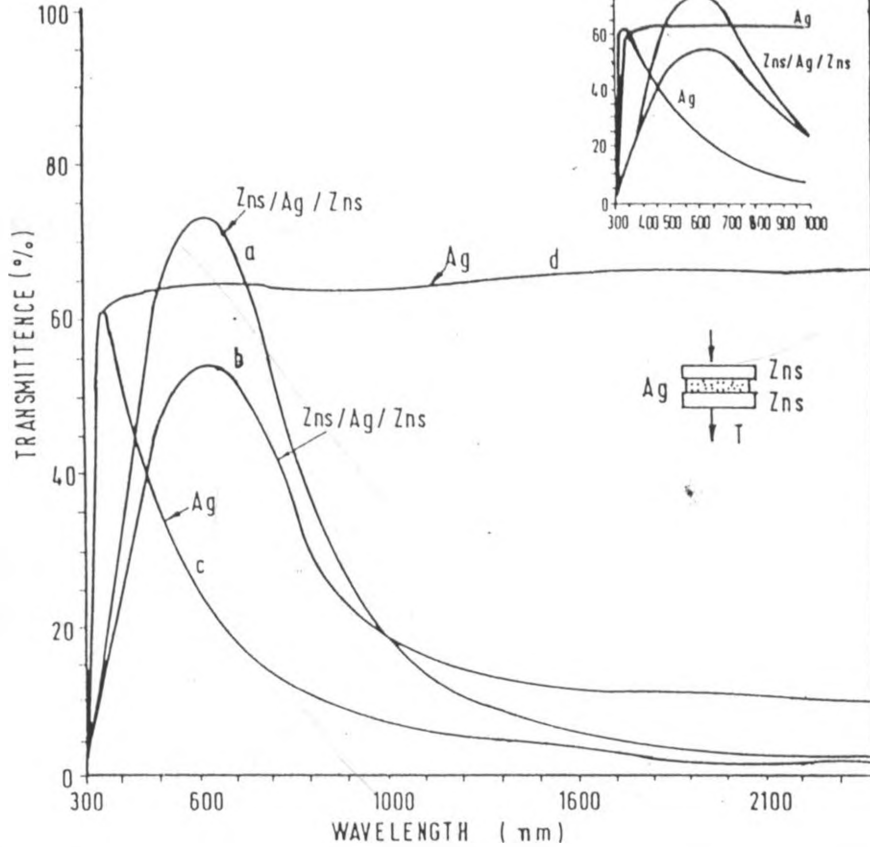


Figure 2.3a Spectral transmittance of Ag and ZnS/Ag/ZnS coatings, deposited on uncleaned substrates. Fresh sample a and c, aged sample b and d. The insert curves are expanded to show the visible region (Mbise, *et. al.* 1990)

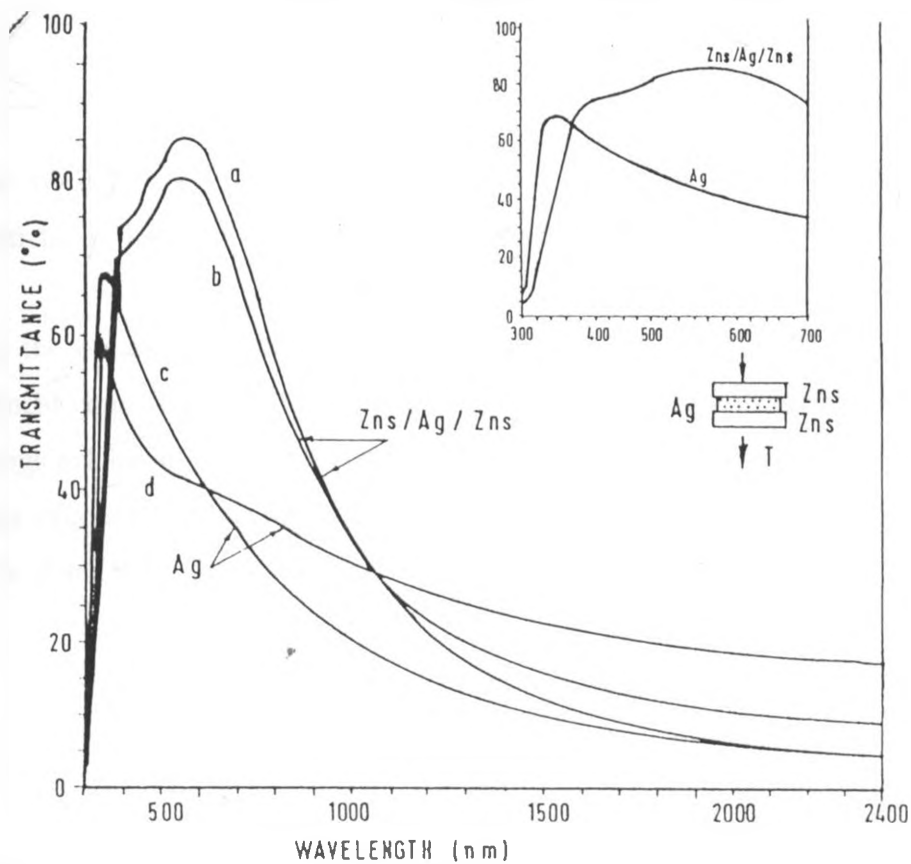


Figure 2.3b Spectral transmittance of Ag and ZnS/Ag/ZnS coatings, deposited on cleaned substrates. Fresh sample a and c, aged sample b and d. The insert curves are expanded to show the visible region (Mbise, *et. al.* 1990)

Table 2.1 Stability of selective coatings in air (Kivaisi, 1976)

Test	Multilayer design	Reflectance of untreated sample %	Reflectance of treated sample %
Heating in air (240° C)	Al-Ge-SiO	79	76
	Ni-Ge-SiO	85	85
	Cr-Ge-SiO	90	93
	Al-PbS-SiO	79	69
	Ni-PbS-SiO	92	88
	Cr-PbS-SiO	94	94
Humidity (90 - 95% RH)	Al-Ge-SiO	79	77
	Ni-Ge-SiO	85	84
	Cr-Ge-SiO	90	90
	Al-PbS-SiO	79	70
	Ni-PbS-SiO	92	88
	Cr-PbS-SiO	94	94

These results revealed that under the given condition, there was very small change in reflectivity of the multilayer coatings; this means that SiO is a good anti-degradation material.

Since the optical properties of thin films changes after long/short duration of exposure to inclement conditions, for this reason, this work is devoted to degradation study of multilayer coatings exhibiting angular dependent transmittance. This type of coating is suitable as static energy efficient window coating. As a window coating it will be exposed to harsh conditions whose changes are sometime drastic, thus the obligation for the study.

## THEORY FOR MULTILAYER COATINGS EXHIBITING ANGULAR DEPENDENT TRANSMITTANCE

### 3.1 Introduction

In this chapter, we describe the theory behind the multilayer coatings exhibiting angular dependent transmittance. Much of it is standard material but for sake of completeness of this work it is worth being included. First we describe the Maxwell's equations for the homogeneous media and then associated Fresnel's equations and the subsequent solutions for unpolarized light are evaluated. The characteristic matrix and the general formula for calculating the quantitative performance parameters are derived towards the end of the chapter.

### 3.2 Maxwell's Equations

In principle, the determination of the amplitudes and intensities of beam of light reflected or transmitted by a thin film(s) on glass is straightforward. The incidence of an electromagnetic (EM) wave upon the interface between two homogeneous media of different optical properties (e.g. glass substrate and air) is followed by the splitting of the EM wave into two waves, namely, the transmitted wave which proceeds into the second medium and the reflected wave which propagates back into the first medium.

The two vectors, namely the electric vector,  $\mathbf{E}$ , measured in electrostatic units and the magnetic induction vector,  $\mathbf{B}$ , measured in electromagnetic units, are used in representing an electromagnetic field. To describe the effect of EM field on material objects, it is necessary to introduce another set of vectors, namely, the electric current density  $\mathbf{J}$  ( $= \sigma\mathbf{E}$ ), the electric displacement  $\mathbf{D}$  ( $= \epsilon\mathbf{E}$ ) and the magnetic vector  $\mathbf{H}$  [ $=$

$(1/\mu)\mathbf{B}]$ . Here  $\sigma$ ,  $\epsilon$  and  $\mu$  are conductivity, dielectric constant, and magnetic permeability, respectively (Heavens, 1965; Born and Wolf, 1975).

For an isotropic medium, the laws of electromagnetism are represented by the Maxwell's equations. These equations (Heavens, 1965; Born and Wolf, 1975) are: -

$$\nabla \cdot \mathbf{D} = \epsilon \nabla \cdot \mathbf{E} = \rho \quad 3.1a$$

$$\nabla \cdot \mathbf{B} = \mu \nabla \cdot \mathbf{H} = 0 \quad 3.1b$$

$$\nabla \times \mathbf{E} = \mu \frac{\partial \mathbf{H}}{\partial t} \quad 3.1c$$

$$\nabla \times \mathbf{H} = \sigma \mathbf{E} + \epsilon \frac{\partial \mathbf{E}}{\partial t} \quad 3.1d$$

where  $\rho$  is the charge density.

If we consider a medium in which there is no space charge, the above equations lead to Maxwell's (2nd order differential) equations representing the propagation of electromagnetic disturbances in the medium

$$\epsilon\mu \frac{\partial^2 \mathbf{E}}{\partial t^2} + \mu\sigma \frac{\partial \mathbf{E}}{\partial t} = \nabla^2 \mathbf{E} \quad 3.2a$$

$$\epsilon\mu \frac{\partial^2 \mathbf{H}}{\partial t^2} + \mu\sigma \frac{\partial \mathbf{H}}{\partial t} = \nabla^2 \mathbf{H} \quad 3.2b$$

The above equations are valid for regions of space throughout which the physical properties of the medium characterized by  $\epsilon$  and  $\mu$  are continuous (Heavens, 1965).



### 3.3 Boundary Conditions

Since in multilayer coatings the physical or/ and optical properties of the coating materials are different and change abruptly across one or more surfaces, all the vectors thus mentioned above are expected to be discontinuous.

We need to consider boundary conditions that apply across these abrupt changes in optical or/ and physical properties that apply to multilayer coatings.

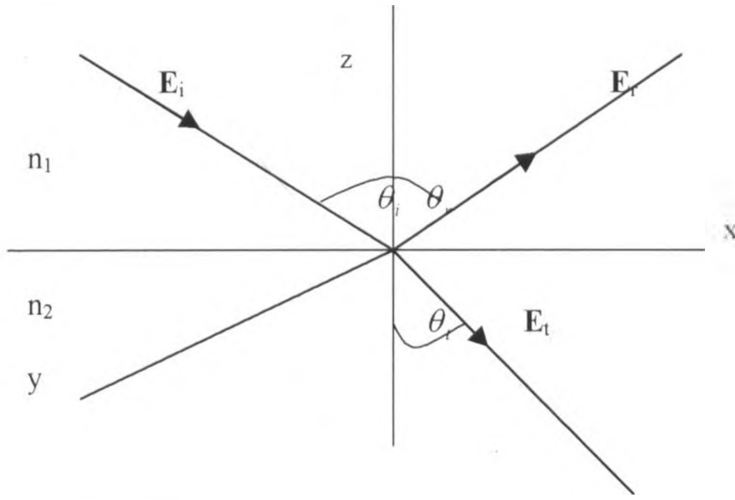


Fig. 3.1. Light path passing from a less dense medium into denser medium; the incidence, reflected and transmitted rays and angles are indicated.

Figure.3.1 illustrates the path taken by a light wave moving from one medium into another (e.g. from air into film). If we let  $\hat{n}$  to be the normal unit vector for the boundary, oriented out of the second medium, then the boundary conditions demand that the normal component should behave (subscript denote the media as shown in Fig.3.1) as

$$\hat{n} \cdot (\mathbf{B}_2 - \mathbf{B}_1) = 0 \quad 3.3$$

which is equation of continuity, meaning that the magnetic induction is continuous across the surface of discontinuity, and

$$\hat{n} \cdot (\mathbf{D}_2 - \mathbf{D}_1) = \rho \quad 3.4$$

That is, the presence of a layer of surface charge density, on the surface of discontinuity, leads to an abrupt change in the normal component of the electric displacement by the amount equal to  $\rho$ .

The tangential components of the electric vector should behave as

$$\hat{n} \times (\mathbf{E}_2 - \mathbf{E}_1) = 0 \quad 3.5$$

which is also another continuity equation, implying that the tangential component of the electric vector should be continuous across the surface while

$$\hat{n} \times (\mathbf{H}_2 - \mathbf{H}_1) = \mathbf{J} \quad 3.6$$

Equation 3.6 implies that, the presence of a surface with current density  $\mathbf{J}$  (considered to be a vector quantity), the tangential component of the magnetic vector should change abruptly; its discontinuity is given by  $\mathbf{J} \times \hat{n}$  (Heavens, 1965; Born and Wolf, 1975).

### 3.4 Fresnel's Equations for Angle Dependent Coatings

Applying the boundary conditions deduced in the previous section, we obtain equations that may be solved to give the amplitudes of the transmitted and reflected vectors in terms of those of the incident vectors. Denoting incident and transmitted waves by the subscripts  $i$  and  $t$ , respectively, we obtain

$$r_{2p} = \frac{\mathbf{E}_{rp}}{\mathbf{E}_{ip}} = \frac{n_1 \cos \theta_i - n_2 \cos \theta_t}{n_1 \cos \theta_i + n_2 \cos \theta_t} \quad 3.7a$$

$$r_{2s} = \frac{\mathbf{E}_{rs}}{\mathbf{E}_{is}} = \frac{n_1 \cos \theta_i - n_2 \cos \theta_t}{n_1 \cos \theta_i + n_2 \cos \theta_t} \quad 3.7b$$

$$t_{2p} = \frac{\mathbf{E}_{tp}}{\mathbf{E}_{ip}} = \frac{2n_1 \cos \theta_i}{n_1 \cos \theta_i + n_2 \cos \theta_t} \quad 3.7c$$

$$t_{2s} = \frac{\mathbf{E}_{ts}}{\mathbf{E}_{is}} = \frac{2n_1 \cos \theta_i}{n_1 \cos \theta_i + n_2 \cos \theta_t} \quad 3.7d$$

where  $\theta_i$  and  $\theta_t$  are the angles of incident and angles of transmission respectively, while  $n$  is the refractive index,  $r_{2s}$ ,  $r_{2p}$  are known as the Fresnel reflection coefficient and  $t_{2s}$ ,  $t_{2p}$  the Fresnel transmission coefficient. The subscript  $s$  and  $p$  denote the perpendicular and parallel plane of polarization.

It should be noted, that  $\epsilon_j = n_j^2$  since  $\mu = 1$  at optical frequencies.

We now apply the above Fresnel's relations to determine the optical properties of a thin film on a transparent substrate.

Let us consider the schematic diagram shown in Fig.3.2. Let 1 denote the medium surrounding the coated substrate; 2 to denote the film of thickness  $d$  and 3 to denote the substrate. If the effect of the backside of the substrate is ignored, the amplitude coefficient for reflectance,  $r_2$ , and transmittance,  $t_2$ , of the film are obtained from

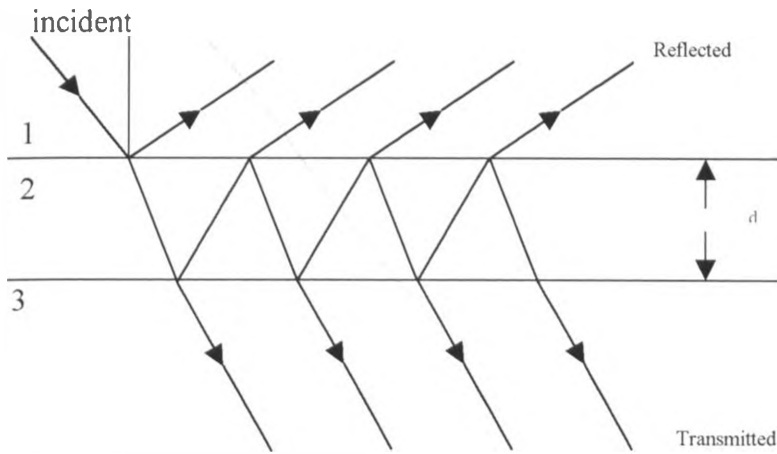


Fig.3.2. The path of light ray passing from air, across the film into the air or another medium of refractive index less than that of the film.

$$r_2^f = \frac{r_{12} + r_{23}e^{2i\delta_2}}{1 + r_{12}r_{23}e^{2i\delta_2}} \quad 3.8$$

and

$$t_2^f = \frac{t_{12} + t_{23}e^{i\delta_2}}{1 + r_{12}r_{23}e^{2i\delta_2}} \quad 3.9$$

where  $\delta_2$  represents the change in phase of the beam on traversing the film and is given by  $\delta_2 = \frac{2\pi}{\lambda} n_2 d \cos\theta_2$  and the superscript  $f$  signify light incident from the front-side.

The relations shown above are applicable for unpolarized light. Those for s and p polarized light as well as for light incident onto the substrate from the backside take the form shown above by equation (3.8) and (3.9) (Granqvist, 1991; Heavens, 1965; Mbise, 1989).

Since we have considered a wave of unit amplitude (and not unit energy) the reflectance and transmittance (defined as ratios of reflected and transmitted energy to the incident energy) are given by (Heavens, 1965; Born and Wolf, 1975):

$$R = \frac{r_{12}^2 + 2r_{12}r_{23} \cos 2\delta_2 + r_{23}^2}{1 + 2r_{12}r_{23} \cos 2\delta_2 + r_{12}^2 r_{23}^2} \quad 3.10$$

$$T = \frac{n_3}{n_1} \frac{t_{12}^2 t_{23}^2}{1 + 2r_{12}r_{23} \cos 2\delta_2 + r_{12}^2 r_{23}^2} \quad 3.11$$

If the substrate is transparent, and if the backside effects are considered, a more complicated situation exists, and multiple reflections in the substrate as shown in Fig.3.2 must be taken into account.

The final expression for the reflectance and the transmittance are given by the following expressions (Granqvist, 1991; Born and Wolf, 1975).

$$R = \frac{R_2^f - R_3(R_2^f R_2^b - T_2^f T_2^b)}{1 - R_2^b R_3} \quad 3.12$$

$$T = \frac{T_2^f T_3}{1 - R_2^b R_3} \quad 3.13$$

where  $R_3 = |r_{31}|^2$  and  $T_3 = \frac{n_3}{n_1} |t_{31}|^2$ , and  $R_2^b(R_2^f)$  denoting reflectance at the film interface for light coming from the back (front) of the film; similar notation (i.e.

$T_2^f$  and  $T_2^b$ ) is used for transmittance. The subscript, 1,2 and 3 signify the medium in which the wave is traversing (Palik, 1985; Granqvist, 1991).

The treatment above can easily be generalized to multiple layer films (Heavens, 1965; Born and Wolf, 1975). Among the various techniques used for multilayer (Heaven, 1965), the characteristic matrix technique is discussed in the next section.

### 3.5 The Characteristic Matrix of a Homogeneous Media

A stratified medium is a medium whose characteristics are constant throughout each plane perpendicular to a fixed direction. If the z-axis of a Cartesian reference system is taken along this special direction, then  $\varepsilon = \varepsilon(z)$  and  $\mu = \mu(z)$

For a homogeneous film  $\varepsilon$  and  $n = \sqrt{\varepsilon}$  are constant. If  $\theta$  denotes the angle which the normal to the wave makes with the z -axis, through a simple algebraic manipulation, the characteristic matrix for s-polarized wave is given by (Born and Wolf, 1975).

$$\mathbf{M} = \begin{pmatrix} \cos(knz \cos\theta) & -\left(\frac{i}{\alpha}\right) \sin(knz \cos\theta) \\ -i\alpha \sin(knz \cos\theta) & \cos(knz \cos\theta) \end{pmatrix} \quad 3.14$$

where  $k = \frac{\omega}{c} = \frac{2\pi}{\lambda}$  with  $\omega$  and  $c$  denoting frequency of the radiation and speed of light respectively, and  $\alpha = \sqrt{\varepsilon} \cos\theta$ . For a p-polarized wave, all the equations and the same characteristic matrix holds, with  $\alpha$  replaced by  $\beta = \sqrt{(1/\varepsilon)} \cos\theta$ .

After evaluating all the elements  $m_{ij}$  for  $z = z_1$  of the characteristic matrix

$\mathbf{M} = \begin{pmatrix} m_{11} & m_{12} \\ m_{21} & m_{22} \end{pmatrix}$  of a given stratified medium, the expression for the reflection and transmission coefficient of the film are given by (Born and Wolf, 1975; Granqvist 1991)

$$r = \frac{(m_{11} + m_{12}\alpha_l)\alpha_1 - (m_{21} + m_{22}\alpha_l)}{(m_{11} + m_{12}\alpha_l)\alpha_1 + (m_{21} + m_{22}\alpha_l)} \quad 3.15$$

$$t = \frac{2\alpha_l}{(m_{11} + m_{12}\alpha_l)\alpha_1 + (m_{21} + m_{22}\alpha_l)} \quad 3.16$$

where  $l$  and  $l$  denote the first and the last medium respectively (Born and Wolf, 1975). In terms of  $r$  and  $t$  the reflectivity and transmissivity are given by (Born and Wolf, 1975; Granqvist, 1991)

$$R = |r|^2 \quad \text{and} \quad T = \frac{\alpha_l}{\alpha_1} |t|^2 \quad 3.17$$

### 3.6 Quantitative Performance Parameters

Having calculated the reflectivity and transmissivity of a multilayer, it is also desirable to specify suitable performance parameters which indicate how far off a window coating is from certain design goals. The various types of average properties commonly used as figures of merit for the glazing system can be calculated using the general equation (Rubin, *et. al.*, 1998).

$$P_q = \frac{\int_a^b P(\lambda)\Phi_q(\lambda)d\lambda}{\int_a^b \Phi_q(\lambda)d\lambda} \quad 3.18$$

Where P is the measured spectral radiometric property such as reflectance or transmittance; q denotes the type of average taken (cf. solar or luminous);  $\Phi$  is the weighing function for the strength of source (sunlight or thermal radiation) under appropriate condition at each wavelength,  $\lambda$ . In this work data for AM1.5 irradiance, ISO 9845 were used for solar, whereas CIE D65 illuminant ISO/CIE 10526 data were used for luminous performance evaluation, and finally, a,b is the practical wavelength limit (cf. a = 300 nm, b = 2500 nm for solar; a = 380 nm; b = 780 nm for luminous)

The above formula in equation 3.18 is utilized using a computer programme to obtain the integrated luminous\* (transmittance and reflectance) and solar\* (transmittance and reflectance) as detailed in appendix B page 91.

\*Integrated luminous/ solar: this is the calculated area under the curve and normalized using standard data that is ISO 9845 and ISO/CIE 10526.



## **EXPERIMENTAL TECHNIQUES**

### **4.1 Introduction**

In this chapter, we describe the experimental techniques that were followed in: fabricating, thickness measurement, characterization of angular dependency and studying optical (transmittance and reflectance) degradation of multilayer coatings.

### **4.2 Cleaning the Substrate**

The substrates were 1 mm thick ordinary microscope glass slides of dimensions 76 cm × 26 cm which could withstand high temperature (~ 500 °C).

The following are the cleaning steps that were followed in this work.

1. The substrates were soaked in a warm soap solution for 5 to 10 minutes.
2. The substrates were degreased using a soapy soft cotton wool by gently drag wiping the surface to avoid any possible scratch marks.
3. When satisfied that the substrates were properly degreased, they were then rinsed using distilled water.
4. The substrates were hang in a rack and immersed into distilled water in a beaker. The beaker was then hang in ultrasonic bath (Model Decon FS 300). The ultrasonic cleaning was done for 20 minutes.

5. Step 4 above was repeated, but with distilled water replaced by 99.8% pure ethanol.
6. After ultrasonic cleaning, the rack and substrates were transferred and suspended over a boiling ethanol in another beaker and rinsed. Thus the ethanol vapour would pass over the substrates surfaces to finely rinse them.
7. The substrates still standing on the rack, were either transferred into a dessicator for storage or were mounted onto the substrate holder in the deposition chamber.

### 4.3 Deposition of the Films

The samples were fabricated by resistive evaporation using Edward's high vacuum coating system (Model E306A). The system is equipped with Edwards E04 diffusion pump and a modern high performance direct drive E2M8 rotary pump. The system is also equipped with Pirani-Penning gauge combination that was used to monitor pressure inside the chamber.

The system has special features that are meant to ensure vacuum chamber contamination is kept to negligible proportion. These features include: -

1. Liquid nitrogen trap, which is located between the diffusion pump and the high vacuum valve. This trap is meant to capture migrating oil vapour and also provides considerable pumping speed for condensable vapours.
2. Fluoro-elastomer chamber seals and low outgassing construction materials, such as stainless steel, make a major contribution to contamination free conditions.
3. Vacuum brazing and non-decay welding techniques have been used for construction of the pumping stalk.

2 2

The base of the coating system is fitted with a circular plate that can hold up to four hearths. Therefore, it is possible for four different materials to be evaporated one at a time, thus making it possible to coat different layer combination without breaking the vacuum.

The evaporants used are shown in Table 4.1. Note that different hearths were used due to different melting points of the different evaporants.

Table 4.1. Material used in this work, their purity and the type of hearth used

Evaporant	Form of evaporant	Purity of evaporant material	Hearth	Hearth's material
MgF <sub>2</sub>	Granules	99.99%	Boat	Molybdenum
Ag	Pellets	99.99%	Boat	Molybdenum
TiO <sub>2</sub>	Granules	99.99%	Boat	Molybdenum
Al	Wire rods	99.99%	Basket	Tungsten

Prior to deposition of the coating, the evaporant material was well soaked by heating it for 3-5 minutes at temperatures close to its melting point. This process aims at degassing the adsorbed gas or impurities from the surface of the source, as well as the boat and other parts of the deposition chamber.

During the soaking process, the pressure in the chamber was slightly going up. To prevent any possible deposition during the soaking process, (or after the desired film thickness has been deposited) the coating system is equipped with a large shutter that is located approximately 5 cm above the evaporant source, while the substrate were positioned ~17.5 cm above the evaporant source.

The ultimate background pressure attained was about  $2.4 \times 10^{-6}$  mbar. During deposition process, the pressure could slightly go up sometimes reaching  $\sim 2 \times 10^{-4}$  mbar.

mbar. The rate of deposition was kept in the range of  $4.5 < r < 6 \text{ \AA/s}$  and  $25 < r < 30 \text{ \AA/s}$  for metals (Ag, Al), for the dielectric ( $\text{MgF}_2$ ), respectively. It should however be noted that the rate of deposition of  $\text{TiO}_2$  was slightly lower in the range of  $6 < r < 10 \text{ \AA/s}$ . The rate of deposition as well as the thickness of the film was controlled by a quartz crystal monitor attached to the system.

#### 4.4 Optical Characterization

The optical properties of the samples were studied by using the Perkin Elmer Lambda 9 spectrophotometer. This is a double beam instrument covering the ultraviolet, visible and near infrared spectral regions.

The instrument is quite accurate and has good resolution provided that initialization procedures, including background correction, are performed prior to actual measurement's are taken.

Each sample was carefully cut into two equal pieces using a sharp diamond glasscutter, and assuming the coating is isotropic, one piece was kept as reference and the other piece was subjected to ageing treatment. Different post treatments were performed for different samples, as detailed in section 4.5.

The spectrophotometry analysis was done before and after treatment of the samples. A large amount of data for transmittance and reflectance were obtained and plotted on the same axes for each sample. The transmittance data were obtained for normal incident beam and for light incident at an oblique angle of  $50^\circ$  onto the sample. Reflectance data were obtained for near normal (i.e.  $15^\circ$ ) incident beam and for light incident at an oblique angle of  $50^\circ$ . Spectrophotometry was done in the 300 nm to 2500 nm wavelength range. The data collected was later analyzed using a computer program given in page 90.

## 4.5 Ageing Treatment

This section summarizes the various ageing treatment methods employed in this study. The approach was performed either in (i) accelerated test – whereby the factors leading to degradation were elevated to extreme (ii) non-accelerated test – whereby factors leading to degradation were let to take their natural course.

### 4.5.1 Elevated Temperatures

The effect of extreme high temperature was investigated by heating the samples in air in an oven at fixed temperatures. The temperature inside the oven was monitored using an in-built digital thermometer with an accuracy of  $\pm 1$  °C. The thermometer was calibrated prior to actual measurements.

1. A number of samples were heated for periods ranging from 12 hrs to 120 hrs in an oven maintained at 50 °C.
2. A number of samples were heated for periods ranging from 12 hrs to 120 hrs in an oven maintained at 100 °C.
3. A number of samples were heated for periods ranging from 12 hrs to 120 hrs in an oven maintained at 200 °C.

Two pieces were kept as references for each of 1, 2 and 3 above.

### **4.5.2 Low Temperatures**

The effect of low temperature was studied by laying the samples inside the freezer compartment of the convectional refrigerator. The temperature inside the freezer was monitored by using an analog in-built thermometer with an accuracy of about  $\pm 1$  °C. The thermometer was calibrated prior to taking actual measurements. Before any samples were exposed to low temperature environment, the freezer was first let to stabilize at the set temperature.

1. A number of samples were laid in a freezer maintained at  $-10$  °C for periods ranging from 1 week to 12 weeks
2. A number of samples were laid in a freezer maintained at  $-18$  °C for periods ranging from 1 week to 12 weeks
3. A number of samples were covered in frost (ice) at  $-20$  °C for 12 weeks

Two pieces were kept as references for each of 1,2 and 3 above.

### **4.5.3 Humid Environment**

The samples were kept in compartment of controlled humidity. The following ingenious method was devised to simulate and maintain the humidity at derived percentages. Given masses of sodium hydroxide (NaOH) or calcium chloride (CaCl) when mixed with given volume of water, can give constant humidity if the temperature of the ambient does not fluctuate much (Rugumamu, 2001). The derived percentages are shown in Table 4.2.

Table 4.2 Concentration of graded solution used to maintain the atmosphere at constant humidity at  $29^{\circ}\text{C} \pm 1^{\circ}\text{C}$

Relative humidity %	NaOH gm/100 ml of water	CaCl <sub>2</sub> gm/100ml of water.
86	22.88	33.20
84	26.30	37.70
74	32.70	46.50
69	35.90	50.90

An ordinary dessicator was adopted as the container. The humidity was measured using an analog hygrometer (accuracy  $\pm 1\%$  RH), which was suspended inside the dessicator. A vaseline lining was applied on the lid of the dessicator to ensure that it was airtight and outside environment did not interfere with the simulated environment. The above table shows derived humidity's that can be obtained at various concentration of NaOH or CaCl<sub>2</sub>.

A number of samples were exposed in high relative humidity (RH) environment maintained at  $86 \pm 1\%$  RH at  $29 \pm 1^{\circ}\text{C}$  for different durations (viz. 3 weeks to 12 weeks). Four pieces were kept as references.

#### 4.5.4 Saline Solution

The effect of saline solution was investigated by soaking the samples in salt (NaCl) solution of concentration 20gm/100ml.

A number of samples were soaked in the salt solution for different duration viz. 5 hrs, 24 hrs and 2 weeks; and 2 pieces were kept as references. In each case before any spectral characterization were done, the samples were exposed to dry in air for duration of 8 hrs.

#### **4.5.5 Organic Solvents**

The effect of organic solvents on multiplayer films was investigated by using acetone and absolute ethanol. The two solvents were both of purity 99.8%. The study is as detailed below.

A number of samples were soaked in acetone and others in absolute ethanol for duration ranging between 12 hrs to 96 hrs respectively. In each case, the samples were exposed in air to dry for duration of 8 hrs before any optical characterizations were done.

#### **4.5.6 Outdoor Environment**

The effect of atmospheric conditions was studied by exposing the samples in outdoor environment. The samples were strategically placed on rooftop where they could not be blown away by wind. A number of samples were exposed for different durations ranging from 2 weeks to 12 weeks. 4 pieces were kept as references. In between the durations of exposure (i.e. 2 weeks, 4 weeks and 12 weeks) the samples were taken to the laboratory and spectral analysis done and then returned back. Atmospheric humidity ranged around  $60 \pm 1\%$  RH to  $70 \pm 1\%$  RH, while the temperature ranged between 20 – 34 °C.

#### **4.5.7 Aquatic Condition**

The effect of water on the coated samples was investigated by keeping a number of samples submerged in distilled water for 48 hrs to 3 weeks. All samples kept in water for duration longer than 48 hrs were being cycled between aquatic condition and dry environment for 8 hrs; 2 pieces were kept as references.



## RESULTS AND DISCUSSION

### 5.1 Introduction

This chapter summarizes the findings of this work. The quantified graphical presentations of the results have been discussed, citing possible factors thought to have attributed to degradation.

The study findings are presented for different degradation tests done on different samples, for given range of time. Initially layer combination that gives the best optical characteristics was determined. The desired optical characteristics are: the samples should transmit substantially in the luminous region, that is 400 nm to 700 nm wavelength; the samples should be able to block most of the near infrared region; and finally, the samples should possess substantial angular performance (defined in page 1). The layer combinations that were studied with their respective thickness combination starting from the topmost layer included:  $\text{MgF}_2/\text{Ag}/\text{MgF}_2$  (240/12/340 nm);  $\text{MgF}_2/\text{Al}/\text{MgF}_2$  (220/12/340 nm);  $\text{TiO}_2/\text{Ag}/\text{TiO}_2$  (240/12/340 nm) and  $\text{TiO}_2/\text{Al}/\text{TiO}_2$  (340/12/220 nm). The layer thicknesses had theoretically been optimized by the authors predecessor (Mbise, 1995).

The  $\text{MgF}_2/\text{Ag}/\text{MgF}_2$  coating out performed the other layer combination (based on the above criteria) and therefore was chosen to be used for degradation studies. The findings for  $\text{MgF}_2/\text{Ag}/\text{MgF}_2$  multilayer are discussed in section 5.2. The  $\text{MgF}_2/\text{Al}/\text{MgF}_2$  and  $\text{TiO}_2$  based multilayer coatings are discussed in sections 5.3 and 5.4, respectively.

## 5.2 Degradation Studies

Below is detailed description of the results obtained from various degradation tests on  $\text{MgF}_2/\text{Ag}/\text{MgF}_2$  based multilayer coatings. The wavelength integrated solar optical properties have been obtained from the graphical spectral data obtained empirically.

### 5.2.1 Elevated Temperatures

The physical appearance of the samples annealed at the temperatures and durations specified in section 4.5.1 (page 33) remained pale blue in colour for the whole duration they were exposed. The spectral data for samples annealed at 50 °C, 100 °C and 200 °C, are given in figures 5.2.1a, 5.2.1b and 5.2.1c, respectively.

The wavelength integrated luminous transmittance data are given in figures 5.2.1aa,bb and cc, for samples annealed at 50 °C, 100 °C and 200 °C, respectively. These graphs have been extrapolated from the tabulated data given in table A1, A2 and A3 of appendix A, respectively, and they show changes in luminous transmittance with time the samples were exposed in elevated temperatures. The angular performance of respective samples can be found by finding the difference in luminous transmittance between A and C for fresh/reference sample, and between B and D for aged sample. In graphs 5.2.1aa,bb and cc, A and B denotes the oblique incidence transmittance while C and D the normal incidence transmittance.

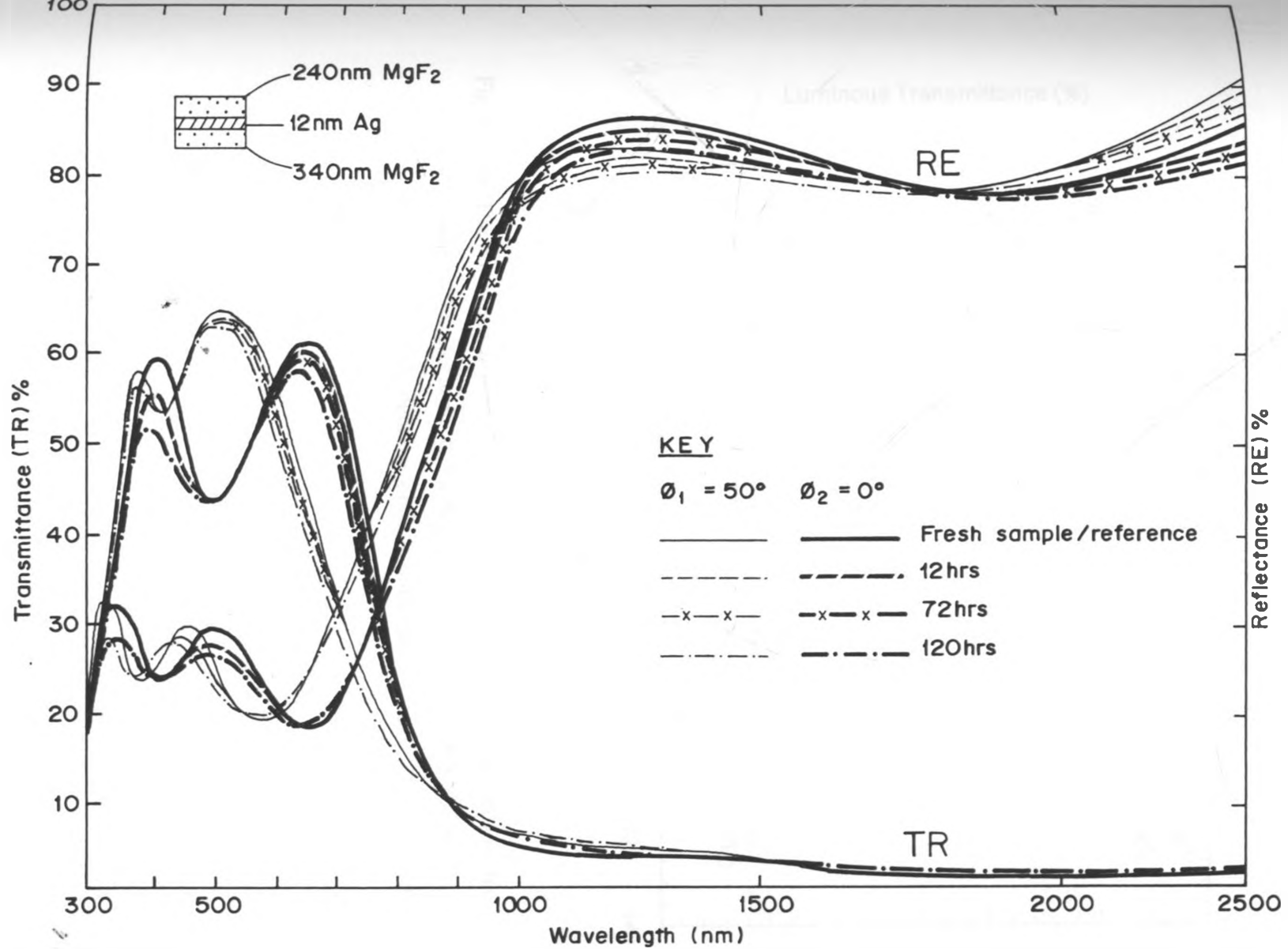


Fig.5.2.1a Spectral transmittance and reflectance of MgF<sub>2</sub>/Ag/MgF<sub>2</sub> multilayer for fresh sample and a sample laid in an oven maintained at  $50^\circ \pm 1^\circ\text{C}$  for indicated duration.

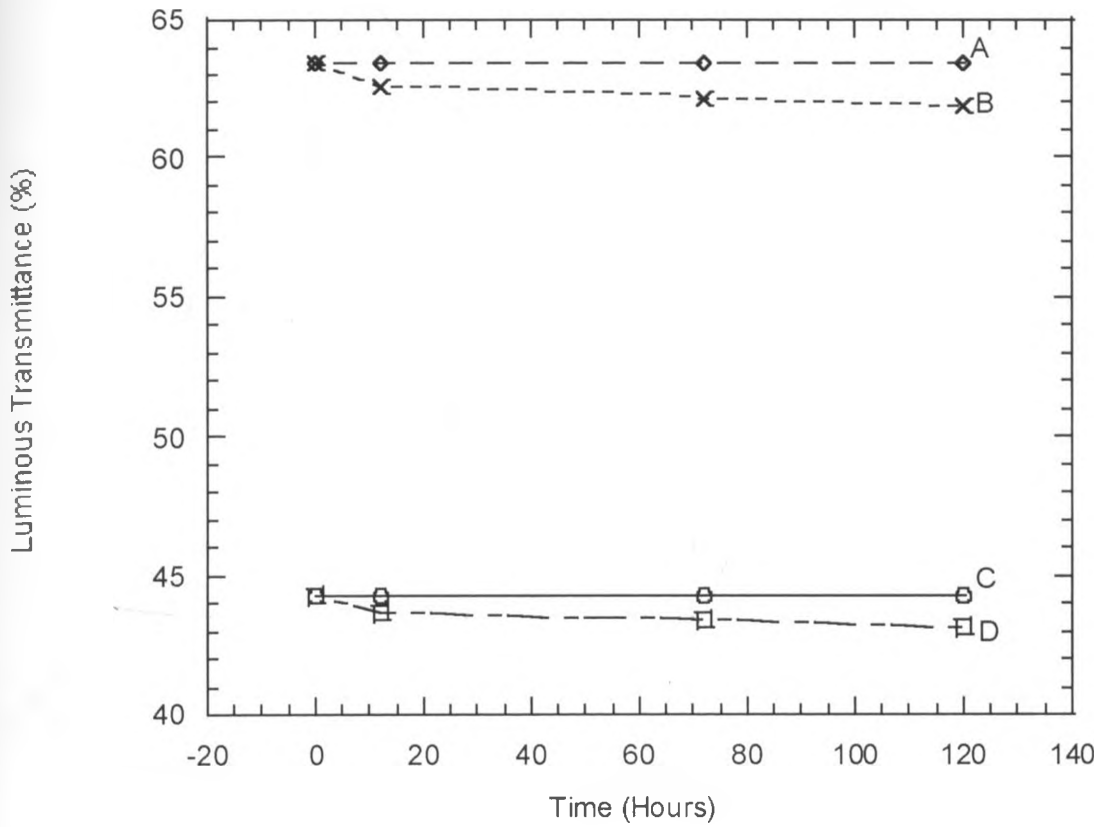


Fig. 5.2. Iaa. The variation with time of wavelength integrated luminous transmittance for samples annealed at 50 °C. Fresh sample A and C; aged sample B and D. (NB. A and B denotes oblique incidence; C and D denotes normal incidence)

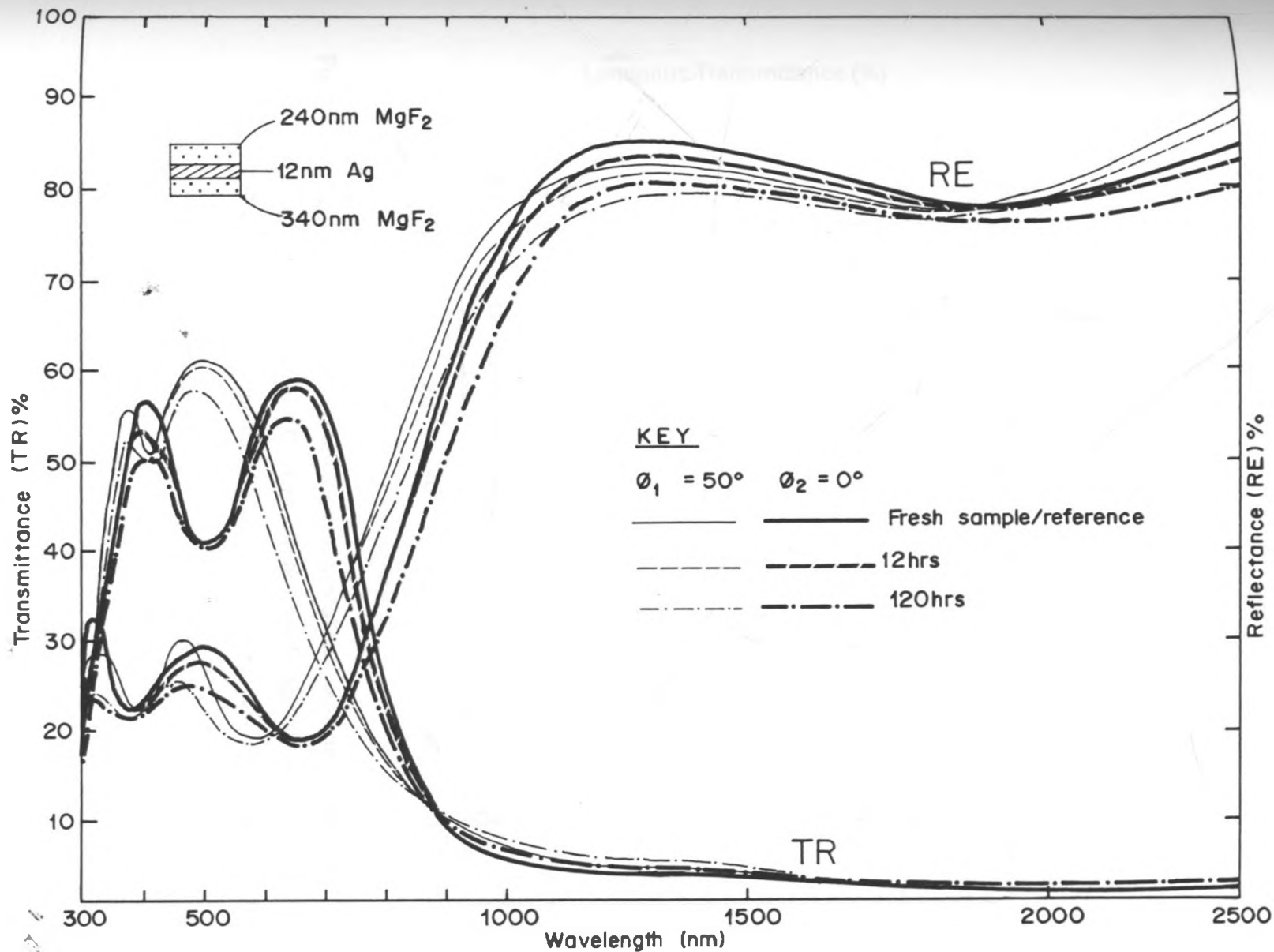


Fig.5.2.1b Spectral transmittance and reflectance of MgF<sub>2</sub> /Ag/MgF<sub>2</sub> multilayer for fresh sample and a sample laid in an oven maintained at  $100 \pm 1^\circ\text{C}$  for indicated duration.

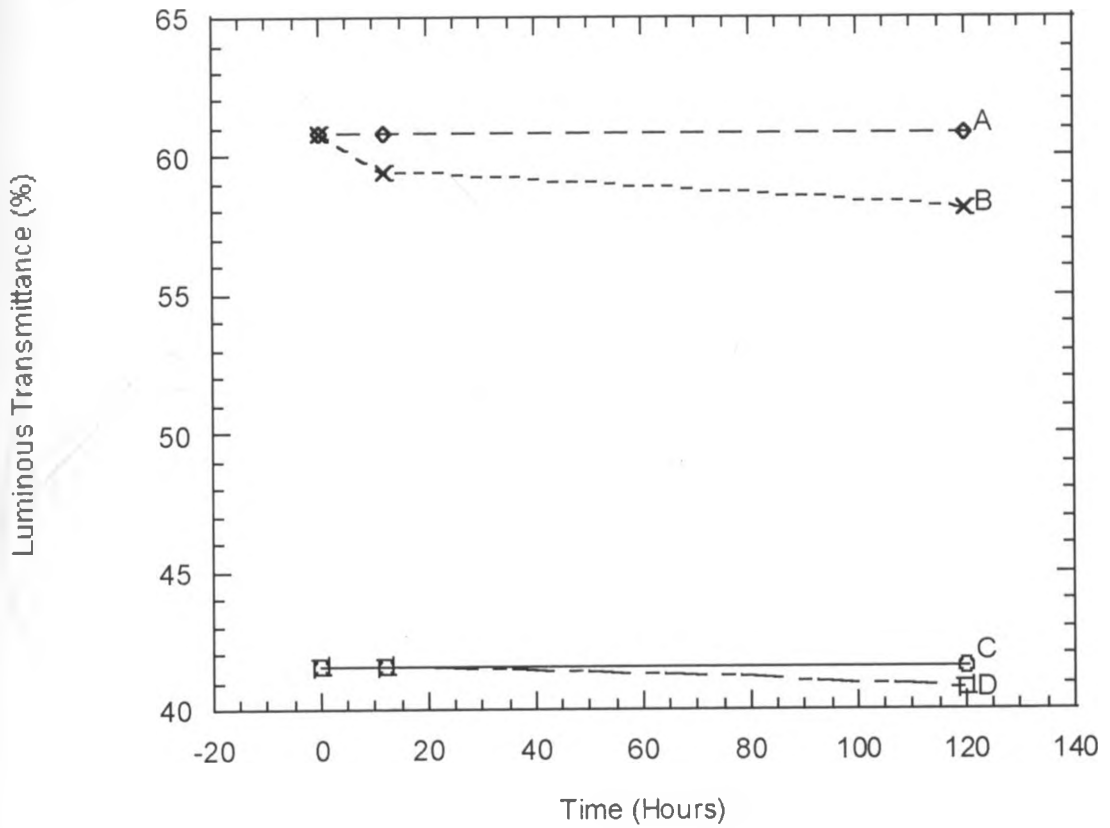


Fig. 5.2.1bb. The variation with time of wavelength integrated luminous transmittance for samples annealed at 100 °C. Fresh sample A and C; aged sample B and D. (NB. A and B denotes oblique incidence; C and D denotes normal incidence)

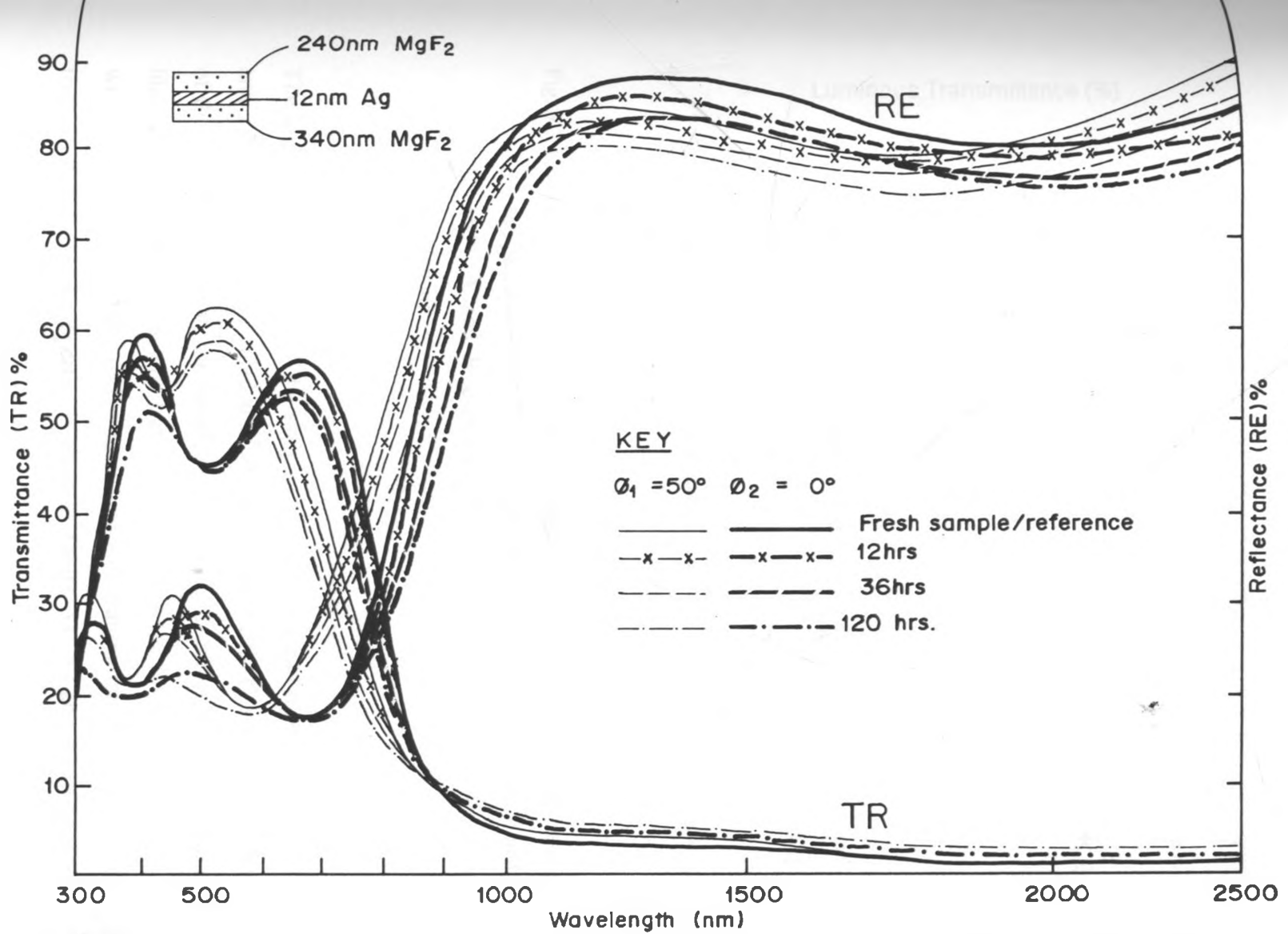


Fig. 5.2.1c Spectral transmittance and reflectance of MgF<sub>2</sub> /Ag/MgF<sub>2</sub> multilayer for fresh sample and sample laid in an oven maintained at  $200 \pm 1^\circ\text{C}$  for indicated duration.

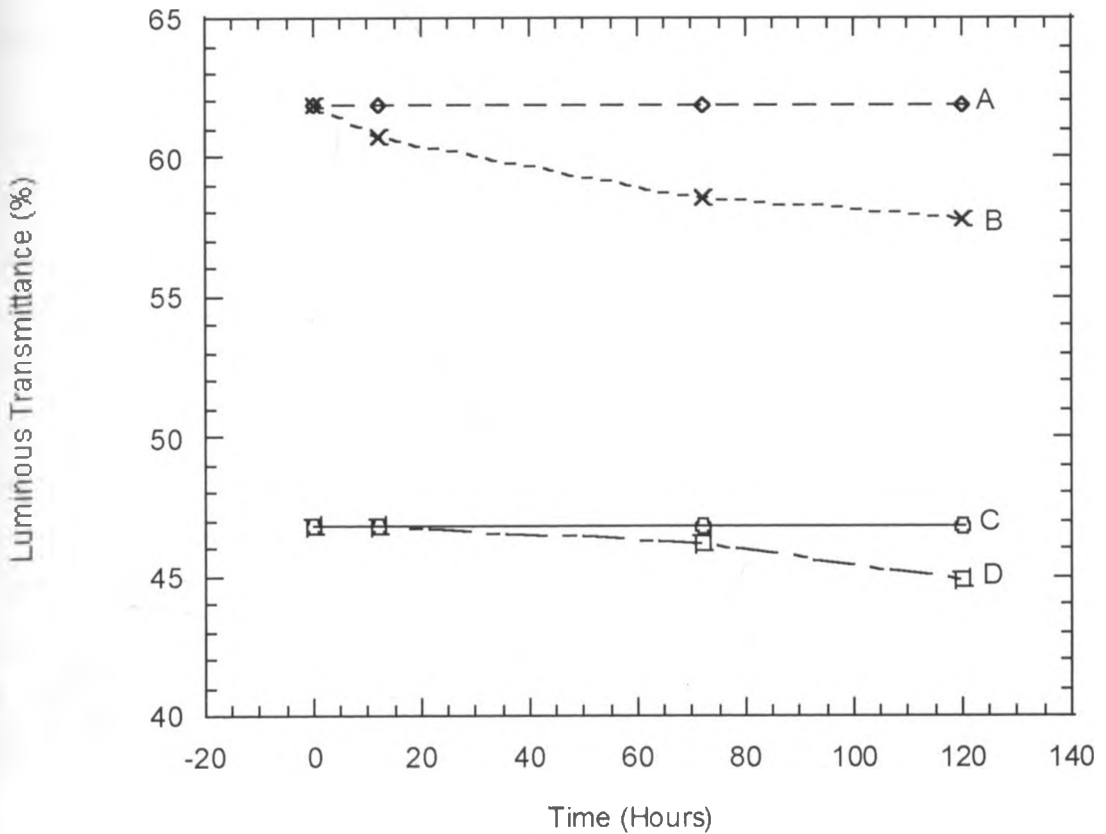


Fig. 5.2.1cc. The variation with time of wavelength integrated luminous transmittance for samples annealed at 200 °C. Fresh sample A and C; aged sample B and D. (NB. A and B denotes oblique incidence; C and D denotes normal incidence)

The angular performance of the samples after 120 hrs had decreased by 0.3%, 1.9% and 2.2% for samples annealed at 50 °C, 100 °C and 200 °C, respectively. An analysis of the results shows that, the samples were not highly affected by annealing since the highest decrement in luminous transmittance was 4.1% for those heated at 200 °C, which represents only 6% of the total luminous transmittance. A detailed tabulated treatise of the optical properties is given in Tables A1, A2 and A3 of appendix A. In



all the samples studied at elevated temperatures, luminous reflectance registered the highest decrement ranging from 3.8% for samples annealed at 50 °C (for 120 hrs) to 7.3% for those annealed at 200 °C (for 96 hrs). The changes observed in samples annealed at temperatures stated, can be regarded as insignificant since they represent a small percentage of the total transmittance/ reflectance under consideration.

The changes observed in spectral properties after the samples were annealed at different temperatures are thought to be because of expansion when the samples were heated and contraction as they cool down to their original state. These changes lead to stresses of considerable magnitude in the films. The main cause of this is the mismatch of the expansion coefficient between the substrate and the multilayer film and even between one layer and another. These stresses eventually affect the packing density, crystallographic structure, rough internal boundaries and other micro-structural properties of the samples (Besancon, 1986; Rubin, *et. al.* 1998; Mbise and Kivaisi, 1993). According to Hoffman (1976), the optical (transmittance and reflectance) changes observed can be reduced even further by depositing the film onto a hot substrate (since this process determines the size of grains of the film) and by post deposition annealing.

### **5.2.2 Low Temperatures**

The spectral data obtained on low temperature tests are given in figures 5.2.2a,b and c, for sample exposed in freezing environment at -10 °C; -18 °C and -20 °C, respectively. Detailed tabulated spectral data is given in Tables A4, A5 and A6 of appendix A. Figures 5.2.2aa,bb and cc gives the variation of luminous transmittance with time as discussed under section 4.5.2.

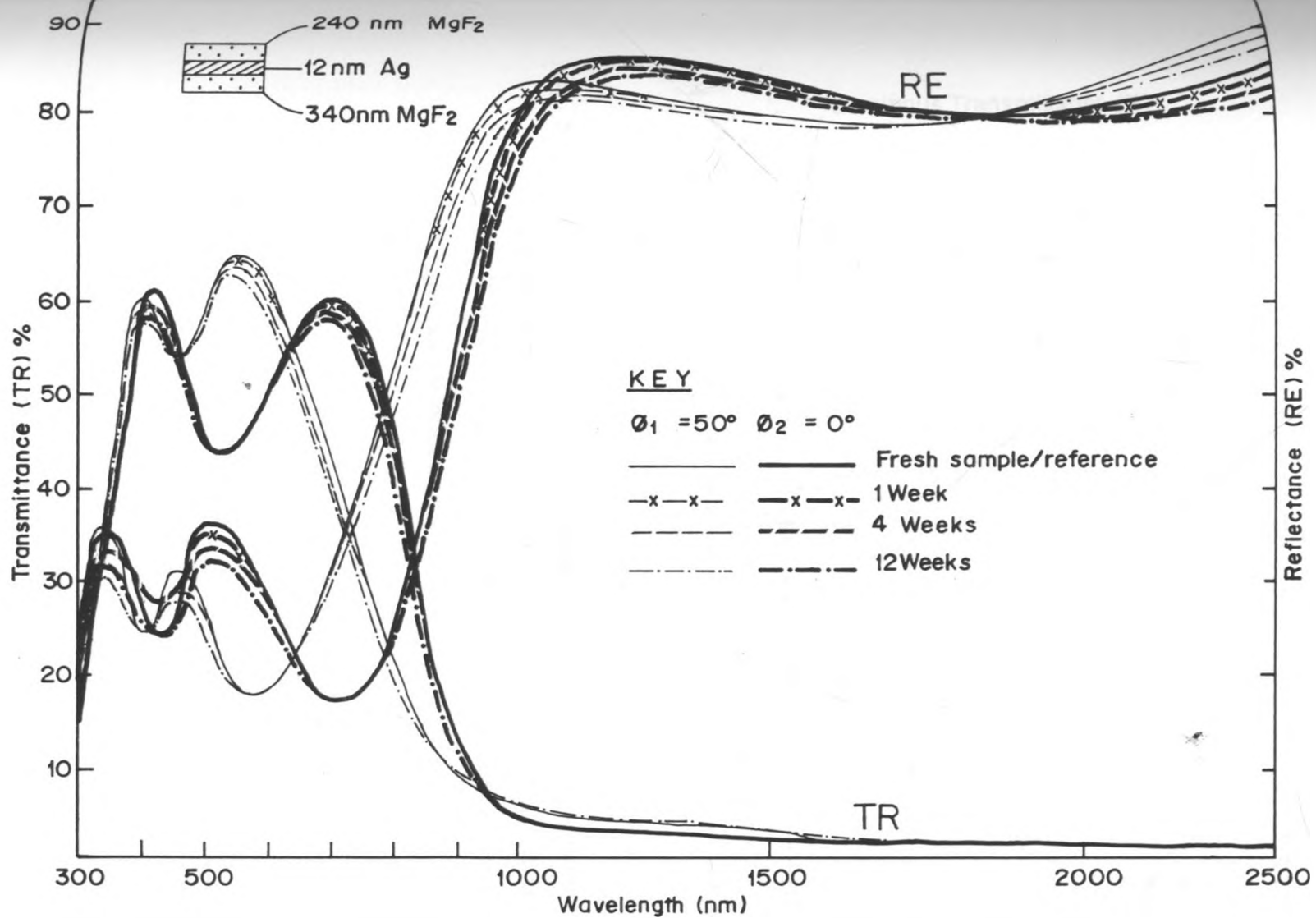


Fig.5.2.2a Spectral transmittance and reflectance of MgF<sub>2</sub>/Ag/MgF<sub>2</sub> multilayer for fresh sample and sample laid in freezer maintained at  $-10 \pm 1^\circ\text{C}$  for indicated duration.

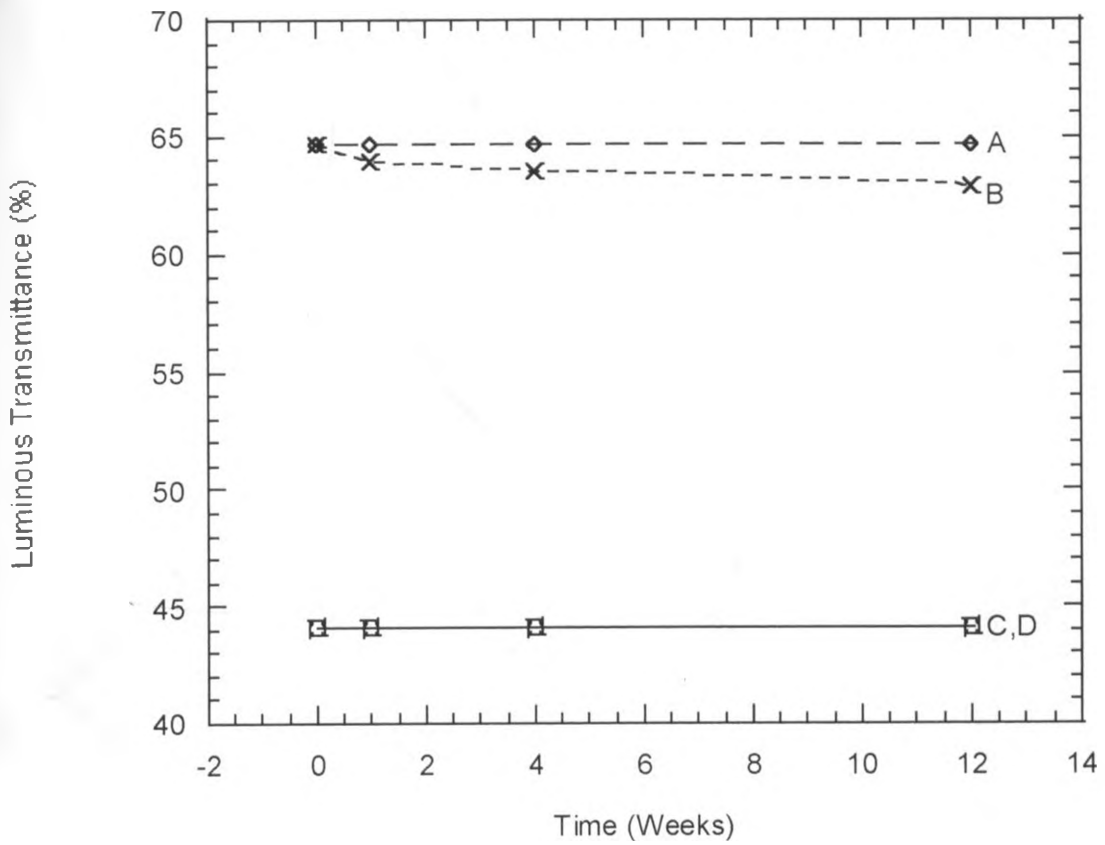


Fig. 5.2.2aa. The variation with time of wavelength integrated luminous transmittance for samples laid in freezer maintained at  $-10^{\circ}\text{C}$ . Fresh sample A and C; aged sample B and D. (NB. A and B denotes oblique incidence; C and D denotes normal incidence).

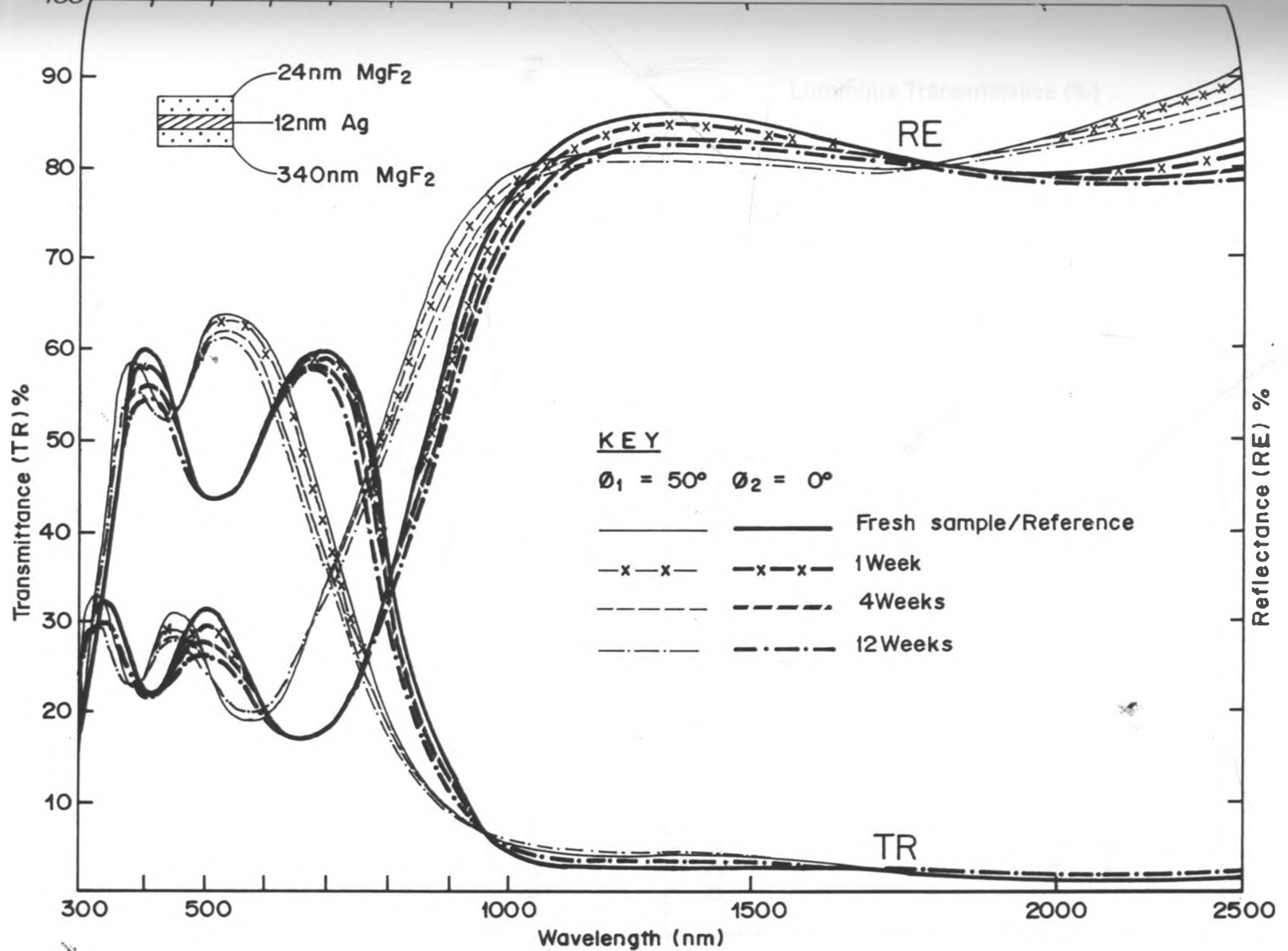


Fig. 5.2.2b Spectral transmittance and reflectance of MgF<sub>2</sub>/Ag/MgF<sub>2</sub> multilayer for fresh sample and sample laid in freezer maintained at  $-18 \pm 1^\circ\text{C}$  for indicated duration.

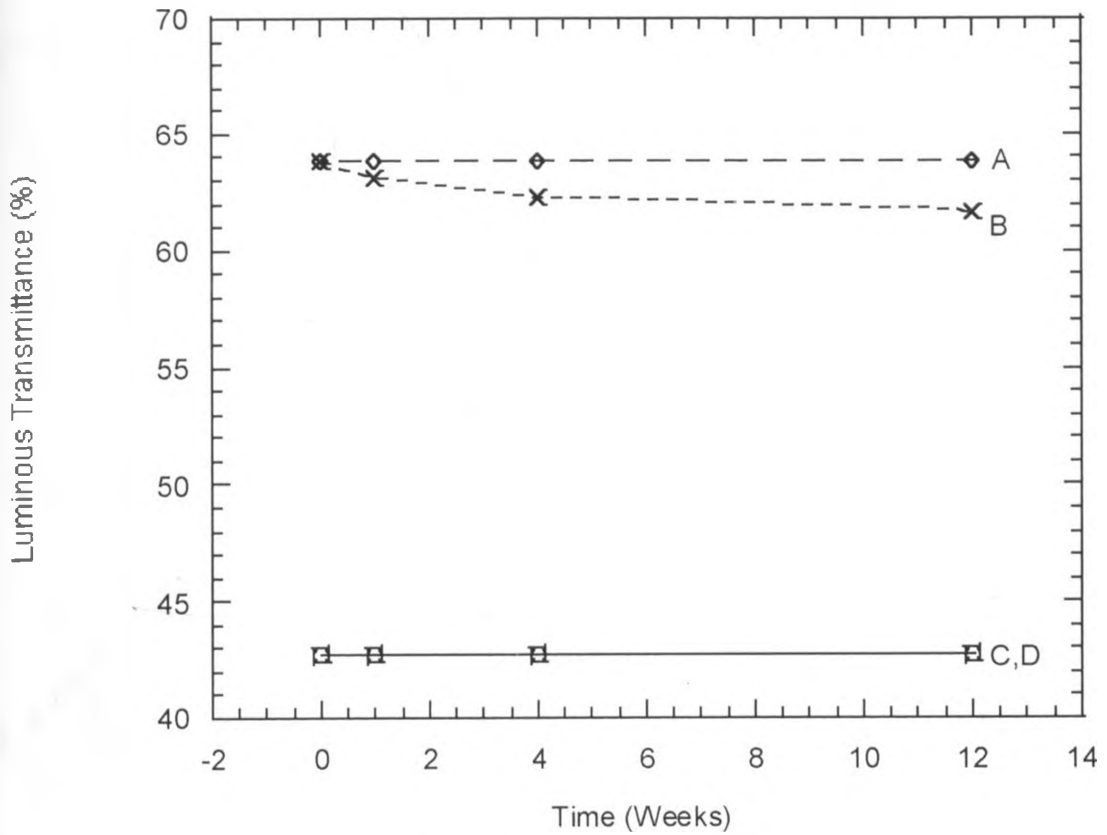


Fig. 5.2.2bb. The variation with time of wavelength integrated luminous transmittance for samples laid in freezer maintained at  $-18^{\circ}\text{C}$ . Fresh sample A and C, aged sample B and D. (NB. A and B denotes oblique incidence; C and D denotes normal incidence).

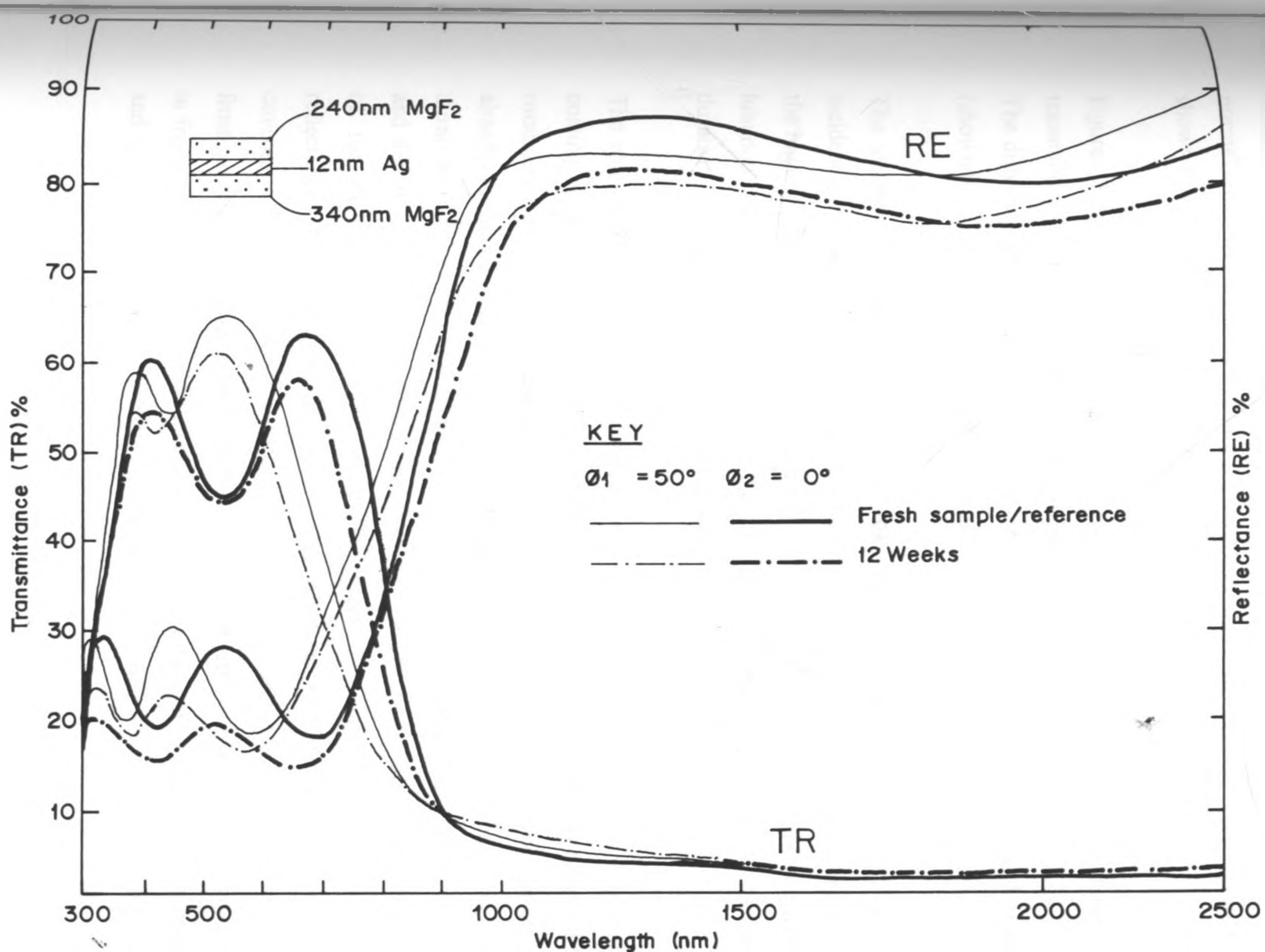


Fig. 5.2.2c Spectral transmittance and reflectance of MgF<sub>2</sub> / Ag / MgF<sub>2</sub> multilayer for fresh sample and a sample covered in Ice (frost) at  $-20 \pm 1^\circ\text{C}$  for indicated duration.

The changes observed in luminous transmittance after 12 weeks for samples kept in freezing environment for equal duration, at different temperatures that is  $-10\text{ }^{\circ}\text{C}$  (Fig. 5.2.2a;aa) and  $-18\text{ }^{\circ}\text{C}$  (Fig. 5.2.2b;bb) recorded a decrement of 1.8% and 2.2%, respectively, for oblique incidence transmittance. The luminous transmittance at normal incidence remained constant for the entire period the samples were exposed, as shown in figures 5.2.2aa and 5.2.2bb.

Figures 5.2.2aa and 5.2.2bb, further shows that, the rate of decrement in luminous transmittance was higher for samples exposed at  $-18\text{ }^{\circ}\text{C}$  to those exposed at  $-10\text{ }^{\circ}\text{C}$ . The difference between the fresh sample (shown by reference line A) and aged sample (shown by line B) demonstrates this difference, in both figures.

The samples covered in ice after 12 weeks, the luminous transmittance at oblique incidence had decreased by 3.5%. In these samples, luminous reflectance registered the highest decrement of 7.8% for normal incidence after 12 weeks of exposure, while luminous transmittance decreased by 0.1% for the same angle of incidence in the same duration, as detailed in Table A6 of appendix A.

The changes observed in these samples are thought to be due to contraction of the coating material when exposed to low temperatures. When the sample is removed to room environment, it will tend to relax, these changes may lead to stress changes as already explained under section 5.2.1, though of lower magnitude considering the duration of exposure. These changes can in one way or another cause lattice defects and defects in internal boundaries, meaning this will affect crystallographic structure of the multilayer and whence eventually affect the optical transmittance and reflectance of the sample (Besancon, 1986; Hoffman, 1976). The samples kept covered in frost suffer the same effect and also micro abrasions (surface roughness) by frost particles contribute to the changes in optical properties. Also the samples covered in frost showed reduced reflectance a factor that was thought to be due to absorption and scattering of the incident beam by the coating material. We did not perform total

reflectance measurements or surface profiling to ascertain the roughness changes; neither did we confirm our results by structural analysis.

### **5.2.3 Humid Environment**

There was no notable change in the physical appearance of the samples after 12 weeks inside the chamber with elevated humidity. Due to saturation inside the chamber, moisture was forming on the surface of the samples making them wet.

The spectral data are shown in figure 5.2.3a. In this figure, it shows that there was insignificant decrease in transmittance and reflectance in the visible region. In the NIR region, reflectance registered a decrement for both near normal and oblique incidence, while transmittance had a small increment of nearly the same magnitude for the two angles of incidence.

Figure 5.2.3b, shows variation with time of luminous transmittance. The figure further shows that, the change in luminous transmittance was more pronounced when the beam is at oblique incidence (difference in A and B) than at normal incidence (difference in C and D).

The analysis of the tabulated data given in Table A7 of appendix A, shows that, the highest change was recorded in oblique incident solar reflectance of 3.3% after 12 weeks. On the other hand, there was no change observed in luminous transmittance and luminous reflectance at normal incidence after the sample had been exposed for 3 weeks. The aged samples still retained their luminous transmittance angular dependency, whereby angular performance changed from 18.7% to 16.7% after the samples had been exposed into humid environment for 12 weeks.



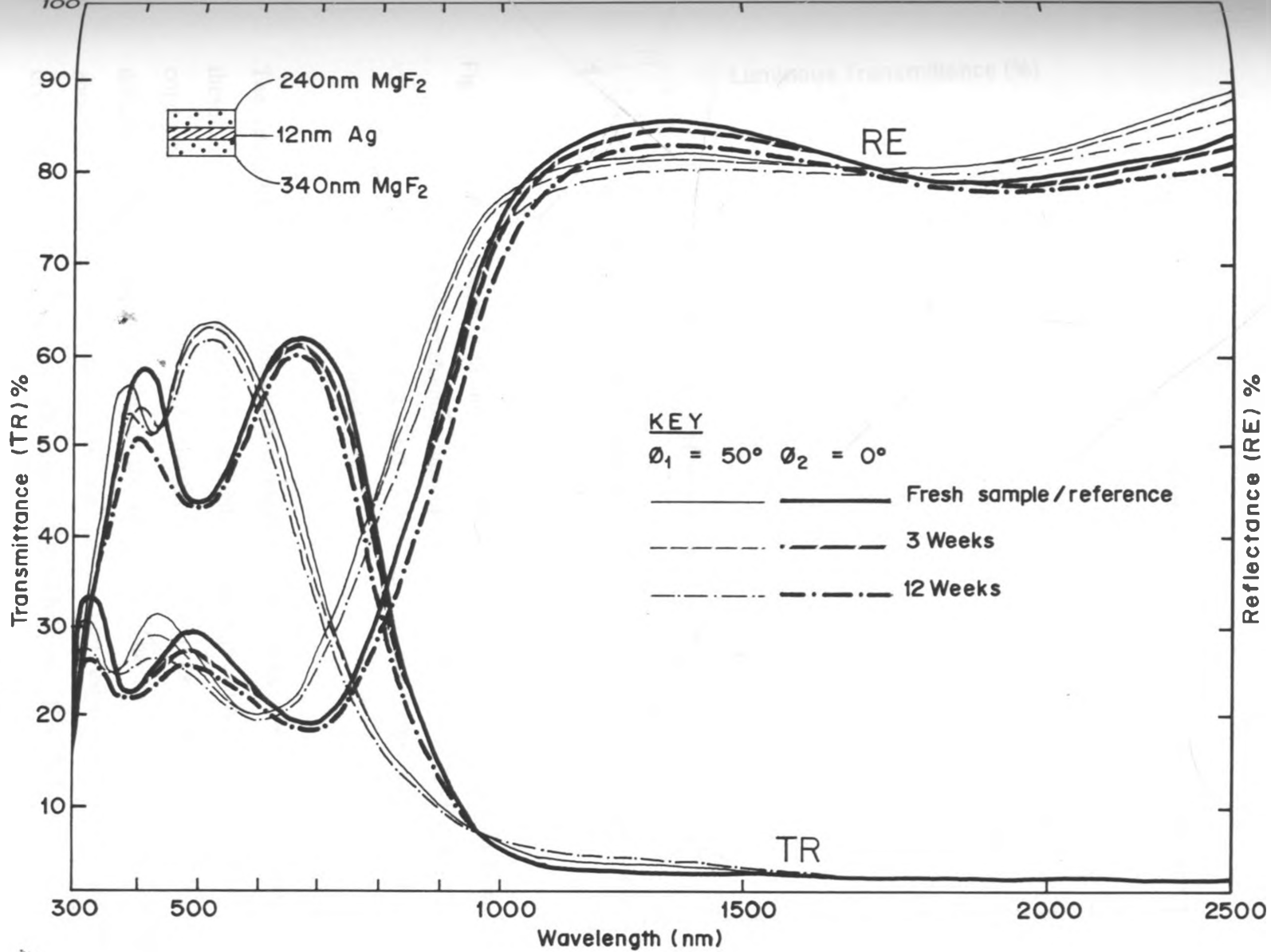


Fig. 5.2.3a Spectral transmittance and reflectance of MgF<sub>2</sub>/Ag/MgF<sub>2</sub> multilayer for fresh sample and sample laid in humidity chamber maintained at  $86 \pm 1\%$  relative humidity for indicated duration.

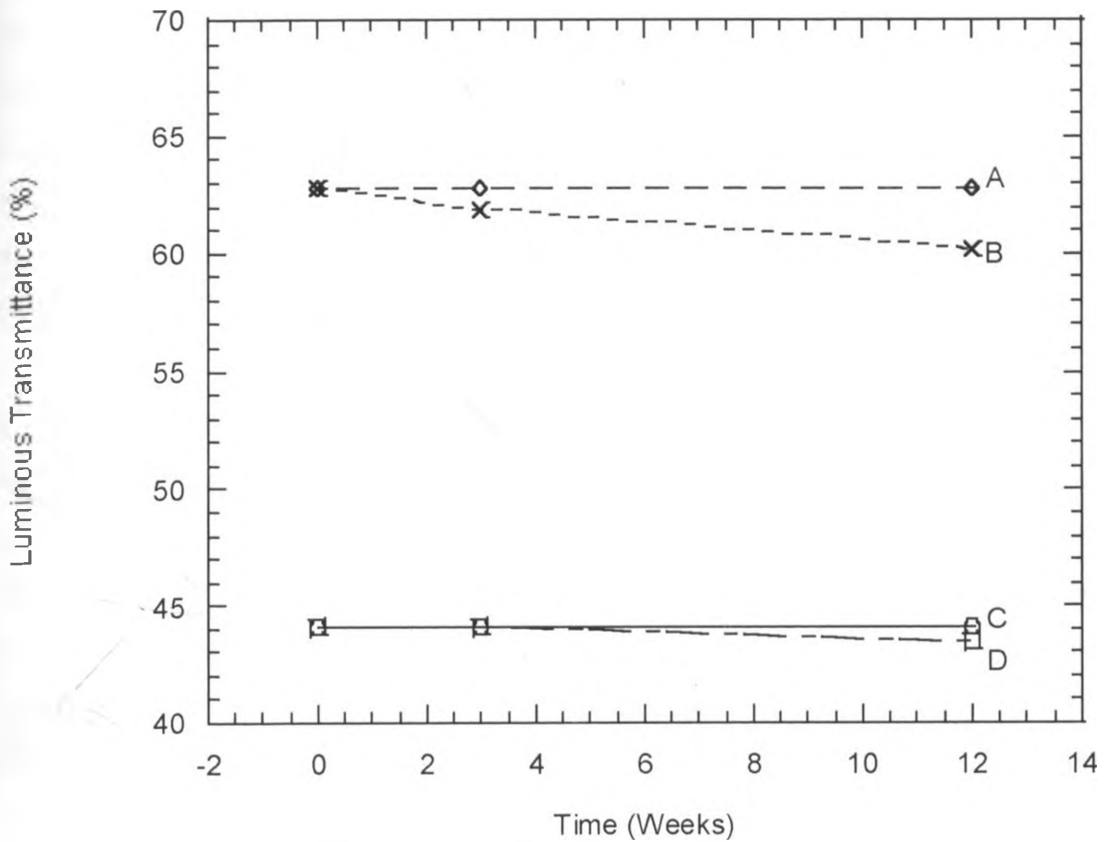


Fig. 5.2.3b. The variation with time of wavelength integrated luminous transmittance for samples laid in chamber maintained at 86% relative humidity: Fresh sample A and C; aged sample B and D. (NB. A and B denotes oblique incidence; C and D denotes normal incidence).

The saturated moisture in the chamber mainly brought about the changes observed in these samples. The moisture compounded with high pressure in the chamber after condensing, it finds its way inside the film via the porous surface of the film or by diffusing between the interfaces of the multilayer. The moisture eventually brings about the changes in structure of the coated film especially packing density, crystallinity and refractive index (Besancon, 1986; Hoffman, 1976; Pulker, 1999).

#### 5.2.4 Saline Solution

The physical appearance of the samples changed from pale blue colour to faded blue with the texture of the film changing completely after 24 hrs. The texture was having small-granulated particles on it, possibly of crystalline salt; also the surface had formed minute cracks. After two weeks, the appearance was that of the uncoated glass except that crystals of salt had formed on the surface after it was allowed to dry. The spectral data are given in figure 5.2.4a,b and c, for different duration of time, while figure 5.2.4d shows the variation with time of wavelength integrated luminous transmittance.

It was observed that after 5 hrs in the solution (figure 5.2.4a; figure 5.2.4d), the luminous transmittance of the sample at oblique incidence remained the same, while at normal incidence; an increment of 8.6% was recorded. After two weeks (figure 5.2.4c; figure 5.2.4d), the optical properties of the sample had changed completely registering an increment of 42.1% and 21.2% for normal and oblique incidence luminous transmittance. For the case of uncoated glass,  $T_{sol} = 91.4\%$  and  $T_{lum} = 92.4\%$ ; while the aged sample after two weeks in the solution,  $T_{lum} = 84.3\%$  and  $T_{sol} = 84.8\%$ , the difference with the uncoated glass is thought to be due to scattering or absorption of the surface. It can be observed that, while transmittance (solar and luminous) for both normal incidence and oblique incidence recorded an increment, the reflectance (solar and luminous) for respective angles of incidence decreased to the lowest values. This was to be expected, as the coating was peeling off, transmittance and reflectance were changing to those of uncoated glass. More details are given in Table A8 of appendix A.

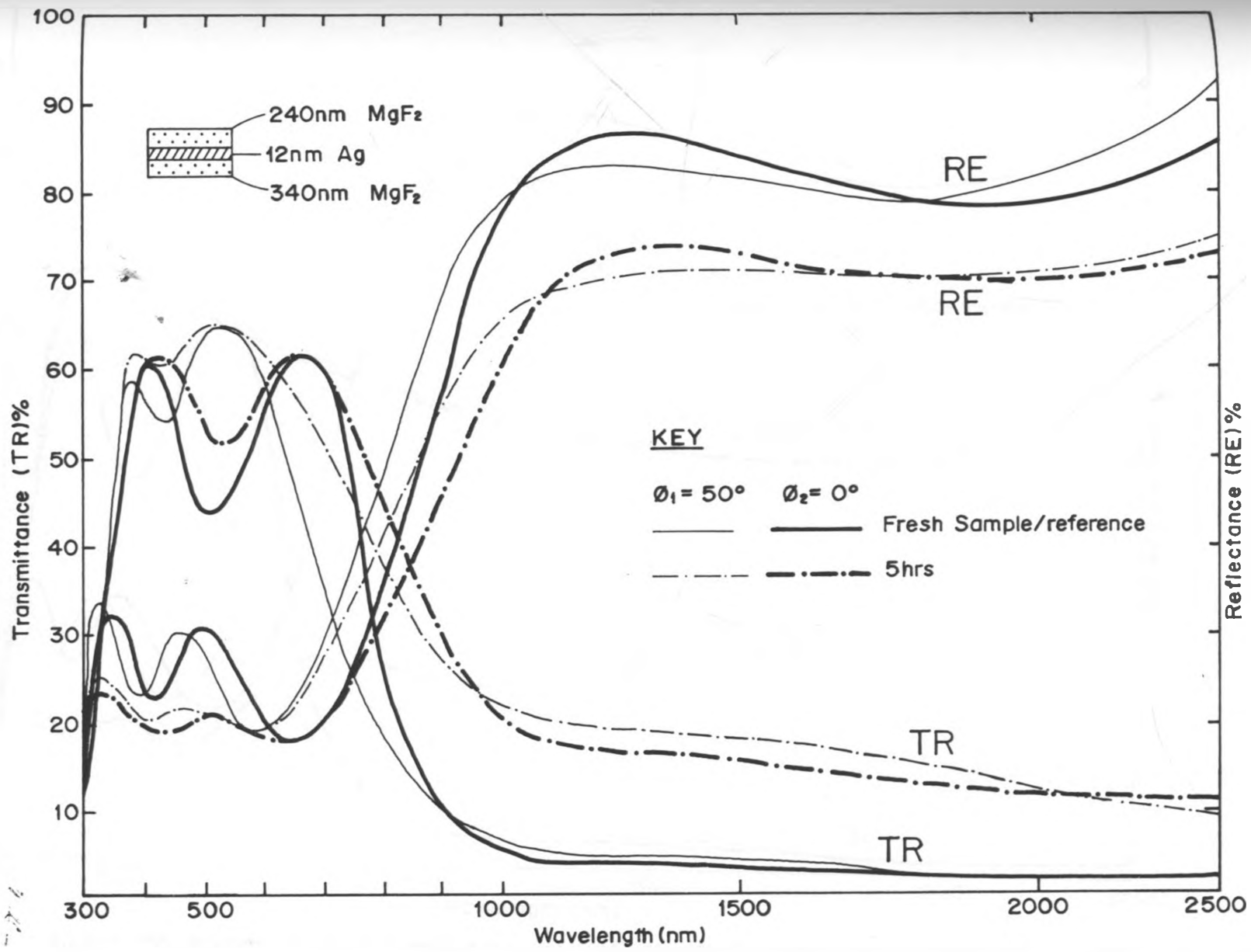


Fig. 5.2.4 a Spectral transmittance and reflectance of MgF<sub>2</sub>/Ag/MgF<sub>2</sub> multi layer for fresh sample and sample soaked in salt (NaCl) solution of concentration 20gm/100ml water for indicated duration.

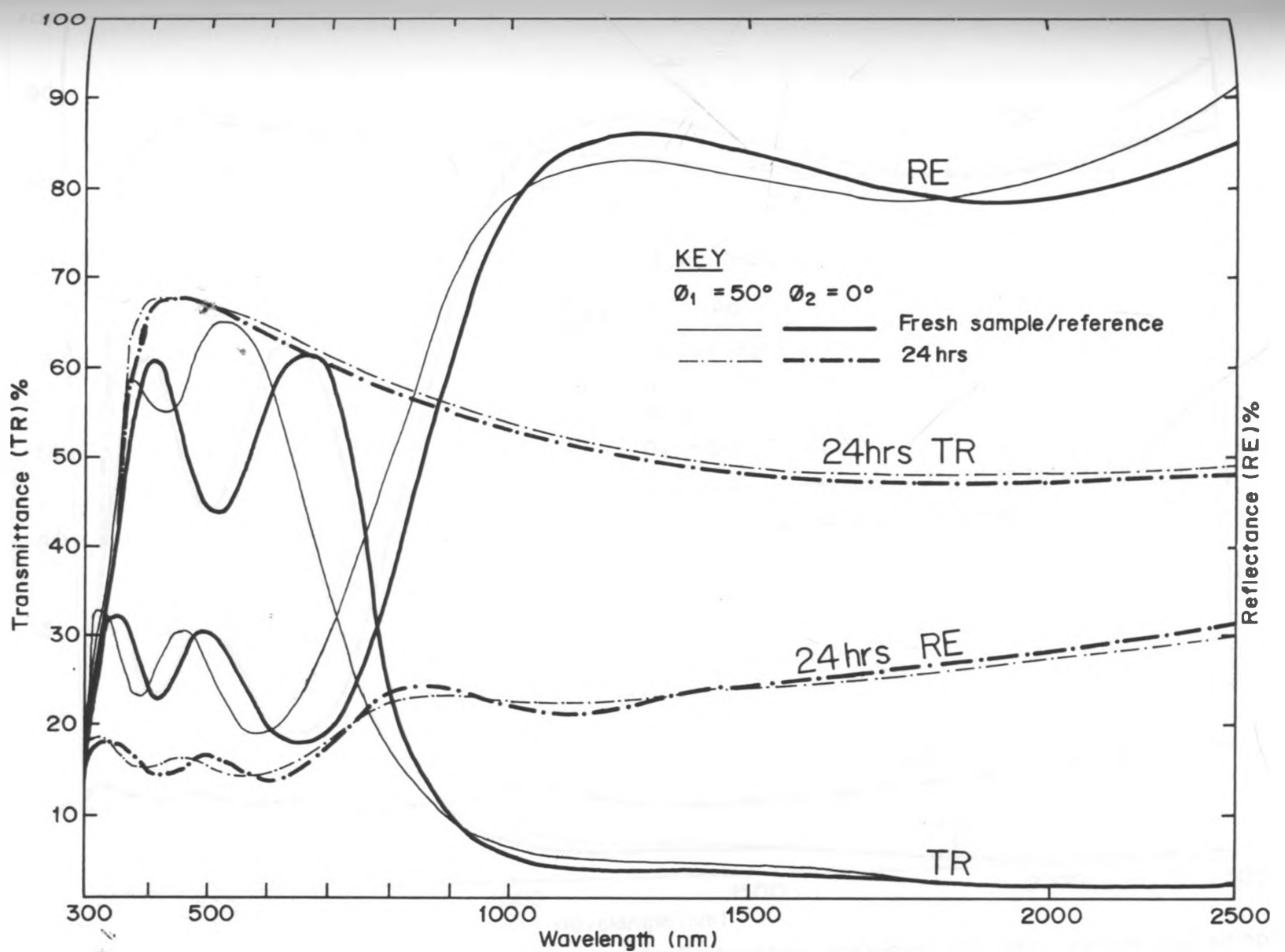


Fig.5.2.4b Spectral transmittance and reflectance of  $MgF_2/Ag/MgF_2$  multi layer for fresh sample and sample soaked in salt (NaCl) solution of concentration 20gm/100ml water for indicated duration.

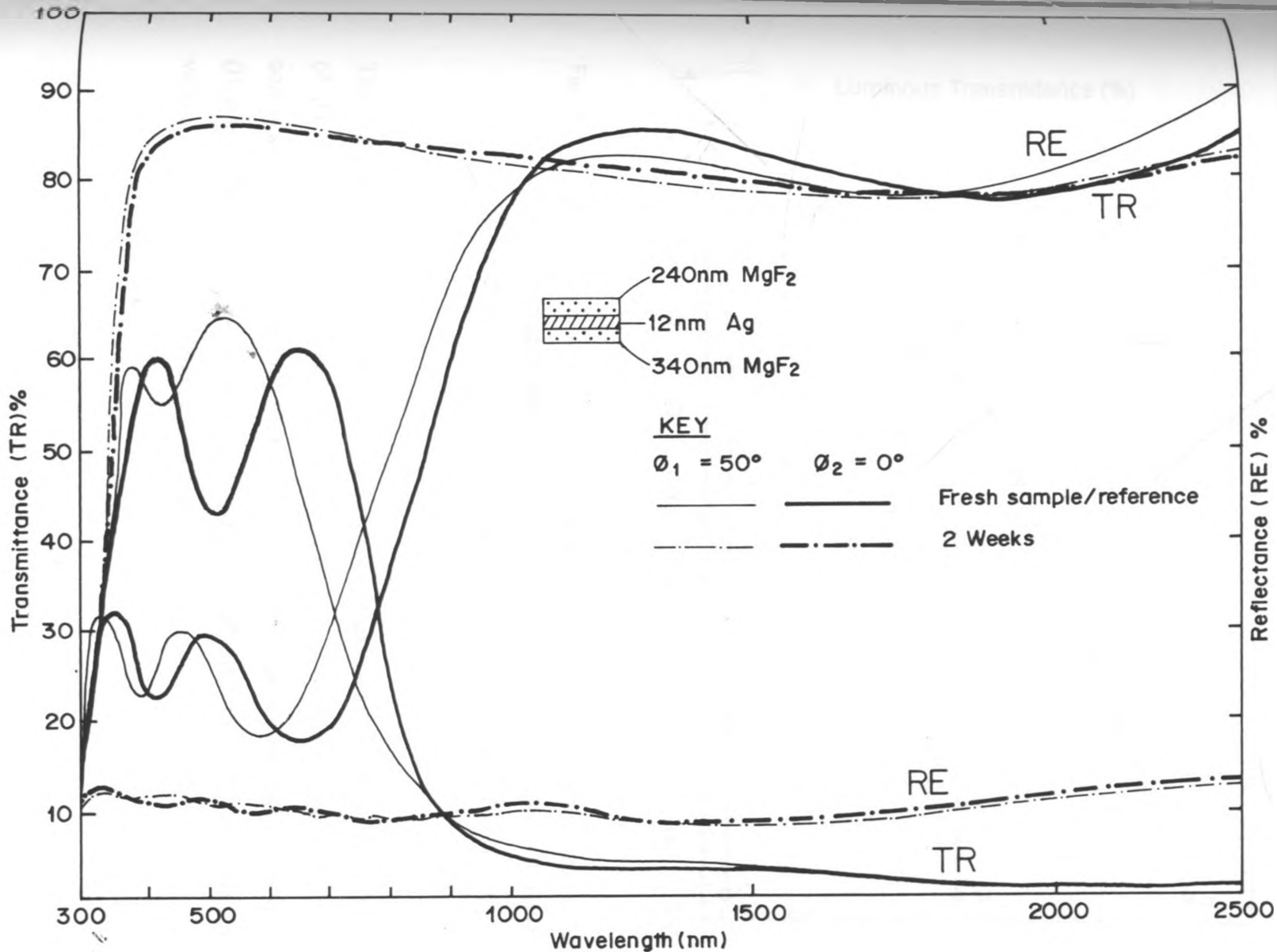


Fig.5.2.4c Spectral transmittance and reflectance of MgF<sub>2</sub>/Ag/MgF<sub>2</sub> multilayer for fresh sample and sample soaked in salt (NaCl) solution of concentration 20gm/100ml Water for indicated duration.

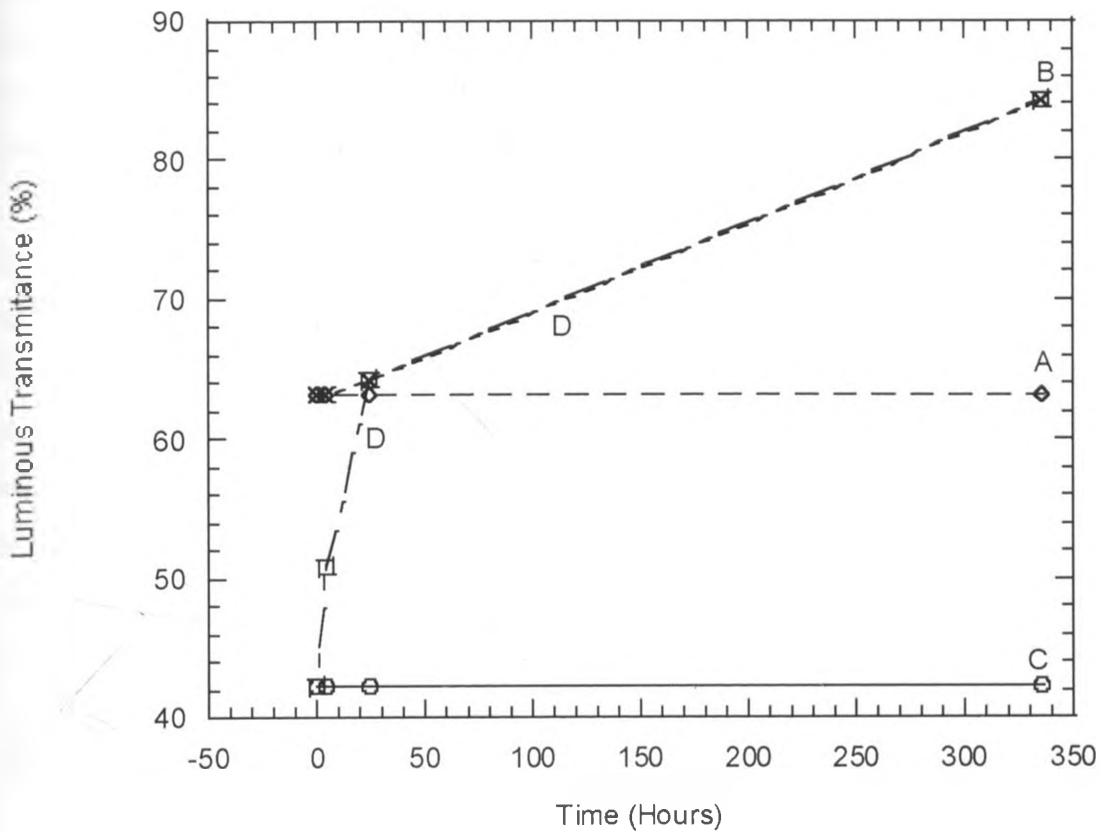


Fig. 5.2.4d. The variation with time of wavelength integrated luminous transmittance for samples soaked in saline solution. Fresh sample A and C; aged sample B and D. (NB. A and B denotes oblique incidence; C and D denotes normal incidence).

The changes observed in transmittance and reflectance can be attributed to the reaction of the  $MgF_2$  and Ag coatings with the NaCl solution eventually peeling off the coatings. Our results compare well to those obtained earlier by Hass and Scott (Heavens, 1965). In their report, the coatings peeled off after subjecting them to vapour of boiled 5% salt solution for 10 days.

### 5.2.5 Organic Solvents

The physical appearance of the sample remained unchanged for those soaked in acetone, while those that were soaked in ethanol, the colour changed from pale blue colour to light blue with yellowish colouration. The effect of acetone on the optical properties seemed less severe as it can be observed in figure 5.2.5a; than those samples soaked in ethanol, as shown in figure 5.2.5b.

In figures 5.2.5aa, and bb, shows the variation with time of luminous transmittance for samples soaked in acetone and ethanol, respectively. The samples soaked in either of the solvents retained their angular dependency with good angular performance. Those samples that were soaked in ethanol (figure 5.2.5bb), their angular performance decreased from 17.8% to 14.8% while those soaked in acetone (figure 5.2.5aa) it decreased from 23.0% to 20.3%. The values for solar transmittance and reflectance remained reasonably high for fresh and aged samples from either of the solvents as shown in Table A9 and A10 of appendix A. The luminous reflectance registered the highest decrement of 6.7% for normal incidence beam for samples soaked in ethanol, while those that were soaked in acetone it was 4.4% after 96 hrs in either of the solvents.

The above changes are thought to be as a result of photonic interband absorption thus leading to the loss in transmittance (Mark and Scalora, 1998). The reflectance is thought to have been affected by the surface scattering, though our work did not touch the area of investigating total reflectance measurements and surface profiling which could have established whether the loss was due to scattering. At the time of presenting these results, no documented work similar to this was available to the author for possible comparison, although Pulker (1999) has suggested use of organic solvents for degradation study.



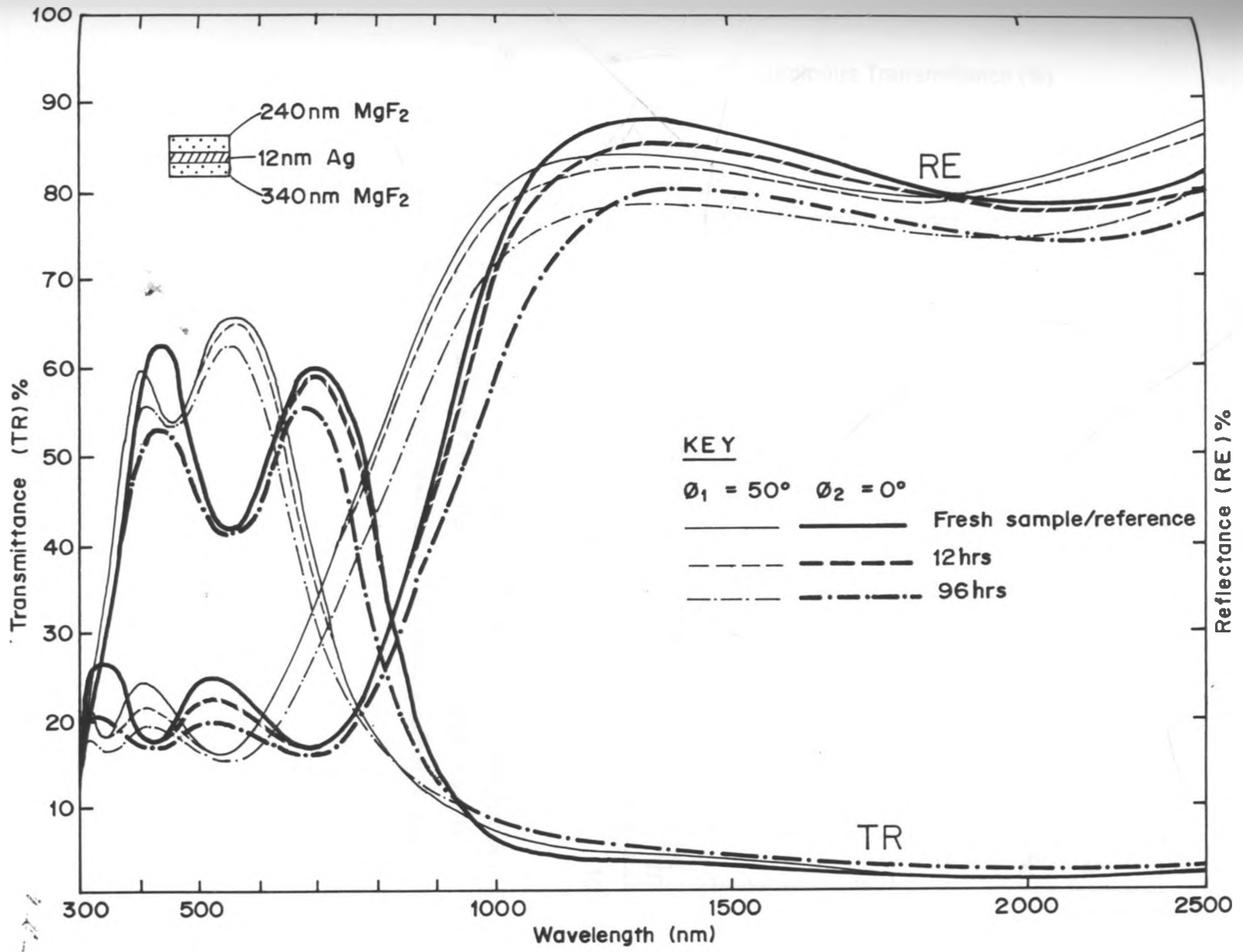


Fig.5.2.5a Spectral transmittance and reflectance of MgF<sub>2</sub>/Ag/MgF<sub>2</sub> multilayer for fresh sample and a sample soaked in acetone of purity 99.8% for indicated duration.

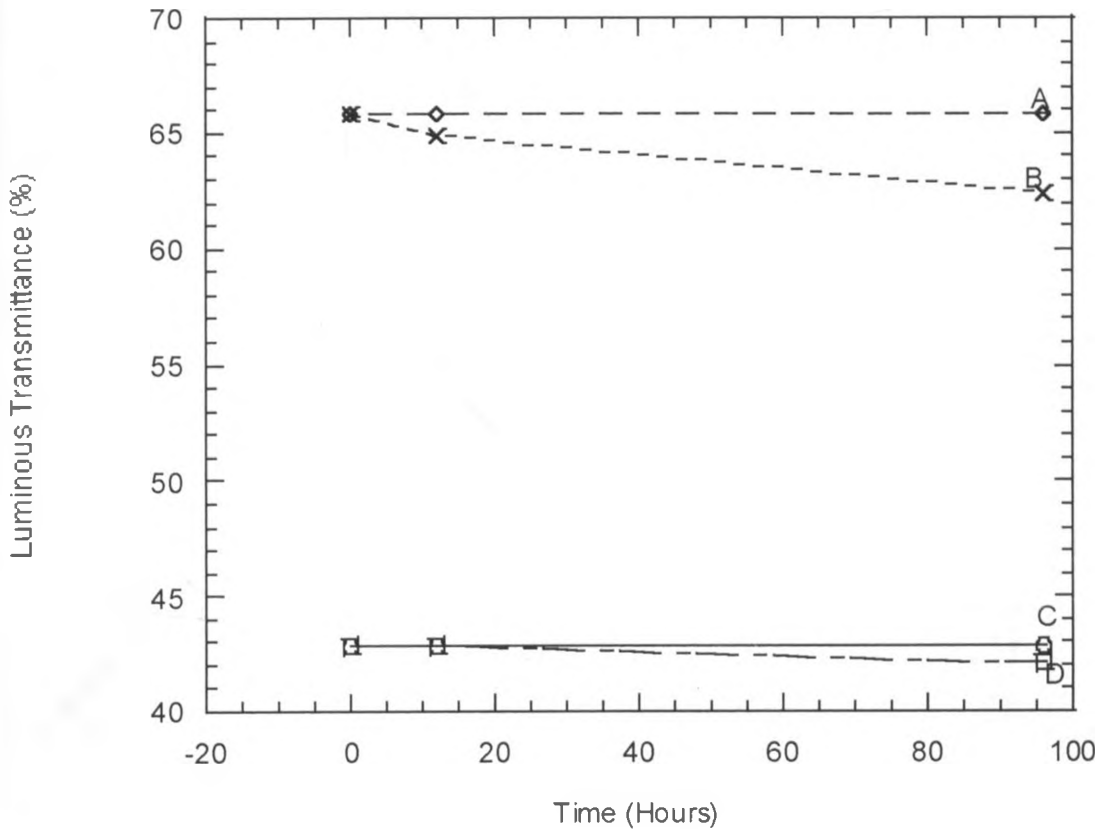


Fig. 5.2.5aa. The variation with time of wavelength integrated luminous transmittance for samples soaked in acetone. Fresh sample A and C; aged sample B and D. (NB. A and B denotes oblique incidence; C and D denotes normal incidence).

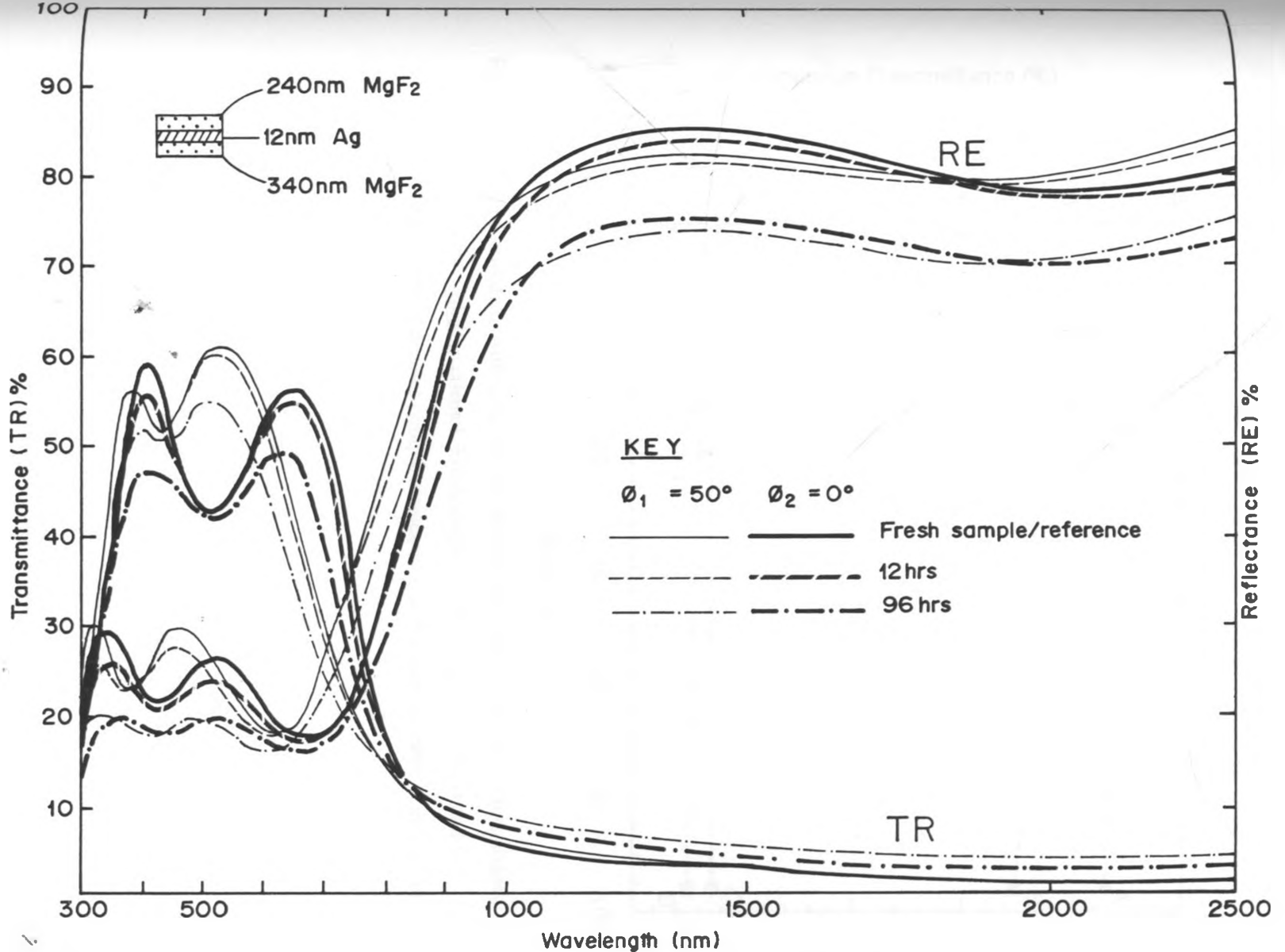


Fig.5.2.5b Spectral transmittance and reflectance of MgF<sub>2</sub>/Ag/MgF<sub>2</sub> multilayer for fresh sample and a sample soaked in ethanol of purity 99.8% for duration indicated.

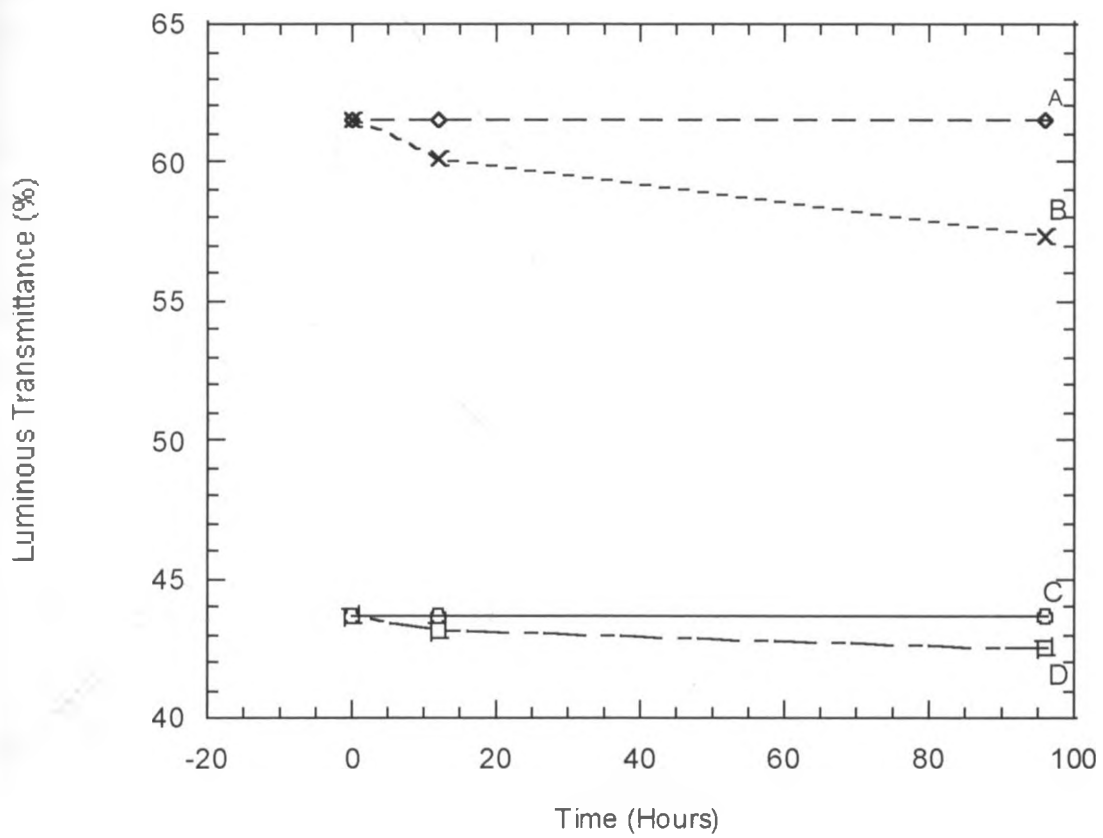


Fig. 5.2.5bb. The variation with time of wavelength integrated luminous transmittance for samples soaked in ethanol. Fresh sample A and C; aged sample B and D. (NB. A and B denotes oblique incidence; C and D denotes normal incidence).

### 5.2.6 Outdoor Environment

The spectral results obtained for samples exposed into the outdoor environment are as shown in figure 5.2.6a. Figure 5.2.6b, shows the quantitative variation with time of luminous transmittance of the samples.

In figure 5.2.6b, it can be observed that the rate of change in luminous transmittance was highest in the first four weeks the samples were exposed, especially when we consider the oblique incidence transmittance (i.e. difference in A and B). At normal incidence transmittance, observable change was between the 4<sup>th</sup> week to 12<sup>th</sup> week (difference in C and D).

The analysis of the results show that, transmittance (luminous and solar) and reflectance (luminous and solar) registered a decrement ranging between 0.2% – 8.3%, except for the luminous transmittance at normal incidence, which remained constant as detailed in table A11 of appendix A. After the sample had been exposed for duration of 12 weeks, the oblique incidence luminous transmittance of the sample had decreased by 3.7% while the luminous reflectance of the sample at normal incidence decreased by 8.3% in the same duration. At oblique angle, solar reflectance remained more than 50%, with the samples still maintaining a 60% luminous transmittance.

The changes in transmittance and reflectance of the samples are thought to be due to the effect of the weather conditions. Degradation due to air pollutants such as sulphur dioxide (sulphur dioxide forms weak acids which leads to reaction with the surface coating), which exists in small parts per billion, can play a substantial role, especially because of the existence of industries (Brunold, *et. al.*, 2000). Moreover, the water vapour in the coastal regions contains small percentages of NaCl whose effect were discussed under section 5.2.4.

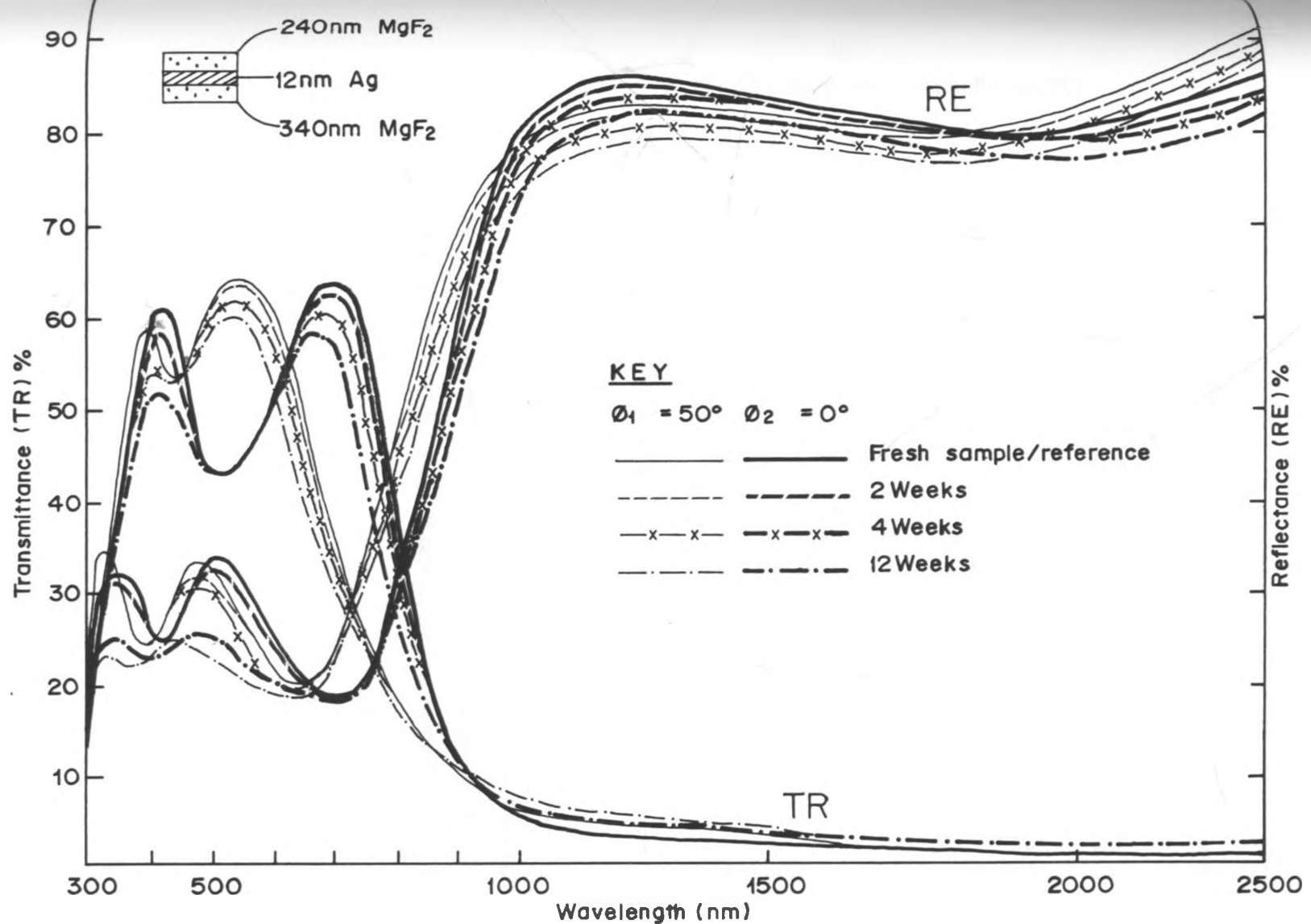


Fig.5.2.6a Spectral transmittance and reflectance of MgF<sub>2</sub>/Ag/MgF<sub>2</sub> multilayer for fresh sample and a sample exposed into normal outside atmosphere environment, temperature range 20–34 ± 1°C, humidity range 60–70 ± 1% RH for duration indicated.

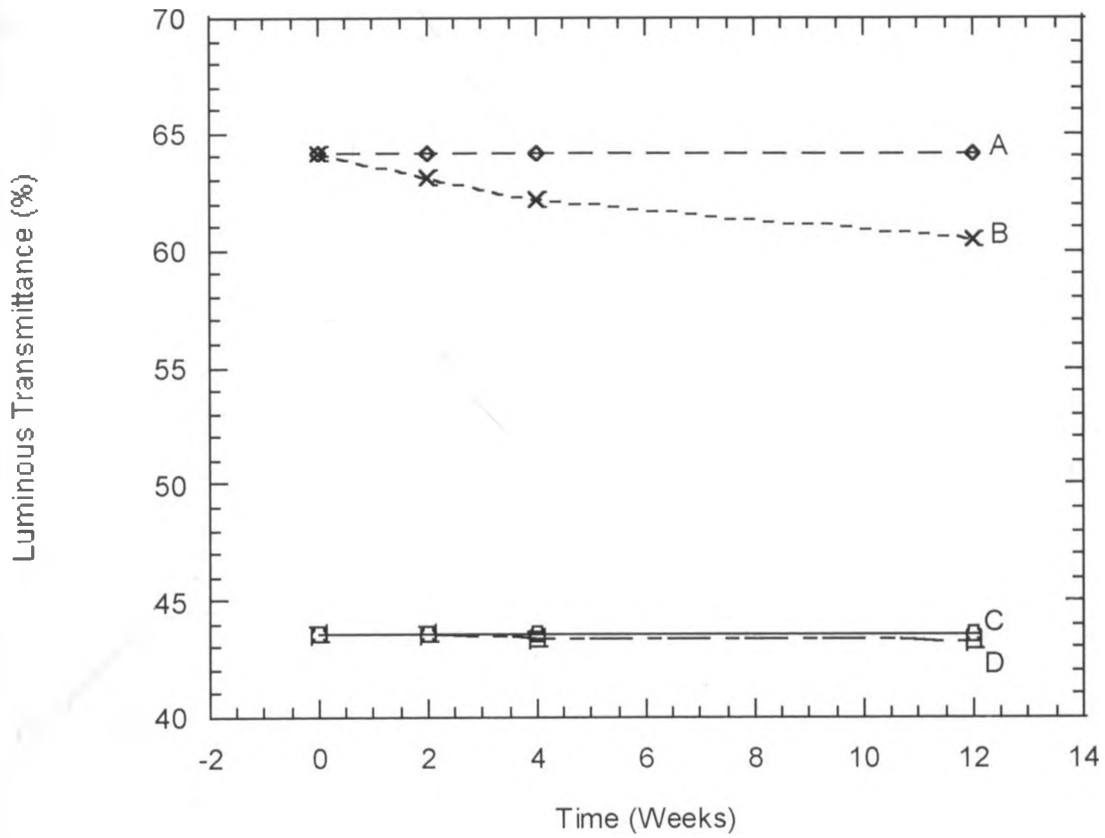


Fig. 5.2.6b. The variation with time of wavelength integrated luminous transmittance for samples exposed into outdoor environment. Fresh sample A and C; aged sample B and D. (NB. A and B denotes oblique incidence; C and D denotes normal incidence).

### 5.2.7 Aquatic Condition

The spectral results obtained after exposing the sample into aquatic environment for three weeks are as shown in figure 5.2.8a. Both transmittance and reflectance decreased in the visible region while in the NIR region, reflectance showed decrement, but transmittance had a small increment.

In the visible region, the oblique incidence luminous reflectance remained constant for fresh and aged sample; also for the same angle of incidence, a decrease of 1.6% was observed for luminous transmittance (figure 5.2.8b) after the sample had been soaked for 504 hrs (3 weeks). The reflectance in the visible region, at oblique incidence remained constant also for fresh and aged samples, respectively, while a 4.7% change was noted in the normal incidence reflectance. The other factors, i.e.  $T_{sol}$  and  $R_{sol}$  registered ~1.5% decrease as detailed in Table A12 of appendix A.

The changes observed in transmittance and reflectance are thought to be due to the changes in surface roughness and porosity of the coating after being exposed into aquatic environment. The increase in surface roughness leads to scattering, which brings about the optical changes. Our results were not confirmed by total reflectance measurement to conclusively say the scattering of the sample is the main cause of the difference. From the results obtained, we can say that water does not easily penetrate the magnesium fluoride coating, because, if it could have soaked in the material, swelling of the layers could have resulted with changes of great magnitude, since thickness will be completely altered; void fraction will also have been adversely affected and the entire crystal structure.



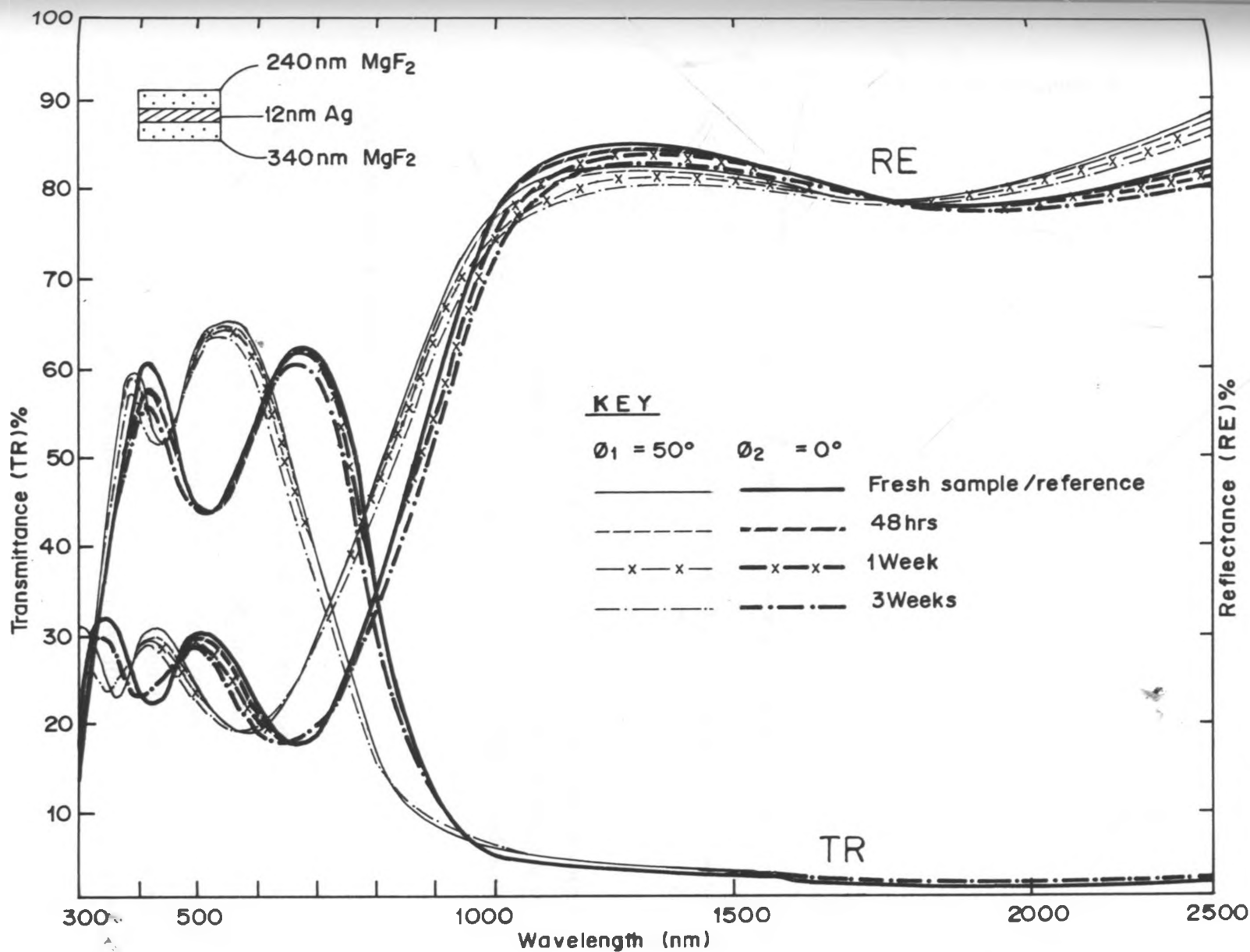


Fig.5.2.7a Spectral transmittance and reflectance of MgF<sub>2</sub>/Ag/MgF<sub>2</sub> multilayer for fresh sample and a sample soaked in water in room environment for indicated duration.

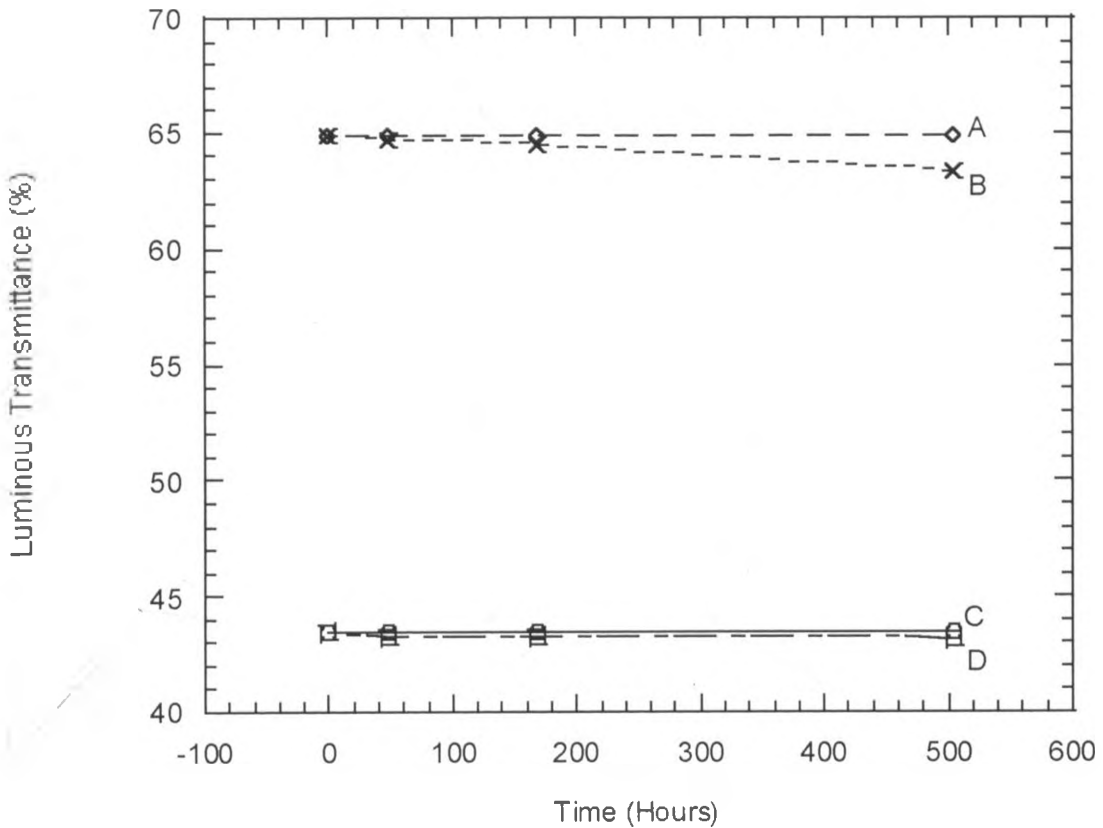


Fig. 5.2.7b. The variation with time of wavelength integrated luminous transmittance for samples soaked in distilled water. Fresh sample A and C; aged sample B and D. (NB. A and B denotes oblique incidence; C and D denotes normal incidence).

### 5.3 MgF<sub>2</sub>/Al/MgF<sub>2</sub> Coatings

The MgF<sub>2</sub>/Al/MgF<sub>2</sub> based coatings were not subjected to degradation studies because they did not meet the pre-set criteria as explained in section 5.1. The spectral transmittance and reflectance for 3 layer MgF<sub>2</sub>/Al/MgF<sub>2</sub> coatings are as shown in figure 5.3.1 below. The transmittance in the visible region for normal and oblique incidence beam were observed to be lower than ~10%. At  $300 \text{ nm} \leq \lambda \leq 2500 \text{ nm}$ , the

reflectance was less than 10% in the visible region, but was gradually increasing to 40% towards the long wavelength region.

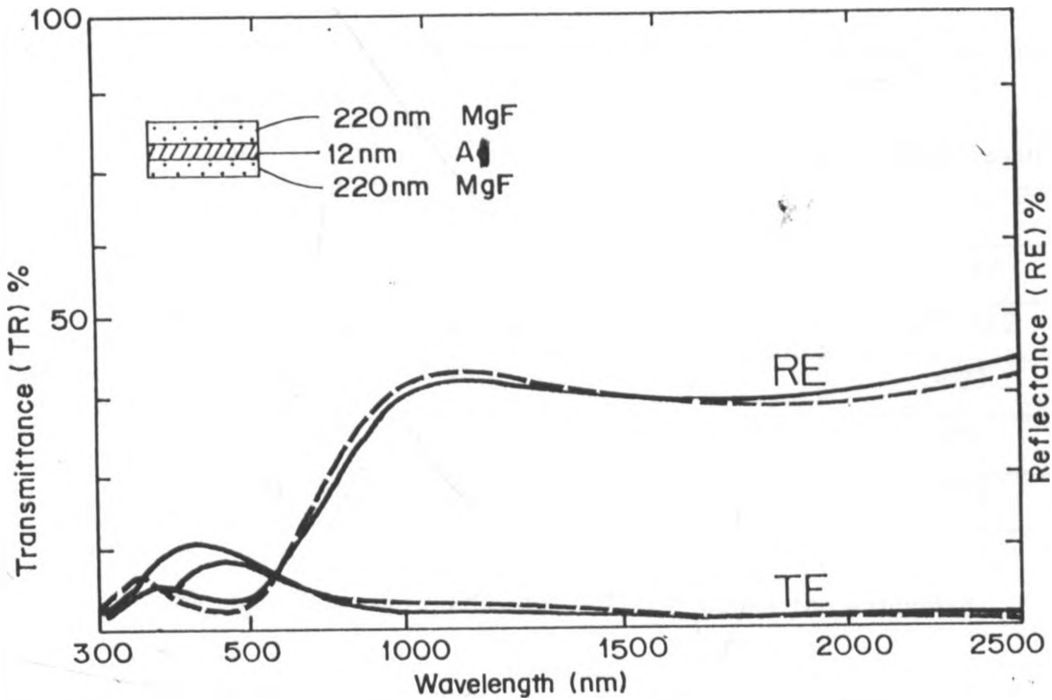


Figure 5.3.1 Spectral transmittance (TR) and reflectance (RE) for  $\text{MgF}_2/\text{Al}/\text{MgF}_2$  coatings

The luminous transmittance was 9.6% for oblique incidence transmittance and as low as 6.2% for normal incidence transmittance. On the other hand, reflectance registered very small difference of the order of 0.1% between the two angles of incidence.

The poor results obtained for this type of coating ( $\text{MgF}_2/\text{Al}/\text{MgF}_2$ ) are attributed to be due to the fact that, under certain growth conditions, films exhibit preferential crystal orientation or even epitaxy (epitaxy means that the film structure is determined by the crystal structure and orientation of the underlying substrate) (Besancon, 1986). In our case of multilayers, for the aluminium layer, its underlying substrate material in this case was  $\text{MgF}_2$ . The two materials have completely different polycrystalline crystal structures, see table 5.3.1. This difference is thought to bring about high photonic

interband absorption especially in aluminium metal (Mark and Scalora, 1998). The other losses can be attributed to scattering of the surface material.

Table 5.3.1. Material type used in this work with respective crystal structure and density (Besancon, 1986; Pulker, 1999).

Material		Crystal structure	Density g/cm <sup>3</sup>
Al		cub	2.70
Ag		fcc	10.49
MgF <sub>2</sub>		tetr	2.9 – 3.2
TiO <sub>2</sub> (iv)	Rutile	tetr	4.23
	Anatase	tetr	3.90
	Brookite	rho	4.13

Where: cub – cubic; fcc – face centred cubic; tetr – tetragonal; rho – rhombic.

#### 5.4 TiO<sub>2</sub> Based Coatings

The TiO<sub>2</sub> based coatings can suitably be deposited by reactive evaporation, whereby reactive gas is introduced inside the chamber during deposition of Ti followed by annealing at high temperature.

The physical appearance of the TiO<sub>2</sub> based coatings was darkish; when the samples were annealed (in air) in an oven maintained at 400 °C, the colour changed to milkish with some black color still visible. The spectral transmittance and reflectance for the TiO<sub>2</sub>/Ag/TiO<sub>2</sub> and TiO<sub>2</sub>/Al/TiO<sub>2</sub> samples are as shown in figures 5.4.1 and 5.4.2, respectively.

The TiO<sub>2</sub>/Ag/TiO<sub>2</sub> samples were observed to transmit luminous transmittance of approximately 52% and 50% at oblique and normal incidence transmittance, respectively. There was small but noticeable difference in transmittance and

reflectance between the normal incidence and oblique incidence as illustrated in figure 5.4.1. The  $\text{TiO}_2/\text{Al}/\text{TiO}_2$  coatings were transmitting as little as  $\sim 18\%$  in the luminous region, while in the NIR region, the transmittance was decreasing gradually towards the long wavelength region. The  $\text{TiO}_2/\text{Al}/\text{TiO}_2$  coating registered small, but defined difference in transmittance and reflectance for oblique and normal incidence of approximately  $0.5\% - 1\%$ .

The results predicted by theory (Granqvist, 1991) for  $\text{TiO}_2/\text{Ag}/\text{TiO}_2$  are as shown in figure 5.4.3. Because of the stoichiometry of  $\text{TiO}_2$ , the shapes predicted by theory are difficult to obtain and furthermore, theory considers ideal case whereas empirically other factors may influence the end results (Besancon, 1986), e.g. rate of deposition, condition of the deposition chamber and even the substrate temperature whether pre and in process annealing (insitu) or post annealing (exsitu), in both cases,  $\text{TiO}_2$  is known to change when deposited at different substrate temperature  $T_s$ , see Table, 5.4.1 below.

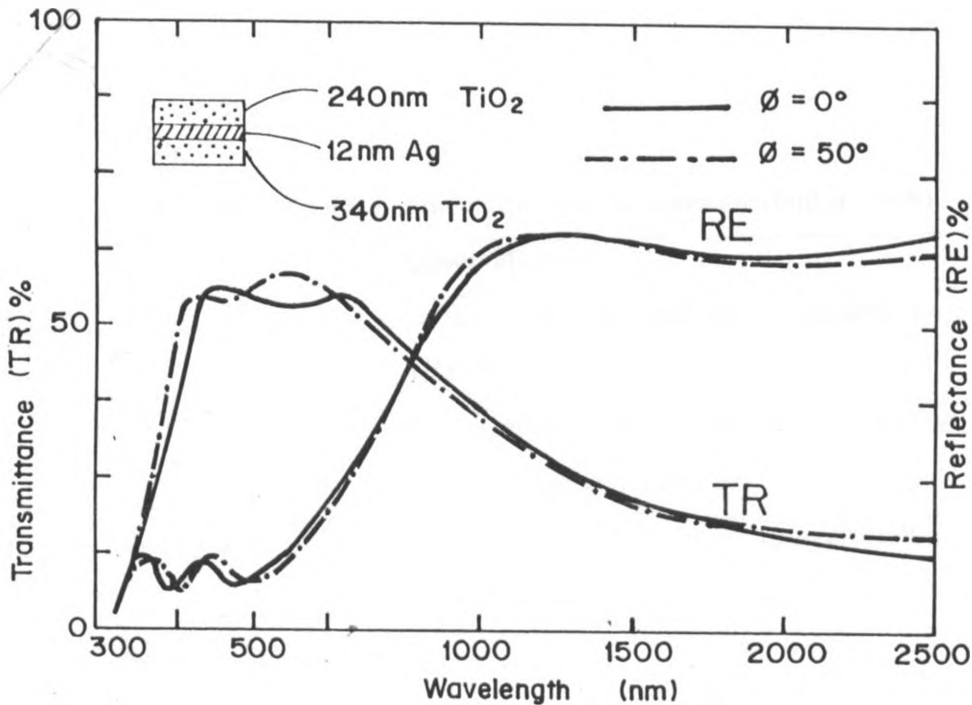


Figure 5.4.1 Spectral transmittance (TR) and reflectance (RE) for  $\text{TiO}_2/\text{Ag}/\text{TiO}_2$  coatings

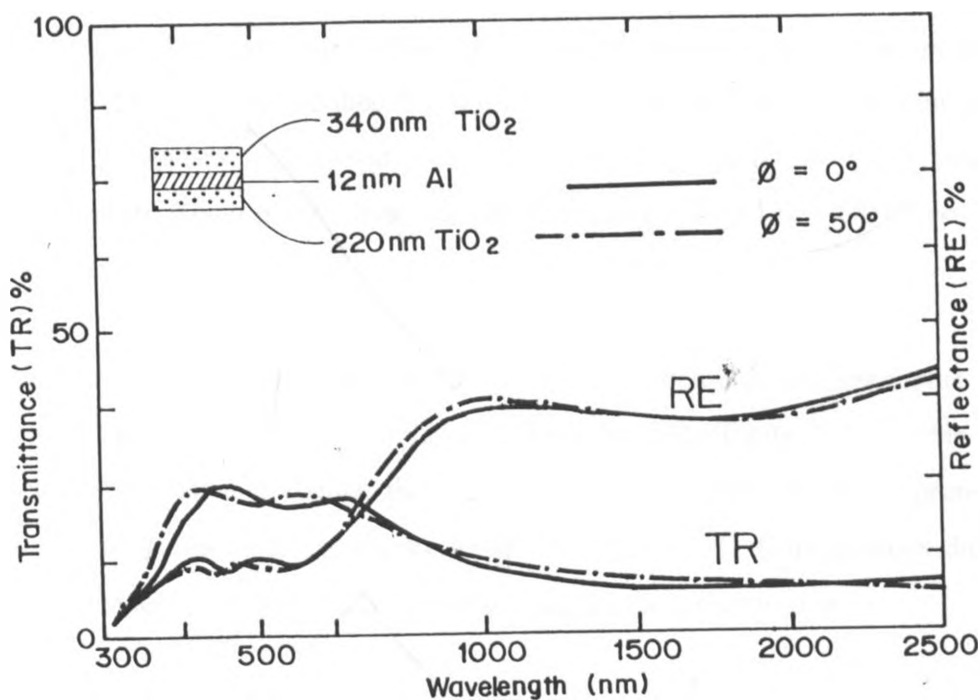


Figure 5.4.2 Spectral transmittance (TR) and reflectance (RE) for TiO<sub>2</sub>/Al/TiO<sub>2</sub> coatings

Table 5.4.1. Properties of TiO<sub>2</sub> at different substrate temperature (Pulker, 1999)

Substrate temperature, T <sub>s</sub>	Observations
T <sub>s</sub> ≤ 280 °C	Diffuse electron diffraction pattern i.e. amorphous TiO <sub>2</sub> films
T <sub>s</sub> ≥ 310 °C	Sharp diffraction pattern, polycrystalline TiO <sub>2</sub> films contain rutile and anatase
T <sub>s</sub> = 380 to 470 °C	Sharp diffraction fringes, polycrystalline TiO <sub>2</sub> films consisting purely of rutile.

From Table 5.3.1, we notice that, tetragonal crystal structure combined with cubic crystal structure give marked low transmittance (less than 50%) as it is observed in...

figure 5.3.1 and 5.4.2, respectively. According to Mark and Scalora, (1998) the losses in incidence energy, can be ascribed to photonic interband absorption as the incidence photon makes transition between the two completely different polycrystalline materials a feature which is not observed between tetragonal and face centered cubic crystals.

By the time this work was compiled, the author had only come across one report done by John and Bachner (1976) for multilayer of  $\text{TiO}_2/\text{Ag}/\text{TiO}_2$  (figure, 5.4.4). This is an experimental study for non-angular dependent coating. The method used in preparing the films was rf-sputtering at a substrate temperature of 600 °C. Current study did not investigate whether sputtering produces better samples than evaporation.

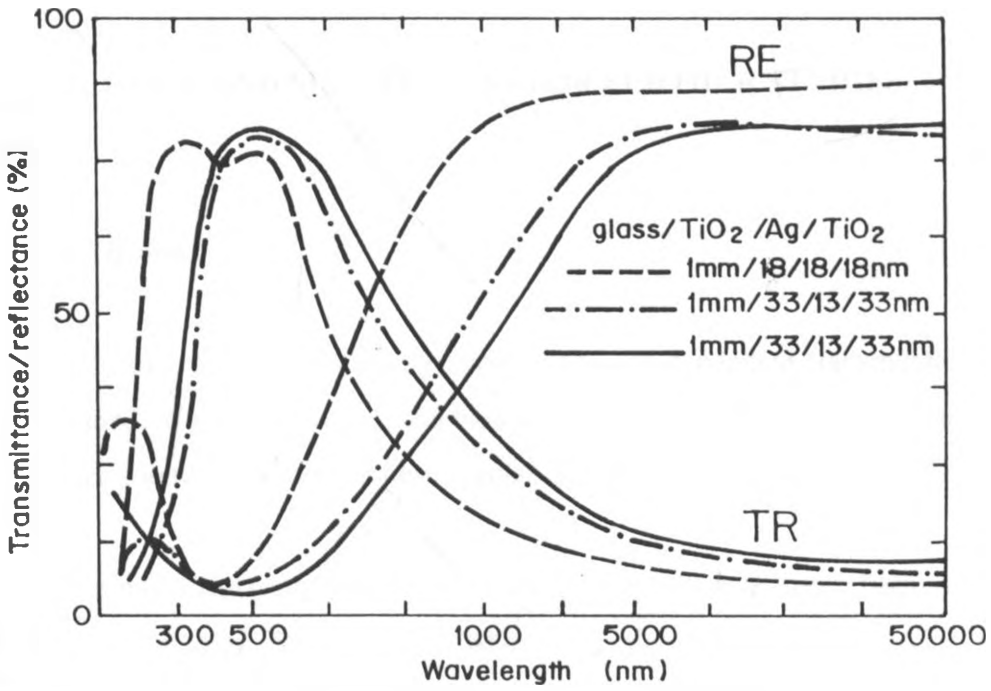


Figure 5.4.3 Spectral normal transmittance (TR) and near normal reflectance (RE) for TiO<sub>2</sub>/Al/TiO<sub>2</sub> coatings (Granqvist, 1991)

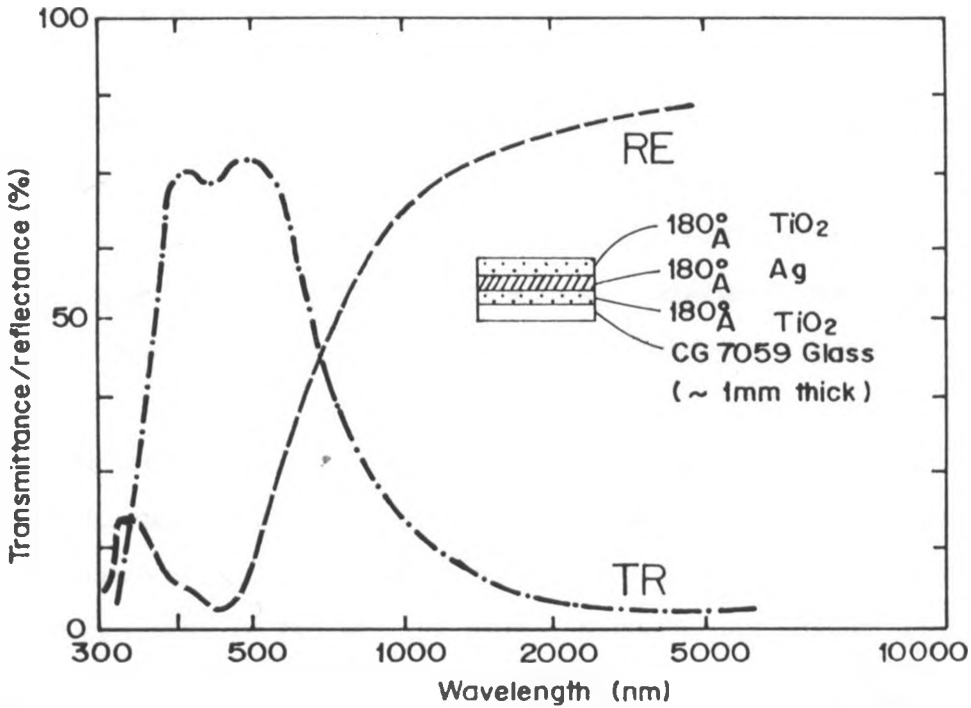


Figure 5.4.4 Measured optical transmittance (TR) and reflectance (RE) of a TiO<sub>2</sub>/Ag/TiO<sub>2</sub> film on Corning 7059 glass (John and Bachner, 1976)



## CONCLUSION AND SUGGESTIONS FOR FURTHER STUDIES

### 6.1 Conclusion

The study of multilayer coatings exhibiting angular dependent transmittance has been investigated. Among the layer combinations studied,  $MgF_2/Ag/MgF_2$  based coatings have been found to display the best angular dependent transmittance.

The coatings displaying angular dependent transmittance have been subjected to degradation studies. Some factors have been identified as the possible causes of degradation of optical properties. The factors can be classified as (i) natural factors, which include: - temperature (high and low), humidity, aquatic (damp) environment and saline environment (ii) man made factors, which include cleaning agents. The process of degradation study was divided into accelerated test and non-accelerated study. In accelerated studies, the samples were subjected to extreme conditions, while in non-accelerated studies; the samples were exposed to natural conditions.

It has been established that multilayer coatings of  $MgF_2/Ag/MgF_2$  are severely affected by high concentration of NaCl, and are reasonably resistant to concentrated organic solvents. From the results, it can be deduced that, multilayer coatings are insignificantly affected by such factors such as: temperature (high or low), elevated humidity, aquatic conditions or when exposed to natural environment.

From the various studies conducted, it is probably that the main cause of degradation in coating materials can be attributed to (i) change in packing density (void fraction) which mainly affects: the refractive index, stress, geometrical and optical thickness and homogeneity of the film (ii) change in crystallinity (amount of defects and dislocation) of the film (iii) change in surface in surface morphology leading to

increased scattering (iv) the effect of atmospheric pollutants such as sulphur dioxide and also the presence of NaCl in the moisture. (v) Chemical compatibility with organic solvents is also a factor. These factors lead to changes in optical properties of the multilayer film.

We can also conclude that, the  $\text{MgF}_2/\text{Ag}/\text{MgF}_2$  multilayer coatings exhibiting angular dependent transmittance can be used for energy efficient window coating because they have the following characteristics (i) stability against weather condition (ii) high transmittance in the luminous region (iii) angular dependency (iv) infrared filter, thus satisfying the objective of energy efficiency in window.

## 6.2 Suggestions for Further Studies

The following studies should be conducted as continuation of this work.

1. Structural characterization of the samples by use of: Surface profiler, Atomic Force Microscopy, Transmission Electron Microscopy (TEM), Scanning Electron Microscopy (SEM), X-Ray Diffraction (XRD) etc. The suggested studies ageing process, i.e. the changes that occur in packing density, crystallographic structure (amount of defects and dislocation), roughness in internal boundaries, surface roughness, grain size and shape will be better understood, thereby explain the ageing process.

2. Try to develop a model for predicting the ageing of coatings. This can be done by considering: (i) pre-set environment in which the coatings stay (ii) the structural change leading to observed change in optical spectra. Parameterization of the the changes can then be modeled. The advantage of such a model is that, service life will be easily predicted without waiting for the long duration common when conducting long term degradation studies.

3. Study transmissive properties of  $\text{MgF}_2/\text{Al}/\text{MgF}_2$  and  $\text{TiO}_2/\text{Al}/\text{TiO}_2$  coatings' photonic band gaps. Other dielectric materials with different polycrystalline structure should also be included in the multilayer combinations so that a detailed study is obtained. Such a study will assist in understanding the reason why materials of cubic and tetragonal polycrystalline structure have low transmittance when coated together as multilayer, and try to suggest alternatives to overcome this problem.

## REFERENCES

- Born, M. and E. Wolf** (1975). *Principals of Optics*. Pergamon Press, Oxford.
- Behrens, H. and G. Ebel** (1981). *Optical Properties of Metals, Physics Data*, vol. 2. Academic Press, New York.
- Behrndt, K.H.** (1964). *Thin Film*, American society for metals, Metals park, Ohio.
- Besancon, R.M.** (1986) Ed. *The Encyclopedia of Physics*, Van Nostrand Reinhold Company, New York.
- Brunold, S., U. Frei, B. Karlsson, K. Moller and M. Köhl** (2000). Accelerated Life Testing of Solar Absorber Coatings, *Solar Energy*, **68**, 313.
- Catalan, L.A.** (1961). Some Computed Optical Properties of Antireflection Coating, *Journal of Optical Society of America*, **52** (4), 437.
- Coleman, R.V.** (1978). *Method of Experimental Physics. Solid State Physics, Vol. II*, p 620 –665, Academic Press, New York.
- Cox, J.T., G. Hass and R.F. Rowntree** (1954). Two Layer Antireflection Coatings for Glass in the Near Infrared, *Journal of Optical Society of America*, **IV**. (4), 445.
- Cox, J.T., G. Hass and A. Thelen** (1962). Triple Layer Antireflection Coatings on Glass For the Visible and Near Infrared, *Journal of Optical Society of America*, **3** (9), 965.
- Driscoll, W.G. and W. Vaughan** (1978). *Handbook of Optics*, McGraw Hill, New York.

**Granqvist, C.G.**, (1984). *Compendium Notes for Solar Energy Materials*, Pergamon, Oxford.

**Granqvist, C.G.** (1989). *Spectrally Selective Surfaces for Heating and Cooling Applications, Tutorial texts in Optical Engineering, Vol. T11*, SPIE, Bellingham.

**Granqvist, C.G.** (1991). In *Energy Efficient Windows: Present and Forthcoming Technology*, edited by C.G. Granqvist, Material Science for Solar Energy Conversion System. Pergamon, Oxford.

**Granqvist, C.G.** (1995). *Handbook of Inorganic Electrochromic Materials*, Elsevier, Amsterdam.

**Heavens, O.S.** (1965). *Optical Properties of Thin Solid Films*, Dover publications, Inc., New York.

**Hilger, A.** (1986). *Thin Film Optical Filters*, 2<sup>nd</sup> ed., Bristol, Bristol.

**Hoffman, R.W.** (1976) Stresses In Thin Film: Relevance of Grain Boundaries and Impurities, *Thin Films*, **34**, 180.

**John, C.C. and F.J. Bachner** (1976). Transparent Heat Mirrors for Solar Energy Applications, *Applied Optics*, **15** (4), 1012.

**Johnson, P.B. and R.W. Christy** (1972). Optical Constants of Noble Metals, *Physics Review*, **B 6**, 4370.

**Johnson, P.B. and R.W. Christy** (1974). Optical Constants of Transition Metals: Ti, V, Cr, Mn, Fe, Co, Ni and Pd, *Physics Review*, **B 9**, 5056.

- Karlsson, J. and A. Roos** (2000) Modelling the Angular Behaviour of the Total Solar Energy Transmittance of Windows. *Solar Energy*, **69** (4) 321.
- Karlsson, J., M. Rubin and A. Roos** (2001) Evaluation of Predictive models for The Angle Dependent Total Solar Energy Transmittance of Glazing materials *Solar Energy*, **71** (1) 23.
- Kazem, M.J., J.A. Woollan and A. Belkind** (1988). Variable Angle of Incidence Spectroscopic Ellipsometric Characterization. *Journal of Applied Physics*, **64** (7), 3407.
- Kivaisi, R.T.** (1976). *Selective Absorbing Coatings for Photo-Thermal Solar Energy Conversion and Some Useful Factors in the Design of Flat Solar Collectors*, M.Sc. Thesis, University of Dar es Salaam, Dar es Salaam, Tanzania.
- Kivaisi, R.T.** (1982). Optical Properties of Obliquely Evaporated Aluminium, *Thin Solid Films*, **97**, 153.
- Ling, S.D. and W. Cheng** (1987). Design and Test of Coatings Deposited on Window Glass for Energy Efficiency, *Optik*, **78** (3), 87
- Mark, J. B. and M. Scalora** (1998). Transmissive Properties of Ag/MgF<sub>2</sub> Photonic Band gaps, *Applied Physics Letters*, **72** (14) 1575.
- Mbise, G.W.** (1989). *Angular Selective Window Coatings: Some Theoretical and Experimental Studies*. M.Sc. Thesis, University of Dar es Salaam, Dar es Salaam, Tanzania.
- Mbise, G.W.** (1995). *Optical and Structural Properties of Obliquely Evaporated Thin Films*, Ph D. Thesis, University of Dar es Salaam, Dar es Salaam, Tanzania.

- Mbise, G.W.** (1998). Spectral and Angular Selective Surfaces. Proc. Fifth College On Thin Film Technology, Vol. 5.7 ( Dar es Salaam, Tanzania).
- Mbise, G.W. and R.T. Kivaisi** (1993). Angular Dependent Transmittance in Multilayer Coating. *Solar Energy Materials and Solar cells*, **30**, 1.
- Mbise, G.W., D. Le Bellac., G.A. Niklasson and C.G. Granqvist** (1997). Angular Selective Window Coatings: Theory and Experiment. *Journal Physics, D: Applied Physics*, **30**, 2103.
- Mbise, G.W., G.B. Smith, G.A. Niklasson and C.G. Granqvist** (1989a). Angular Selective Optical Properties of Cr Films Made by Oblique Angle Evaporation. *Applied Physics Letter*, **54**, 987.
- Mbise, G.W., G.B. Smith, G.A. Niklasson and C.G. Granqvist** (1989b). Optical Materials Technology for Energy Efficiency and Solar Conversion, VIII. Proc. SPIE (San Diego, California), **1149**, 179
- Mbise, G.W., G.B. Smith, and C.G. Granqvist** (1989c). High Resolution Studies of Columnar Growth in Obliquely Deposited Metal Films. *Thin Solid Films*, **174**, L123.
- Mbise, G.W., T. Otit and R.T. Kivaisi** (1990). Angular and Selective Coatings with Induced Transmission. Proc. 1<sup>st</sup> World Renewable Energy Congress, Reading, UK.
- Meinel, A.B. and M.P. Meinel** (1979). *Applied Solar Energy, An Introduction*. Addison Wesley, Massachusetts.
- Mwamburi, M** (2001). Program Moonraker 7, Private Communication.

**Nestel Jr, J.E. and R.W. Christy** (1980). Optical Conductivity of bcc Transition Metals: V, Nb, Ta, Cr, Mo, W. *Physics Review*, **B 21**, 3173.

**Palik, E.D.** (1985). Ed., *Handbook of Optical Constants for Solid Part 1*, Academic Press, New York.

**Pulker, H.K.** (1999). *Coating on Glass*, Elsevier, Amsterdam.

**Randlett, M., E. Stroberg and K.L. Chopra** (1966). Mechanical System of Multiple Film Deposition, *Review of Scientific Instruments*, **37**, 1378.

**Rubin, M., R. Powles and K. von Rottkay** (1999). Models for the Angle Dependent Optical Properties of Coated Glazing Materials, *Solar Energy* **66**, (4) 267.

**Rubin, M., R. Powles and K. von Rottkay** (1998). Window Optics, *Solar Energy* **62**, (8) 149.

**Rugumamu, H.** (2001) Humidity Simulation Using CaCl or NaOH, Private Communication

**Smith, G.B.** (1989). Theory of Angular Selective Transmittance in Obliquely Columnar Thin Film Containing Metal and Void, *Applied Optics*, **29**, 3685.

**Turbadar, T.** (1964a). Equi - Reflectance Contours of Double Layer Anti - Reflectance Coatings, *Optical Acta.*, **11**, 159.

**Turbadar, T.** (1964b). Equi - Reflectance Contours of Triple Layer Anti - Reflectance Coatings, *Optical Acta.*, **11**, 195.

**Tremblay, C., F. Rhealt, R. Boulay and R. Tremblay** (1987). Angular Dependent Total Internal Reflector, *Applied Optics*, **26**, 570.



**Valkonen, E. and C.G. Ribbing** (1984). Optical Selectivity of Thin Silver Films  
Prepared By rf Assisted dc Magnetron Sputtering, *Material Letters*, **3**, 29.

**Valkonen, E. and B. Karlsson** (1985). Optimization of Metal Based Multilayer for  
Transparent Heat Mirrors, Proc. ICPT, Stockholm, Sweden.

# APPENDIX A : TABULATED OPTICAL PROPERTIES OF MgF<sub>2</sub>/ Ag /MgF<sub>2</sub> MULTILAYER COATINGS

N.B. N = New (Fresh) sample, A = Aged sample.  $\theta = 0^\circ$  (normal incidence)  
 $\theta = 50^\circ$  (oblique incidence)

Table A1. Changes in optical properties for samples heated at 50 °C for duration shown.

	Time (hrs)	T <sub>lum</sub>		R <sub>lum</sub>		T <sub>sol</sub>		R <sub>sol</sub>	
		N	A	N	A	N	A	N	A
$\theta = 0^\circ$	12h	44.3	43.7	25.6	23.5	31.6	30.0	51.3	50.1
	72h	44.3	43.4	25.6	23.5	31.6	29.6	51.3	49.7
	120h	44.3	43.1	25.6	21.8	31.6	29.4	51.3	49.5
$\theta = 50^\circ$	12h	63.4	62.6	20.0	20.0	28.3	26.8	55.6	54.8
	72h	63.4	62.1	20.0	20.0	28.3	26.6	55.6	54.3
	120h	63.4	61.9	20.0	20.1	28.3	26.5	55.6	54.0

Table A2. Changes in optical properties for samples heated at 100 °C for duration shown.

	Time (hrs)	T <sub>lum</sub>		R <sub>lum</sub>		T <sub>sol</sub>		R <sub>sol</sub>	
		N	A	N	A	N	A	N	A
$\theta = 0^\circ$	12h	41.6	41.6	28.3	26.7	30.1	28.2	50.4	49.0
	120h	41.6	40.8	28.3	23.1	30.1	27.8	50.4	48.1
$\theta = 50^\circ$	12h	60.8	59.4	20.1	20.1	27.8	26.1	54.4	52.8
	120h	60.8	58.1	20.1	19.2	27.8	25.7	54.4	51.8

Table A3. Changes in optical properties for samples heated at 200 °C for duration shown.

	Time (hrs)	T <sub>lum</sub>		R <sub>lum</sub>		T <sub>sol</sub>		R <sub>sol</sub>	
		N	A	N	A	N	A	N	A
$\theta = 0^\circ$	12	46.8	46.8	29.4	26.2	30.9	29.0	51.1	49.0
	36	46.8	46.2	29.4	24.7	30.9	28.7	51.1	48.6
	96	46.8	44.9	29.4	22.1	30.9	28.4	51.1	48.3
$\theta = 50^\circ$	12	61.9	60.7	19.7	19.7	27.8	25.6	55.2	52.4
	36	61.9	58.6	19.7	19.7	27.8	25.4	55.2	52.2
	96	61.9	57.8	19.7	19.1	27.8	23.1	55.2	51.9

Table A4. Changes in optical properties for samples laid in freezer maintained at -10 °C for duration shown.

	Time (weeks)	T <sub>lum</sub>		R <sub>lum</sub>		T <sub>sol</sub>		R <sub>sol</sub>	
		N	A	N	A	N	A	N	A
∅ = 0°	1 wk	44.1	44.1	34.8	33.6	31.6	30.9	50.6	48.9
	4 wk	44.1	44.1	34.8	33.0	31.6	30.7	50.6	48.5
	12 wk	44.1	44.1	34.8	30.8	31.6	30.5	50.6	48.2
∅ = 50°	1 wk	64.7	63.9	20.2	20.2	28.1	27.5	55.4	54.8
	4 wk	64.7	63.5	20.2	20.2	28.1	27.1	55.4	54.5
	12 wk	64.7	62.9	20.2	20.2	28.1	26.9	55.4	54.3

Table A5. Changes in optical properties for samples laid in freezer maintained at -18 °C for duration shown.

	Time (weeks)	T <sub>lum</sub>		R <sub>lum</sub>		T <sub>sol</sub>		R <sub>sol</sub>	
		N	A	N	A	N	A	N	A
∅ = 0°	1 wk	42.7	42.7	27.2	26.8	31.4	30.8	50.3	48.9
	4 wk	42.7	42.7	27.2	26.1	31.4	30.1	50.3	48.6
	12 wk	42.7	42.7	27.2	25.4	31.4	29.8	50.3	48.5
∅ = 50°	1 wk	63.8	63.1	19.8	20.1	28.0	26.6	55.3	54.3
	4 wk	63.8	62.3	19.8	20.1	28.0	26.3	55.3	53.9
	12 wk	63.8	61.6	19.8	20.1	28.0	26.2	55.3	53.6

Table A6. Changes in optical properties for samples covered in ice (frost) at -20 °C for duration shown.

	Time (hrs)	T <sub>lum</sub>		R <sub>lum</sub>		T <sub>sol</sub>		R <sub>sol</sub>	
		N	A	N	A	N	A	N	A
∅ = 0°	12 wk	43.5	43.4	27.4	19.6	31.5	27.9	51.5	47.9
∅ = 50°	12 wk	64.6	61.1	19.6	18.2	28.4	27.0	56.1	52.8

Table A7. Changes in optical properties for samples laid in chamber maintained at 86% relative humidity for duration shown

	Time (weeks)	T <sub>lum</sub>		R <sub>lum</sub>		T <sub>sol</sub>		R <sub>sol</sub>	
		N	A	N	A	N	A	N	A
∅ = 0°	3 wks	44.1	44.1	26.3	25.2	33.4	32.1	51.4	49.6
	12 wks	44.1	43.5	26.3	24.1	33.4	30.9	51.4	48.2
∅ = 50°	3 wks	62.8	61.9	22.1	22.1	31.1	29.6	54.9	53.2
	12 wks	62.8	60.2	22.1	20.9	31.1	28.3	54.9	51.6

Table A8. Changes in optical properties for samples soaked in saline solution of concentration 20gm/100ml, for duration shown.

	Time (hrs)	T <sub>lum</sub>		R <sub>lum</sub>		T <sub>sol</sub>		R <sub>sol</sub>	
		N	A	N	A	N	A	N	A
∅ = 0°	5 hrs	42.2	50.8	27.5	19.4	32.6	39.2	51.8	45.2
	24 hrs	42.2	64.3	27.5	16.5	32.6	51.4	51.6	16.7
	2 wks	42.2	84.3	27.5	11.6	32.6	84.8	51.8	8.2
∅ = 50°	5 hrs	63.1	63.1	21.8	19.4	28.7	39.4	55.7	44.8
	24 hrs	63.1	64.3	21.8	16.8	28.7	84.8	55.7	8.2
	2 wks	63.1	84.3	21.8	11.6	28.7	84.8	55.7	8.2

Table A9. Changes in optical properties for samples soaked in acetone of purity 99.8% for duration shown

	Time (hrs)	T <sub>lum</sub>		R <sub>lum</sub>		T <sub>sol</sub>		R <sub>sol</sub>	
		N	A	N	A	N	A	N	A
∅ = 0°	12 hrs	42.8	42.8	24.3	22.5	34.7	32.5	53.8	51.5
	96 hrs	42.8	42.1	24.3	19.9	34.7	31.5	53.8	49.6
∅ = 50°	12 hrs	65.8	64.9	18.2	18.2	31.4	29.3	57.2	55.1
	96 hrs	65.8	62.4	18.2	17.8	31.4	28.1	57.2	53.4

Table A10. Changes in optical properties for samples soaked in ethanol of purity 99.8% for duration shown

	Time (hrs)	T <sub>lum</sub>		R <sub>lum</sub>		T <sub>sol</sub>		R <sub>sol</sub>	
		N	A	N	A	N	A	N	A
∅ = 0°	12 hrs	43.7	43.1	26.7	23.2	32.5	31.8	52.6	50.4
	96 hrs	43.7	42.5	26.7	20.0	32.5	28.7	52.6	48.7
∅ = 50°	12 hrs	61.5	60.1	24.6	20.6	29.8	29.3	55.9	53.3
	96 hrs	61.5	57.3	24.6	19.3	29.8	26.3	55.9	51.7

Table A11. Changes in optical properties for samples exposed into outdoor environment for duration shown

	Time (hrs)	T <sub>lum</sub>		R <sub>lum</sub>		T <sub>sol</sub>		R <sub>sol</sub>	
		N	A	N	A	N	A	N	A
∅ = 0°	2 wks	43.6	43.6	32.8	29.7	31.8	30.1	51.4	49.8
	4 wks	43.6	43.4	32.8	29.7	31.8	29.5	51.4	49.2
	12 wks	43.6	43.2	32.8	24.5	31.8	29.2	51.4	48.8
∅ = 50°	2 wks	64.2	63.1	28.3	27.9	29.4	28.3	56.3	54.3
	4 wks	64.2	62.2	28.3	24.5	29.4	27.3	56.3	53.2
	12 wks	64.2	60.5	28.3	20.9	29.4	26.7	56.3	52.9

Table A12. Changes in optical properties for samples soaked in distilled water for duration shown

	Time (hrs)	T <sub>lum</sub>		R <sub>lum</sub>		T <sub>sol</sub>		R <sub>sol</sub>	
		N	A	N	A	N	A	N	A
∅ = 0°	48 hrs	43.5	43.2	28.3	26.4	31.6	30.4	51.7	51.5
	1 wk	43.5	43.2	28.3	25.1	31.6	30.1	51.7	50.9
	3 wks	43.5	43.1	28.3	23.6	31.6	29.9	51.7	50.1
∅ = 50°	48 hrs	64.9	64.7	19.8	19.8	28.3	27.3	56.4	56.1
	1 wk	64.9	64.5	19.8	19.8	28.3	27.1	56.4	56.4
	3 wks	64.9	63.3	19.8	19.8	28.3	26.7	56.4	54.6

## APPENDIX B: PROGRAM MOONRAKER 7 (Mwamburi, M., 2001)

This program was initially written by Mr. Mghendi Mwamburi, at Physics Department, Moi University Kenya. The program was edited by Musembi, R.J.

The program is written in MathCAD and it uses the formula given in section 3.6 page 28. The computation is done using the trapezoidal rule by: first getting the area under the curve for figures obtained empirically given in section 5.2. The value obtained is then normalized using the standard data for sunlight or thermal radiation i.e. ISO 9845 data for A.M 1.5 irradiance and ISO 10526 data for luminous performance. The practical wavelength limits used are given in section 3.6, page 28.

The software used for computation was **MathCAD 6+**

PROGRAMME MOONRAKER 7  
THIS PROGRAMME CALCULATES SOLAR/ LUMINOUS (transmittance/reflectance)

ORIGIN = 0

m = 938 <= number of data points in files

j := 1..m

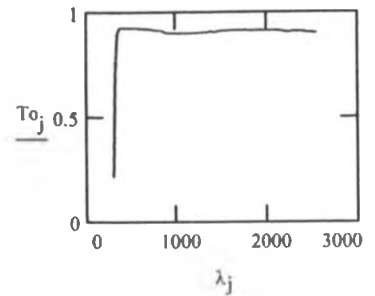
M = READPRN(Tglass.txt)

$$\lambda_j := [M_{(j,0)}]$$

$$T_{o(j)} = M_{(j,1)}$$

$$T_{o_{938}} = 0.902$$

PLOT TRANSMITTANCE OF PLAIN GLASS

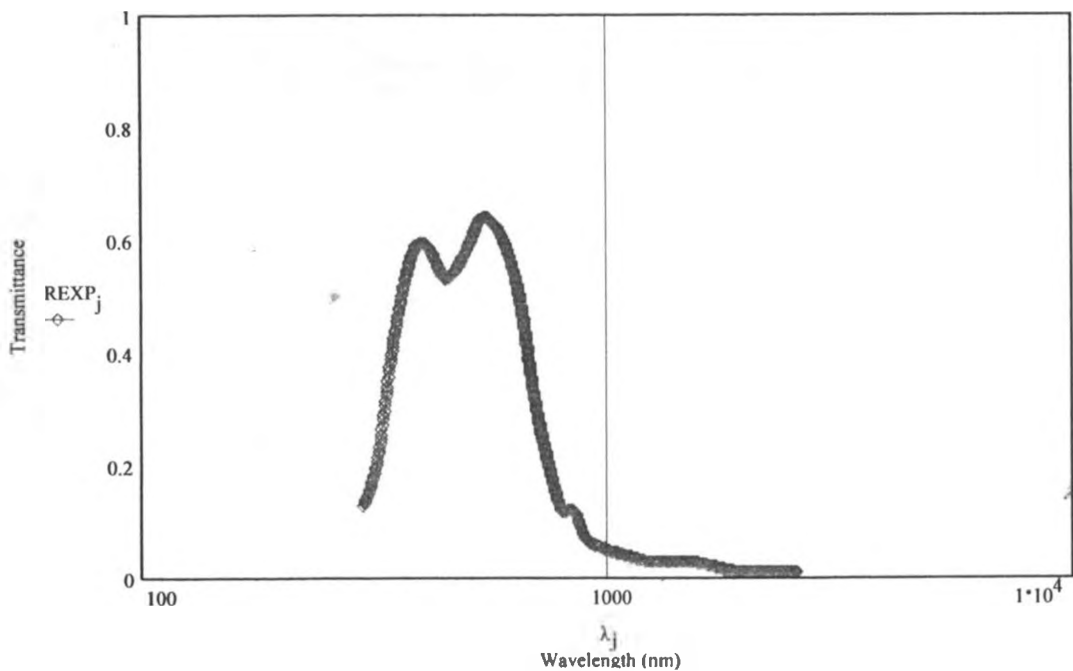


j = 0..m for data

M = READPRN(explcotfr.txt) <= READ EXPERIMENT DATA FILE AND PLOT

$$\lambda_j = M_{(j,0)}$$

$$REXP_j = M_{(j,1)}$$



**CALCULATION OF SOLAR (TRANSMITTANCE/ REFLECTANCE)**

AM1.5 Irradiance DATA

ORIGIN = 0

j = 0..m

M = READPRN(am15.txt)

$$\lambda_j = M_{(j,0)}$$

$$Sam_{(j)} = \frac{M_{(j,1)}}{1100}$$

$$\lambda_0 = 300$$

$$X_j = Sam_j \cdot REXP_j$$

Eye sensitivity DATA

j = 0..m

M = READPRN(eyadata2.txt)

$$\lambda_j = M_{(j,0)}$$

$$eyemax = 0.9983$$

$$\lambda_0 = 300$$

$$E_j = REXP_j \cdot Eye_j$$

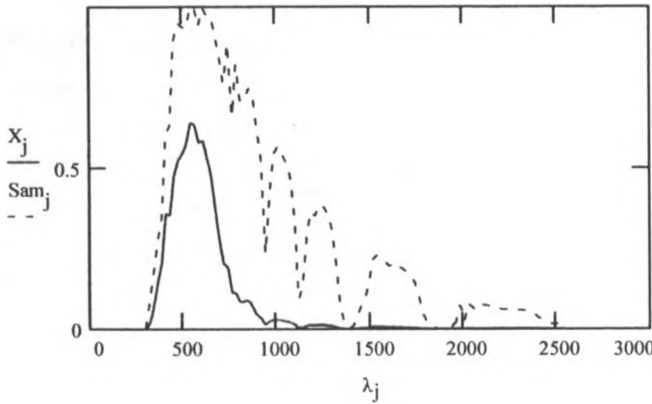
$$Eye_{(j)} = \frac{M_{(j,1)}}{eyemax}$$

Calculation of intergrated solar (transmittance/ reflectance)

j = 1..m

$$Tsolar = \frac{\sum_j \left[ X_{j-1} + \left( \frac{X_j - X_{j-1}}{2} \right) \right] \cdot (\lambda_j - \lambda_{j-1})}{\sum_j \left[ Sam_{j-1} + \left( \frac{Sam_j - Sam_{j-1}}{2} \right) \right] \cdot (\lambda_j - \lambda_{j-1})}$$

$$Tsolar = 0.278$$



Rough approx.

$$Tsolar1 := \frac{\sum_j X_j}{\sum_j Sam_j}$$

$$Tsolar1 = 0.4$$

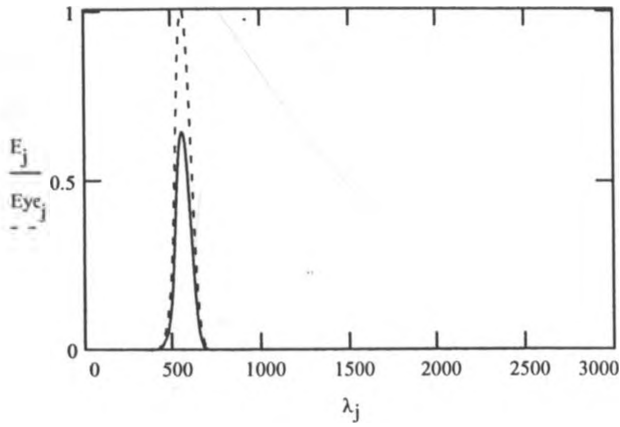
**CALCULATION OF LUMINOUS (TRANSMITTANCE/ REFLECTANCE )**

Calculation of intergrated luminous (transmittance/ reflectance)



$$Tlum = \frac{\sum_j \left[ E_{j-1} + \left( \frac{E_j - E_{j-1}}{2} \right) \right] \cdot (\lambda_j - \lambda_{j-1})}{\sum_j \left[ Eye_{j-1} + \left( \frac{Eye_j - Eye_{j-1}}{2} \right) \right] \cdot (\lambda_j - \lambda_{j-1})}$$

$$Tlum = 0.608$$



Rough approx.

$$Tlum2 = \frac{\sum_j E_j}{\sum_j Eye_j}$$

$$Tlum2 = 0.608$$

Data storage ( not critical)

ORIGIN = 0 j = 0..2

REF<sub>(0,1)</sub> = Tsolar REF<sub>(0,2)</sub> = Tlum

WRITEPRN(Tsolar\_1 PRN) = REF